# POWER ENHANCEMENT AND APPLICATIONS OF MICROBIAL FUEL CELLS

**TANG XINHUA**

*(B Eng) Zhejiang University*

*(MSc) Graduate University of Chinese Academy of Sciences*

**A THESIS SUBMITTED**

**FOR THE DEGREE OF DOCTOR OF PHILOSOPHY**

**NUS GRADUATE SCHOOL FOR INTEGRATIVE SCIENCES AND ENGINEERING**

**NATIONAL UNIVERSITY OF SINGAPORE**

**2016**

**DECLARATION**

**I hereby declare that the thesis is my original work and it has been written by me in its entirety. I have duly acknowledged all the sources of information which have been used in the thesis.**

**This thesis has also not been submitted for any degree in any university previously.**

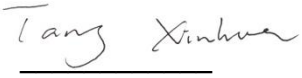

**Tang Xinhua**

**10 May 2016**

**ACKNOWLEDGEMENTS**

This thesis would not have been possible without the assistance from many others. First and foremost, I would like to express my gratitude to my supervisor Professor Ng How Yong for his close guidance, advice and encouragement during the course of my PhD study. Without his support, I could not be able to join the collaborating laboratory overseas to complete my research project. Without his guidance, my thesis work could have been impossible.

Secondly, I would like to thank Professor Li Haoran and Professor Du Zhuwei from Chinese Academy of Sciences They have not only provided advanced research equipments, but also have spent lots of time and efforts on my work. I have benefited a lot from their expertise in environmental biotechnology.

I am grateful to my teammates and friends. Their support is not only helpful to my research, but also very important for my social life. Here, I want to give thanks to Wang Weida, Shailesh Kharkwal, Ten Qing, Du Yunlun, Chen Weiqiang, Zhang Xu, Yang Zhichao, Yi Aifei, Cai Zhenlei and Cheng Yulong. I really enjoy the time we had together, which is and will always be a great memory in my life.

I would like to acknowledge NUS Graduate School for Integrative Sciences and Engineering for the research scholarship. Without the financial support, I

could not have the opportunity to pursue my PhD study in NUS.

Finally, I would like to give my special thanks to my wife, my baby and my parents for their selfless love and support. They are always standing by my side and giving me the confidence and strength to overcome the difficulties. Because of their love, my world is full of sunshine.

**TABLE OF CONTENTS**

## SUMMARY

Microbial fuel cell (MFC) is a bioelectrochemical system that exploits microbial catalysis to directly convert chemical energy in organic matters into electrical energy. Although MFC is a promising environmental biotechnology for energy production and wastewater treatment, it is still in its infancy and is thus far away from practical applications. Currently, MFC technology is primarily constrained by the low power generation and the prohibitive construction cost. Overcoming these barriers will be of great significance to the applications of MFCs.

Firstly, a facile and scalable approach was used to synthesize conductive polypyrrole hydrogels/carbon nanotubes (CPHs/CNTs) that synergized the advantageous features of hydrogels and organic conductor. The high electrocatalytic activity of this anode significantly reduced the interfacial charge transfer resistance and facilitated the direct electron transfer from bacteria to anode in MFCs. The porous structure and hydrophilicity of this composite enhanced the biofilm formation on anode surface. As a result, this anode increased the maximum power density of MFCs by 118%.

Secondly, anthraquinone-2-sulfonic acid (AQS), an electron transfer mediator, was covalently grafted onto graphite felt surface *via* spontaneous reduction of the *in situ* generated AQS diazonium cations. This study demonstrated that

covalently modified AQS functioned as a redox mediator to facilitate the mediated electron transfer from bacteria to electrode. Consequently, AQS modified anode enhanced the maximum power density of MFCs by 94%.

Thirdly, catalyst for oxygen reduction in cathode is vital for power production in MFCs. non-precious metal catalysts comprising carbon, nitrogen and iron were prepared by a high-temperature synthesis method. These catalysts showed very positive onset potentials and less than 3% yield of hydrogen peroxide in the whole potential range, which matched the state-of-the-art Pt/C. These catalysts significantly enhanced the maximum power density from 1.32 $W/m^3$ to 12.54 $W/m^3$ in MFCs. Physical and chemical characterizations of the catalysts indicated that iron coordinated with pyridinic nitrogen hosted in micropores was responsible for the high catalytic activity. This study demonstrates that these catalysts are excellent cathodes for MFCs due to their high catalytic activity, strong stability and very low cost.

Fourthly, bicarbonate buffer was used in MFCs to help stabilize the solution pH for exoelectrogens for electricity production. Compared with the electrolyte with the commonly used phosphate buffer, electrolyte with bicarbonate buffer effectively decreased the suspended bacteria. The reduction of bacteria suspended in the solution allowed more substrate to be consumed by bacteria formed on anode surface for electricity generation. As a result, the electrolyte with bicarbonate buffer significantly enhanced the coulombic

efficiency. This study demonstrates that electrolyte with bicarbonate holds the potential to enhance the feasibility for practical applications of MFCs.

Finally, electrical energy production from wastewater by MFCs was investigated. An energy recovery efficiency of 18.4% and an energy density of 0.89 kWh/(kg COD) was achieved in single chamber MFCs. This study demonstrates that MFCs can be a competitive technology for simultaneous energy recovery and wastewater treatment.

## A LIST OF TABLES

## A LIST OF FIGURES

## A LIST OF ABBREVIATIONS

| | |
|---|---|
| AQS | Anthraquinone-2-sulfonic acid |
| AQDS | anthraquinone-1, 6-disulfonic acid |
| BOD | Biochemical oxygen demand |
| CE | Coulombic efficiency |
| CNTs | Carbon nanotubes |
| COD | Chemical oxygen demand |
| CPH | Conductive polypyrrole hydrogels |
| CV | Cyclic voltammetry |
| EDS | Energy dispersive spectrometry |
| EIS | Electrochemical impedance spectroscopy |
| FESEM | Field emission scanning electron microscope |
| FT-IR | Fourier transform infrared spectroscopy |
| LSV | Linear sweep voltammograms |
| MFC | Microbial fuel cell |
| MEC | Microbial electrolysis cell |
| NHE | Normal hydrogen electrode |
| NQ | 1,4-naphthoquinone |
| $OD_{600}$ | Optical density at 600 nm |
| ORR | Oxygen reduction reaction |
| PANI | Polyaniline |
| RHE | Reversible hydrogen electrode |
| RRDE | Rotating ring disk electrode |
| SEM | Scanning electron microscope |
| SCE | Saturated calomel electrode |
| XPS | X-ray photoelectron spectroscopy |

## A LIST OF PUBLICATIONS

In this thesis

1. **Tang, X.**, Li, H., Du, Z., Wang, W., and Ng, H. Y. (2015) Conductive polypyrrole hydrogels and carbon nanotubes composite as an anode for microbial fuel cells, *Rsc Advances 5*, 50968-50974.
2. **Tang, X.**, Li, H., Du, Z., and Ng, H. Y. (2015) Polyaniline and iron based catalysts as air cathodesfor enhanced oxygen reduction in microbial fuelcells, *Rsc Advances 5*, 79348-79354.
3. **Tang, X.**, Li, H., Du, Z., and Ng, H. Y. (2014) Spontaneous modification of graphite anode by anthraquinone-2-sulfonic acid for microbial fuel cells, *Bioresource Technology 164*, 184-188.
4. **Tang, X.**, Li, H., Du, Z., and Ng, H. Y. (2014) A phosphorus-free anolyte to enhance coulombic efficiency of microbial fuel cells, *Journal of Power Sources 268*, 14-18.
5. **Tang, X.**, Li, H., Wang, W., Du, Z., and Ng, H. Y. (2014) A high-performance electrocatalytic air cathode derived from aniline and iron for use in microbial fuel cells, *Rsc Advances 4*, 12789-12794.

Others

1. Wang, W., Feng, Y., **Tang, X.**, Li, H., Du, Z., Yi, A., and Zhang, X. (2015) Enhanced U(VI) bioreduction by alginate-immobilized uranium-reducing bacteria in the presence of carbon nanotubes and anthraquinone-2,6-disulfonate, *Journal of Environmental Sciences 31*, 68-73.
2. Feng, Y., Wang W., **Tang, X.**, Li, H., Du, Z., Yang, Z., and Du, Y. (2014) Isolation and characterization of an electrochemically active and cyanide-degrading bacterium isolated from a microbial fuel cell, *Rsc Advances 4*, 36458-36463.
3. Yang, B., Zuo, J., **Tang, X.**, Liu, F., Yu, X., Tang, X., Jiang, H., and Gan, L. (2014) Effective ultrasound electrochemical degradation of methylene blue wastewater using a nanocoated electrode, *Ultrasonics sonochemistry 21*, 1310-1317.
4. Wang, W., Li, H.,Feng, Y., **Tang X.**, Du Z., Du Y. (2014) Research and application advances in microbial fuel cell. *Chemical Industry and Engineering Progress*, *33*, 1067-1076.
5. Lai, B., **Tang, X.**, Li, H., Du, Z., Liu, X., and Zhang, Q. (2011) Power production enhancement with a polyaniline modified anode in microbial fuel cells, *Biosensors & Bioelectronics 28*, 373-377.
6. **Tang, X.**, Guo, K., Li, H., Du, Z., and Tian, J. (2011) Electrochemical

treatment of graphite to enhance electron transfer from bacteria to electrodes, *Bioresource Technology 102*, 3558-3560.

7. **Tang, X.**, Du, Z., and Li, H. (2010) Anodic electron shuttle mechanism based on 1-hydroxy-4-aminoanthraquinone in microbial fuel cells, *Electrochemistry Communication 12*, 1140-1143.
8. **Tang, X.**, Guo, K., Li, H., Du, Z., and Tian, J. (2010) Microfiltration membrane performance in two-chamber microbial fuel cells, *Biochemical Engineering Journal 52*, 194-198.
9. Guo, K., **Tang, X.**, Du, Z., and Li, H. (2010) Hydrogen production from acetate in a cathode-on-top single-chamber microbial electrolysis cell with a mipor cathode, *Biochemical Engineering Journal 51*, 48-52.

# Chapter 1 Introduction and literature review

## 1.1 Introduction

Approximately 80% of world energy consumption of 2012 came from fossil fuels, and fossil fuels, such as petroleum, coal and natural gas, are being exhausted, leading to an energy crisis in the near future (1). In order to mitigate this challenge, sustainable energy sources as alternatives to fossil fuels have to be developed.

One untapped resource is the organic matters in wastewater theoretically sufficient to generate about $7.4 \times 10^{18}$ J per year, which is three to four times more energy than the energy that is needed to treat the wastewater (2). Aerobic treatment of wastewater such as activated sludge is an efficient technology for removing organic contaminants because aerobic heterotrophic microorganisms can degrade organic matters very fast due to their high metabolic kinetics (3). However, it is energy intensive and costly because of aeration and sludge treatment. Typically, about 0.4-1.0 kWh of energy is needed for removing one kilogram COD from wastewater by activated sludge treatment (4). Anaerobic digestion is a traditional technology to capture energy from dissolved organic matters in wastewater in the form of biogas (5). Methane produced by anaerobic digestion, however, must be efficiently collected and safely stored, because methane is a greenhouse gas which might cause explosion (6). In addition, anaerobic digestion normally requires a warm temperature higher than 20 ℃, which limits its applications in lots of wastewater treatment plants (2).

Microbial fuel cell is a bioelectrochemical system that exploits microbial

catalysis to directly convert chemical energy in organic matters into electrical energy (7-8). As a promising environmental biotechnology for sustainable energy production from wastewater, MFCs have drawn much attention in the past decade (9-10). Recently, applications of MFCs have been expanded to a much larger scope, such as microbial electrosynthesis of chemicals (e.g., hydrogen, hydrogen peroxide, methane, ethanol), biochemical oxygen demand and toxicity monitoring, sediment bioremediation and water desalination (11-16).

Though MFCs are promising for these applications, this technology is still in its infancy and is thus still far away from practical applications. Currently, MFCs are primarily constrained by the low power generation and prohibitive construction cost (17-19). These technical barriers need to be overcome to enhance the performance and reduce the cost of MFCs.

Anode material plays a key role in determining the power production of MFCs, because it not only influences the biofim formation on electrode surface, but also affects the extracellular electron transfer between microorganisms and the electrode (20). As such, preparation of novel anode with high electrocatalytic activity and excellent biocompatibility is an effective approach to enhance power density in MFCs.

Cathode is another limiting factor for power generation in MFCs (21). Oxygen is the best choice as electron acceptor for MFCs due to the positive redox potential, the harmlessness of the reduction product ($H_2O$) and its virtually inexhaustible availability. So far, platinum-based cathodes have been commonly used in MFCs due to their high catalytic activity towards oxygen reduction reaction. This expensive catalyst, however, severely impedes the

large-scale applications of MFCs. Therefore, development of high-performance and low-cost cathode is of great significance for applications of MFCs.

### 1.2 Working principle of MFCs

Microbial fuel cell (MFC) is a bioelectrochemical device that converts the chemical energy in organic matters into electrical energy through catalytic reactions by microorganism (22-24).

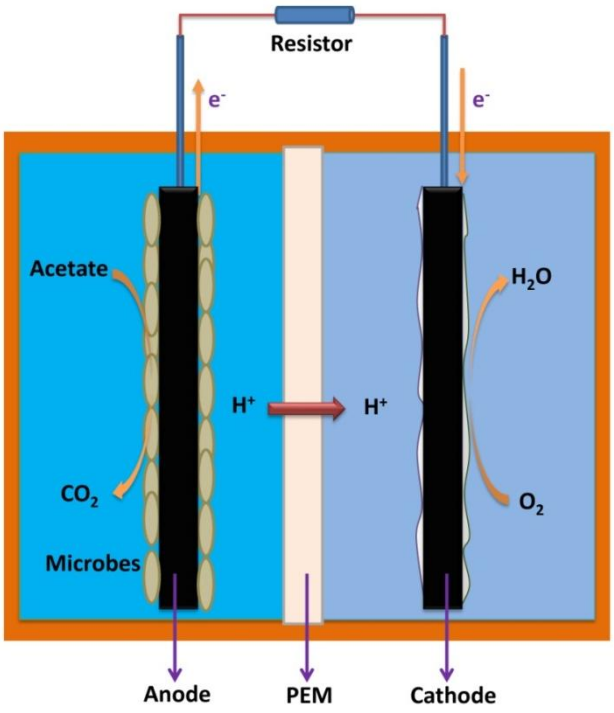


Figure 1. 1 Schematic diagram of a microbial fuel cell for power production.

Typically, a MFC reactor consists of an anode and a cathode, possibly separated by a proton exchange membrane (Figure 1.1). In the anode, electrochemically active microorganisms degrade organic matters and release electrons and protons under anaerobic condition. The electrons transfer from

the microorganisms to the anode and then to the cathode via the external circuit. The protons diffuse to the cathode where they react with electrons and usually oxygen to form water. Consequently, a continuous current is generated while organic compounds in wastewater are degraded. The electrode reactions are demonstrated below using acetate as the substrate.

Anodic reaction: $CH_3COO^- + 6H_2O \xrightarrow{\text{Microbes}} 2HCO_3^- + 9H^+ + 8e^-$

Cathodic reaction: $4H^+ + 4e^- + O_2 \longrightarrow 2H_2O$

The cell voltage that can be generated from MFCs can be calculated from the Nernst potential of the anode and cathode (25):

$$E_{cell} = E_{cat} - E_{an}$$

In which $E_{cell}$ is the cell voltage, $E_{cat}$ is the cathode potential and $E_{an}$ is the anode potential.

The Nernst potential of the anode and cathode is described respectively below (25):

$$E_{an} = E_{an}^0 - \frac{RT}{8F}\ln\left(\frac{\left[CH_3COO^-\right]}{\left[H^+\right]^9\left[HCO_3^-\right]^2}\right)$$

$$E_{cat} = E_{cat}^0 - \frac{RT}{4F}\ln\left(\frac{1}{\left[H^+\right]^4 pO_2}\right)$$

Where $E_{an}$ is the anode potential (V), $E_{an}^0$ is the standard anode potential at 298 K (V), $E_{cat}$ is cathode potential (V), $E_{cat}^0$ is the standard cathode potential at 298 K (V), R is universal gas constant (8.314 J/mol/K), F is the Faraday's constant (96500 C/mol), T is temperature (K), $[CH_3COO^-]$ is acetate concentration (mol/L), $[H^+]$ is proton concentration (mol/L), $[HCO_3^-]$ is

bicarbonate concentration (mol/L), $pO_2$ is partial oxygen pressure (Pa).

Under standard condition, the anode potential using acetate is 0.187 V (vs NHE) and the cathode potential using oxygen is 1.229 V (vs NHE), therefore a cell voltage of 1.042 V can be obtained theoretically.

### 1.3 A brief history of MFC development

The first discovery of current generation from bacteria was reported in 1911 by Potter, who observed electricity from *Escherichia coli* on platinum electrode surface (26). This discovery did not receive well attention until 1990s, when it was found that microorganisms could transport electrons to insoluble minerals, a process known as extracellular electron transfer (26-27).

Two types of mechanisms have been demonstrated for extracellular electron transfer from bacteria to electrode: direct electron transfer and mediated electron transfer (28). Physical contact between the cell membrane or a membrane organelle (pili) and the electrode enables the direct electron transfer from bacteria to anode. For mediated electron transfer, redox mediator shuttles between bacteria and anode and help deliver electron.

In the early stage of MFC research, exogenous redox mediators were added into anodic chambers to drive the extracellular electron transfer, because those microorganisms could not directly transfer electron into electrode surface (29-30). Most of the mediators, however, are expensive, toxic and unstable, which hampers the applications of MFCs (31). The finding that some

microorganisms, such as *Shewanella putrefaciens*, *Geobacteraceae*, *Desulfuromonaceae* and *Rhodoferax ferrireducens* can directly transfer electrons to electrode surface without addition of mediators is a milestone in the history of MFCs, which greatly accelerates the advancement of this technology (31-32). From then on, the study of MFCs has developed very rapidly and this technology has demonstrated its potential for applications such as electricity production, wastewater treatment, biosensors, chemical and fuel synthesis, and desalination (10-11, 16, 33-36).

## 1.4 Applications of MFCs

### 1.4.1 Electricity production

MFCs can directly convert chemical energy in organic matters into electrical energy. Therefore, the theoretical energy conversion efficiency can be very high, as it is not limited by the thermal efficiency of the Carnot cycle (31). Rabaey et al. reported that electron recovery as electricity was up to 89% in a MFC using glucose as the substrate (7). Rosenbaum et al. described a coulombic efficiency of 97% in MFCs during the degradation of the fermentation products formate and ethanol (37).

As a promising technology to extract electrical energy from biomass, MFCs can be used as power sources. Although MFCs cannot contribute to the power grid in the foreseeable future due to the small power production, MFCs have been successfully used as power supplies in remote areas, such as freshwater

and marine environments. For example, sediment MFCs have been used as alternative power sources to batteries in marine studies. Shantaram et al. developed an MFC to power a wireless sensor which was able to monitor the water quality and transit the data to remote receivers (38). Tender et al. prepared a MFC to power a meteorological buoy that measured temperature, humidity and pressure on the bottom of marine environments (39). Currently, however, the power production of MFCs is still too low to supply power intensive devices. In order to improve the application as power sources, the power density has to be enhanced.

### 1.4.2 Wastewater treatment

The greatest advantage of wastewater treatment using MFCs is that, rather than energy consuming, clean energy is produced simultaneously. It is estimated that organic matters in wastewater is theoretically sufficient to generate about $7.4\times10^{18}$ J very year, which is three to four times more energy than what is needed to treat the wastewater (2). Therefore, MFC has the potential to be a self-sufficient technology for wastewater treatment.

Aerobic treatment of wastewater is energy intensive and costly because of aeration and sludge treatment. Currently, about 0.4- 1.0 kWh of energy is needed for removing one kilogram COD from wastewater by activated sludge treatment (4). Anaerobic digestion is a traditional technology to capture energy during wastewater. Methane produced by anaerobic digestion, however, must

be efficiently collected and safely stored (6). Besides, anaerobic digestion normally requires a warm temperature higher than 20 ℃, while MFC can function well over a wide range of temperature (2). Another advantage of MFC over anaerobic digestion is that the former can work over a large range of COD concentration and the latter is more suitable for high COD loading due to the long detention times.

So far, MFCs have been used for various kinds of wastewaters treatment, such as domestic wastewater, swine wastewater, brewery wastewater and food processing wastewater (40). These wastewaters are rich in organic matters, which could be easily degraded by microorganisms in MFCs. The COD removal efficiency typically can be more than 80% (41-42). Besides, inorganic matters, such as sulfide, ammonium, have also been successfully removed by MFCs (43-44). The removal of these organic and inorganic compounds is due to the microbial oxidation in the anode. The reduction of some pollutants in the cathode is another strategy for wastewater treatment. For example, nitrate, copper, uranium and mercury have been reduced and removed by the biocathode in MFCs (35, 45-47).

### 1.4.3 Analytical applications of MFCs

The main analytical application of MFCs is for biochemical oxygen demand (BOD) detection. In 1977, Karube et al. demonstrated the first BOD monitoring by calculating the hydrogen generated in MFCs (48). Later in 2003,

Kim et al. discovered that the BOD concentration was proportional to the coulomb recovered by MFCs (49). This MFC biosensor presented excellent stability for a period of five years. The response time for BOD concentration lower than 6.45 mg/L was less than 30 min. A high BOD concentration of 206.4 mg/L, however, required a long time of approximately 10 h to complete the test, as the coulomb could be obtained only when the BOD had been consumed by the microorganisms.

Researchers also found that the maximum current production was directly proportional to the BOD concentration, when the anodic oxidation was limited by BOD concentration (49-50). As the current reaches steady state in a very short time, this type of MFC has the potential to be used for real-time BOD detection. For example, BOD concentrations up to 100 mg/L showed a good linear relationship to the maximum current during wastewater monitoring and the respond time was about 60 min (51). By optimization the MFC design, the external resistance and the hydraulic retention time, the response time of the MFC biosensor was reduced to about 5 min (52). The short response time, excellent stability and accuracy are the major advantages of MFC biosensor for BOD detection.

MFC biosensors have also been proposed for on-site monitoring of toxic substance in water. The toxic substance inhibits metabolic activity of microorganisms and further electron transfer from microorganisms to anode. Since the current depends on the concentration of toxicants, MFC-type

biosensor has been successfully applied for monitoring chemical toxicants such as lead, mercury, formaldehyde, and organophosphorus compound (53-55). The greatest advantage of MFC biosensor is that it can be used in river or ocean sediment where other technologies have difficulty to access.

### 1.4.4 Chemical synthesis

The electricity produced by MFCs can be used for chemical synthesis. Typically, an additional voltage is required to drive the reaction because the synthesis of these chemicals is thermodynamically unfavorable. Therefore, these reactors are also known as microbial electrolysis cells (MEC). The production of hydrogen from MECs has been studied the most (56-57). In order to reduce the proton and produce hydrogen in the cathode, an additional voltage of about 0.2 V is needed (56). Compared with direct electrolysis of water to generate hydrogen which normally requires a voltage larger than 2.1 V, the applied voltage of MEC is much smaller. Compared with dark fermentation for hydrogen production, MEC has much higher hydrogen recovery efficiency and the substrates can be any biodegradable dissolved organic matters (56, 58). Besides hydrogen, other chemicals such as hydrogen peroxide, methane, ethanol, caustic soda and propanediol have also been produced by MECs (12, 59-63). Because these chemicals are considerably more valuable than the energy supplied, chemical synthesis is a very promising application for MFCs.

## 1.5 Microorganisms in MFCs

Bacteria capable of extracellular electron transfer are known as exoelectrogens or electrochemically active bacteria (64). These microorganisms are able to oxidize organic matters and transfer the electrons outside the cell.

Bacteria have two types of extracellular electron transfer pathways as described previously. In mediated electron transfer, bacteria, such as *Pseudomonas aeruginosa* and *Shewanella oneidensis*, can shuttle the electrons from the cell to anode *via* redox mediators (65-67). Mediators, such as quinone, thionine, new methylene blue, methyl viologen and neutral red, are artificially added into MFC to enhance the electricity production in the early study of MFCs (28). During direct electron transfer, bacteria such as *Geobactersulfurreducens*, *Shewanellaputrefaciens*, and *Rhodoferax ferrireducens*, can transfer the electron to electrode *via* bacterial cell outer membrane cytochromes (23-24, 68). It has also been shown that some bacteria (*Geobacter*, *Shewanella*) can transfer electron directly to electrode via biological conducting pili, also known as nanowires (69). The nanowires typically extend from the transmembrane cytochromes for tens of micrometers with a diameter of 50-150 nm. So far, many exoelectrogens have been investigated in MFCs and Table 1.1 lists some of the bacteria that have been studied in MFCs.

Community analysis of biofilms in MFCs indicates that a variety of strains are present on the anode surface. Besides the electrochemically active bacteria,

other bacteria that cannot generate electricity themselves are also present on anode surface (70). Study demonstrates that pure strains exhibit much lower power density than mixed culture, and one possible explanation is that the electrochemically inactive bacteria produce mediators to facilitate the extracellular electron transfer for the exoelectrogens (66, 71). Therefore, mixed cultures are popularly used in MFCs for power generation.

It has been demonstrated that bacteria biofilms attached on anode surface play the role for electricity generation while bacteria suspended in the solution have not any contribution for power production in MFCs (68, 72-73). Therefore, reducing the suspended microorganisms and enhancing the biofilm formation on anode surface have great benefit for power generation in MFCs.

Table 1.1 Microbes applied in Microbial Fuel Cells.

| Microbes | Substrate | Applications |
|---|---|---|
| *Actinobacillus succinogenes* | Glucose | Neutral red or thionin as electron mediator (74-75) |
| *Aeromonas hydrophila* | Acetate | Mediator-less MFC (76) |
| *Alcaligenes faecalis, Enterococcus gallinarum, Pseudomonas aeruginosa* | Glucose | Self-mediate consortia isolated from MFC with a maximum power density of 4.31 $W/m^2$ (66) |
| *Clostridium beijerinckii* | Starch, glucose, lactate, molasses | Fermentative bacterium (77) |
| *Clostridium butyricum* | Starch, glucose, lactate, molasses | Fermentative bacterium (22, 77) |
| *Desulfovibrio desulfuricans* | Sucrose | Sulphate/sulphide as mediator (78-79) |
| *Erwinia dissolven* | Glucose | Ferric chelate complex as mediators (80) |
| *Escherichia coli* | Glucose | Mediators such as methylene blue |

| | | |
|---|---|---|
| | sucrose | needed (78, 81-82) |
| *Geobacter metallireducens* | Acetate | Mediator-less MFC (83) |
| *Geobacter sulfurreducens* | Acetate | Mediator-less MFC (68, 84) |
| *Gluconobacter oxydans* | Glucose | Mediator (HNQ, resazurin or thionine) needed (85) |
| *Klebsiella pneumoniae* | Glucose | HNQ as mediator biomineralized manganese as electron acceptor (86-87) |
| *Lactobacillus plantarum* | Glucose | Ferric chelate complex as mediators (80) |
| *Proteus mirabilis* | Glucose | Thionin as mediator (88-89) |
| *Pseudomonas aeruginosa* | Glucose | Pyocyanin and phenazine-1-carboxamide as mediator (66-67) |
| *Rhodoferax ferrireducens* | Glucose, xylose | Mediator-less MFC (24) |
| *Shewanella oneidensis* | Lactate | Anthraquinone-2,6-disulfonate (AQDS) as mediator (65) |
| *Shewanella putrefaciens* | Lactate, pyruvate, | Mediator-less MFC but incorporating an electron mediator like Mn (32, 90) |
| *Streptococcus lactis* | Glucose | Ferric chelate complex as mediators (80) |

### 1.6 Anodes in MFCs

Anode in MFCs, as both biofilm carrier and the electron acceptor, plays a key role in determining the power production of MFCs, because anode surface properties not only influence bacteria attachment and biofilm formation, but also affect the extracellular electron transfer between microorganisms and the electrode. Therefore, anode material is of great significance to the performance of MFCs. An ideal anode material for MFCs is supposed to have the following properties: (1) excellent biocompatibility; (2) high conductivity; (3) high specific surface area; (4) high electron transfer rate on the bacteria-anode interface; (5) strong chemical stability; and (6) relatively low cost (91).

### 1.6.1 Anode material classification

Two types of materials have been commonly used as anode materials in MFCs: carbon materials and metal materials.

Carbon materials are the most commonly employed anode materials for MFC anodes due to their excellent properties: excellent biocompatibility, strong chemical stability, large supply and cheap price. Based on their configuration, carbon materials can be classified into a plane structure and a packed structure. Plane structured carbon materials include carbon papers, graphite plates, carbon cloth and carbon meshes. Recently, carbon anodes in packed form have also been widely used in order to increase the surface area for bacteria adhesion and biofilm formation (92). Carbon anodes in packed form include graphite rod, granular graphite, graphite felt, carbon felt, and granular activated carbon. These materials are typically filled tightly in the anode chamber of MFCs to reach high interface area between bacteria and electrode. Carbon materials, however, demonstrate very low electrocatalytic activity for the anode microbial reactions and consequently the modification of carbon materials offers an promising approach to enhance the performance of MFCs (93).

Although the conductivity of metals is much higher than carbon materials, they are not as widely used as carbon materials for anode applications in MFCs. A majority of metals are excluded because they are chemically unstable or can be easily corroded by bacteria. Among those that meet the anode

material requirement, only stainless steels, titanium and gold have been used as anodes in MFCs (94-96). Richter et al. reported that a current of 0.5 mA was generated using a gold anode in MFCs, which was approximately the same as graphite anode (97). However, the prohibitive cost of gold severely limits its application in MFCs. For titanium and stainless steels, due to the poor biocompatibility, the power production was smaller than graphite anode (94-95).

### 1.6.2 Anode modification in MFCs

The surface properties, such as surface chemistry, specific surface area, surface charge, hydrophilicity and topography, have great impact on electricity generation in MFCs (98-99). Anode materials are modified to improve the biocompatibility, conductivity, specific surface area and the electron transfer rate on the bacteria-anode interface. So far, many anode modification methods have been reported to enhance the performance of MFCs.

#### 1.6.2.1 Surface coating

The first modification method is surface coating. For example, metals or metallic oxide have been coated on carbon materials for anode application in MFCs. Au and Pd nanoparticles were coated on graphite surface to enhance the conductivity of the anode, which greatly increased the current production in MFCs (100). $Fe_2O_3$ was deposited on graphite felt by thermal decomposition of $Fe(CO)_5$, which enhanced the biofilm formation and the

electron transfer from bacteria to electrode (101).

Conducting polymers have also been coated on carbon materials to enhance the power production of MFCs due to their high electrocatalytic activity, good conductivity and chemical stability (102-103). Polyaniline was modified on carbon cloth surface through electrochemical polymerization of aniline (102). The maximum power density of the MFCs with modified anode was 2.66 times higher than the control. Further, the modified anode reduced the internal resistance by 65.5%. Nanostructured polypyrrole was decorated on carbon fiber (103). Cyclic voltammetry and impedance spectroscopy indicated that the anode coated by polypyrrole presented smaller electron transfer resistance on the interface between bacteria and anode. As a result, the power density increased 4.5 times compared with the control group.

Carbon nanotubes (CNTs), due to their high specific surface area and excellent conductivity, have been coated on carbon cloth, carbon paper, sponge and textile to improve the power production in MFCs (104-107). Multi-wall CNTs were coated on carbon paper using a layer-by-layer assemble method, and this novel anode reduced the interfacial charge transfer resistance from 1163 Ω to 258 Ω while improved the power density by 20% in MFCs (104). The MFC with carbon cloth anode coated by CNTs was used for simultaneous electricity generation and wastewater treatment (106). Compared with bare carbon cloth anode, the maximum power density, COD removal efficiency and coulombic efficiency of the modified anode were greatly improved. Xie et al. decorated

the sponge and textile with CNTs to form three-dimensional anodes, which allowed the substrate transport and bacteria colonization deep inside the electrodes (105, 107). These anodes showed good biocompatibility, high conductivity, much larger bacteria-anode interface, and 10-fold-lower charge transfer resistance in MFCs.

Electron transfer mediators, such as quinone, thionin, methyl viologen and neutral red, can effectively facilitate extracellular electron transfer from bacteria to anode surface and consequently enhance the power production. In the earlier study of MFCs, mediators were routinely added into MFCs for power production. However, adding these mediators directly into the anolyte not only increases the operating cost, but also poses potential environmental problems. Therefore, coating of mediators onto the anode surface offers an effective approach to enhance the electricity production. For example, anthraquinone-1, 6-disulfonic acid (AQDS) (108-109) and 1,4-naphthoquinone (NQ) (108) were adsorbed on graphite anodes by immersing the anodes in AQDS and NQ solutions respectively, which successfully improved the power output of MFCs. However, the current density of MFCs decreased considerably over time because the mediators physically adsorbed on anode surface with weak interaction could easily be desorbed under normal experimental conditions.

### 1.6.2.2 Surface treatment

The functional groups, charge and area on anode surface have considerable influence on biofilm formation and extracellular electron transfer (98). Therefore, surface treatment of anode materials by physical or chemical method provides and efficient approach to improve the biofilm formation, extracellular electron transfer and ultimately the power production in MFCs (110).

Ammonia gas treatment of carbon cloth anode was firstly conducted by Cheng et al. (111). The treated anode (700 ℃for 1h) increased the power density by approximately 20% and reduced the start up time by 50%. After ammonia treatment, positive surface charge on anode increased from 0.38 meq/$m^2$ to 3.99 meq/$m^2$, which improved the biofilm formation due to the enhanced electrostatic attraction.

Heat treatment of anode materials is cost efficient and more environmentally friendly compared with ammonia treatment. Carbon fiber was heated and used as anode in MFCs; the treated anode improved the maximum power density by 15%, because the electrochemically active surface area was increased and more positive charge was generated (112).

Acid treatment is another strategy that has been used for carbon anode modification. The method increases the specific surface area and nitrogen-containing groups, which allows more microorganisms to adhere on the anode surface. Nitric acid treatment of graphite felt exhibited two-fold

growth in power density and acid treatment of activated carbon fiber felt improved the power density by 58% (113-114).

Electrochemical oxidation of graphite felts anode at a constant current density of 30 $mA/cm^2$ for 12 h generated 39.5% higher current than the untreated anode in MFCs (115). The authors attributed the electricity enhancement to the carboxyl containing functional groups generated during electrochemical oxidation, which could form strong hydrogen bonding with peptide bond in bacterial cytochromes.

Mediator coating brings the problem that the mediator can be easily desorbed due to the poor force between the mediator and the carbon materials. Covalently grafting of mediator on anode surface can effectively solve the problem. For example, neutral red was covalently grafted on graphite anode *via* amidation reaction, which reached a power density of 845 $mW/m^2$ in an MFC using a sewage sludge inoculums, while the control MFC only had a power density of 0.65 $mW/m^2$ (116). Though this method is effective, it consumes large quantity of organic solvents and acids. Therefore, more environmentally friendly methods to covalently immobilize mediators on anode surface are urgently required.

## 1.7 Cathode in MFCs

### 1.7.1 Electron acceptors in the cathode

In the early stage of MFC study, the major research was focused on the

extracellular electron transfer from bacteria to anode surface, while the cathode reaction was nearly ignored and only easily handled reduction of ferricyanide was applied (117).This cathode system, however, is unsustainable because ferricyanide replenishment is required during the electricity production process. Recently, more and more efforts have been made to investigate the cathode reaction, including the use of different electron acceptors and novel cathode materials design (118).

Besides ferricyanide, other electron acceptors such as $O_2$, $MnO_4^-$, $NO_3^-$, $ClO_4^-$, $Cu^{2+}$, $Cr_2O_7^{2-}$ and $VO_2^+$ have also been studied in MFCs (118). Among all of these electron acceptors, oxygen is the best choice due to the very positive redox potential, the harmlessness of the reduction product (water), the virtually inexhaustible availability and the low cost. As a result, oxygen is now the dominant electron acceptor in MFCs. In fact, it has been acknowledged that oxygen reduction reaction (ORR) is the only cathode reaction practically feasible for electricity generation in MFCs.

### 1.7.2 Electrochemical loss in the cathode

Currently, ORR rate is a bottleneck for power generation in MFCs because of the unfavorable reaction condition: ambient temperature, almost neutral pH and small concentration of supporting electrolytes (119). Calculated from the Nernst potential equation, the theoretical cathode potential of ORR to form water is 0.805 V (vs. NHE) at pH 7 and under a partial oxygen pressure of 0.2

bar in MFCs (91). In practice, however, the cathode potential is typically 0.2 V (vs. NHE) under this condition, which indicates that an electrochemical loss (overpotential) of about 0.605 V is lost in the cathode (91). This large electrochemical loss, which dramatically decreases the voltage output, means that much smaller amount of energy is produced than thermodynamically available. Therefore, reducing the electrochemical loss is an effective approach to enhance the voltage production in MFCs. Electrochemical loss relevant to cathode includes electrode kinetic loss, side reaction loss and thermodynamic loss (117).

The electrochemical catalytic reaction rate is typically limited by the slow electrode kinetic. For ORR, the kinetic may be constrained by the slow electron transfer step, the oxygen adsorption step and the product desorption step (117). The kinetic can be measured by the maximum current density in a rotating electrode under which the reaction is not limited by the mass-transfer. Larger interfacial surface area of the electrode, higher temperature and higher oxygen pressure can enhance the electrode kinetic (120-121). However, the use of high-performance catalyst is the most effective method to decrease the kinetic loss (119).

Side reaction loss is caused by reactant crossover and competing reactions (117). The crossover of substrate from anode chamber to cathode chamber can result in direct oxidation of the substrate on cathode surface, which provides electrons for ORR and forms the internal current in cathode. This can lower

the cathode potential as a mixed potential lying between the redox potential of the oxygen and the substrate is formed. The other side reaction loss is due to competing reactions. For ORR, it can proceed either *via* a four-electron pathway to form water or *via* a two-electron pathway to produce hydrogen peroxide. The theoretical potential of the four-electron reaction of ORR is 1.229 V (vs. RHE) under standard condition, while the value is only 0.695 V (vs. RHE) for the two-electron reaction to form hydrogen peroxide (119). Therefore, the four-electron reaction is the target in MFCs for power production. However, the undesirable two-electron reaction competes with the target four-electron reaction, which also causes the formation of a mixed theoretical potential lying between 0.695 V (vs. RHE) and 1.229 V (vs. RHE) (117). The formation of mixed potentials can dramatically reduce the cathode potential and accordingly the cell voltage. Further, the generation of $H_2O_2$ causes damages to electrode material, membrane and even electrochemically active microorganisms, which limits the overall performance of MFCs (122). As such, cathode catalyst with high selectivity for the four-electron reaction can efficiently solve this problem.

When biological catalysts (enzyme or microbial cell) are used in the cathode, a thermodynamic loss may be observed due to the occurrence of redox cascades between the biocatalyst and the cathode (117). The bacteria or enzyme on cathode surface get reduced and then deliver the electron to the final electron acceptor (oxygen). The redox potential of the biocatalyst active site, such as

cytochrome oxidase and bilirubin oxidase, is lower than the redox potential of ORR. Further, the use of redox mediators to shuttle the electron from the biocatalyst to cathode also decrease the cathode potential, as the redox potential of mediators is lower than the redox potential of ORR.

### 1.7.3 Cathode materials in MFCs

Cathode material design is the greatest challenge for the scale up of MFCs for practical applications. As described above, cathode materials have considerable impact on voltage output in MFCs. The electrochemical loss for ORR at bare carbon cathode can be very large, which results in an extremely low current density (119). The application of platinum as a catalyst coated on carbon cathode can improve the maximum current density by 2-3 times (123). This noble catalyst, however, accounts for almost half of the total construction cost of the MFC reactor, which hampers the scale up of MFC technology for practical applications (25). As a result, the exploration of low-cost and high-performance cathode catalyst becomes a major focus in MFC research. Some of the catalysts that have been used in MFCs are reviewed below.

Platinum is the most commonly used cathode catalyst in MFCs due to its high catalytic activity and high selectivity for the four-electron reaction towards ORR. However, the prohibitive cost and reserve shortage of platinum severely limit its application. In order to reduce the cost, researchers reduced the cathode loading of platinum from 0.5 $mg_{pt}/cm^2$ to 0.1 $mg_{pt}/cm^2$ and the

maximum power density was only reduced by 19% (124). However, there are some disadvantages for platinum catalyst in MFCs. First, platinum is vulnerable to poisoning by dissolved hydrogen sulfide in wastewater, which dramatically lowers its catalytic activity. Besides, the crossover of substrate can be easily oxidized on platinum surface. As a result, internal current and mixed potential are formed, which inevitably decrease the cell voltage.

Non-precious metal catalysts have been developed as alternatives to platinum to reduce the construction cost of MFCs. Iron phthalocyanine (FePc) was used as cathode catalyst in MFCs by some researchers (119, 124-125). FePc presented a high open circuit potential (540 mV) and internal current due to substrate crossover was negligible (119, 126). However, hydrogen peroxide was formed *via* the two-electron pathway of the ORR on the surface of this catalyst. These competing reactions caused cathode overpotential due to the formation of a mixed potential as described previously. As hydrogen peroxide is an aggressive agent which corrodes the catalysts, the long time stability is also a problem for this material.

Manganese dioxide was studied as cathode in MFCs. The maximum power density with manganese dioxide reached 172 $mW/cm^3$, while maximum power density in the MFCs with the benchmark platinum was 268 $mW/cm^3$ (127). In another study, manganese dioxide was uniformly dispersed on carbon nanotubes by a hydrothermal method to enhance the specific surface area (128). The maximum power density of this composite was 210 $mW/m^2$, only

slightly smaller than the platinum based cathode (229 $mW/m^2$). Lead dioxide was also applied as cathode catalyst for power production in MFCs (129). However, the lead released could cause serious environmental pollution. Therefore, it cannot be widely used for large scale applications of MFCs.

Besides chemical catalysts, bacteria catalysts on cathode termed as biocathode have also been used to facilitate oxygen reduction. Bacteria catalysts have the benefits of low cost, self-regeneration and high catalytic activity. A seawater biofim on a stainless steel cathode increased the power by a factor of 30 compared with the cathode without biofim in the study (130). In another biocathode MFC, nitrate was completely reduced to nitrogen gas in the cathode chamber, which achieved a cell voltage of 0.214 V, a current density of 35 $A/m^3$ and a maximum power density of 4 $W/m^3$ (131).

Enzyme has also been investigated to catalyze ORR in the cathode of MFCs. For example, a laccase from *Trametes versicolor* was used as the cathode catalyst for ORR in MFC (132). This MFC showed an open circuit voltage of 1.1 V, one of the highest in MFCs studies. The high specificity of this enzyme towards the four-electron reaction of oxygen reduction greatly reduced the overpotential caused by crossover reaction and competing reaction. As a result, the electrochemical loss was greatly decreased and ultimately the cell voltage output was enhanced. However, the long time stability of enzyme was the greatest weakness because enzyme could be easily deactivated in MFCs (117).

## 1.8 Knowledge gaps

Anode material plays a significant role in determining the power generation in MFCs, because it not only influences the biofim formation on electrode surface, but also affects the extracellular electron transfer between microorganisms and the electrode (20). As mentioned previously, an ideal anode material for MFCs is supposed to have the following properties: (1) excellent biocompatibility; (2) high conductivity; (3) high specific surface area; (4) high electron transfer rate on the bacteria-anode interface; (5) strong chemical stability; and (6) relatively low cost (91). However, the lack of such materials severely limits the practical application of MFCs. As such, development of novel anodes that meet the above properties will be an effective approach to enhance power density in MFCs.

Although platinum can significantly reduce the electrochemical loss for ORR in the cathode and consequently improve the power production of MFCs (123). This noble catalyst, however, is prohibitive and hampers the scale up of MFC technology for practical applications (25). The lack of cathode which is cheap and possesses high catalytic activity towards ORR in MFCs severely restricts the performance of MFCs, especially the large-scale application of MFCs. Therefore, development of high-performance and low-cost cathode is of great significance for applications of MFCs.

## 1.9 Research objective and thesis organization

The main objectives of this research are to enhance power generation and reduce the construction cost of MFCs to improve the applications of this

technology.

This thesis is constructed into seven chapters. Chapter 1 provides a general introduction, research objective and organization of the thesis. A literature review on MFCs is also presented in this chapter.

Chapter 2 reports a facile and scalable method to synthesize conductive polypyrrole hydrogels/carbon nanotubes (CPHs/CNTs) using phytic acid as gelator and dopant. The high electrocatalytic activity and excellent biocompatibility of this composite anode facilitates the direct electron transfer from bacteria to anode and consequently increased the power density of MFCs.

In chapter 3, anthraquinone-2-sulfonic acid (AQS), an electron transfer mediator, is covalently grafted onto graphite felt surface *via* spontaneous reduction of the *in situ* generated AQS diazonium cations. This AQS grafted on anode surface works as an electron transfer mediator to facilitate the mediated electron transfer from bacteria to anode, which remarkably enhanced the power production in MFCs.

In chapter 4, non-precious metal catalysts for oxygen reduction reaction comprising carbon, nitrogen and iron are prepared by a high-temperature synthesis method. These catalysts show very positive onset potentials and less than 3% yield of hydrogen peroxide in the whole potential range, which matches the state-of-the-art Pt/C. These low-cost and high-performance cathode catalysts significantly enhance the maximum power density in MFCs.

Chapter 5 investigates electrolyte with bicarbonate as an alternative of phosphate buffer in MFCs. Bicarbonate buffer effectively reduces microorganisms suspended in the solution, which allows more substrate to be

consumed by bacteria formed on anode surface for electricity production. As a result, it considerably enhances the coulombic efficiency (CE) of MFCs.

Chapter 6 studies sustainable energy recovery from wastewater by MFCs. The energy recovery efficiency reaches 18.4% and the energy density achieves at 0.89 kWh/kg COD, which demonstrates that MFC has the potential to be a self-sufficient technology for wastewater treatment.

Chapter 7 gives an overall conclusion of this work and an outlook of MFCs.

## 1.9 References


1. International Energy Agency. (2012) Key World Energy Statistics, *International Energy Agency, Paris*.
2. Logan, B. E., and Rabaey, K. (2012) Conversion of Wastes into Bioelectricity and Chemicals by Using Microbial Electrochemical Technologies, *Science 337*, 686-690.
3. Huggins, T., Fallgren, P., Jin, S., and Ren, Z. (2013) Energy and Performance Comparison of Microbial Fuel Cell and Conventional Aeration Treating of Wastewater, *J Microb Biochem Technol S 6*, 2.
4. Rabaey, K., and Verstraete, W. (2005) Microbial fuel cells: novel biotechnology for energy generation, *Trends in Biotechnology 23*, 291-298.
5. Zeeman, G., Kujawa, K., de Mes, T., Hernandez, L., de Graaff, M., Abu-Ghunmi, L., Mels, A., Meulman, B., Temmink, H., Buisman, C., van Lier, J., and Lettinga, G. (2008) Anaerobic treatment as a core technology for energy, nutrients and water recovery from source-separated domestic waste(water), *Water Science and Technology 57*, 1207-1212.
6. Xie, X., Ye, M., Hsu, P. C., Liu, N., Criddle, C. S., and Cui, Y. (2013) Microbial battery for efficient energy recovery, *Proceedings of the*

*National Academy of Sciences of the United States of America 110*, 15925-15930.

7. Rabaey, K., Lissens, G., Siciliano, S. D., and Verstraete, W. (2003) A microbial fuel cell capable of converting glucose to electricity at high rate and efficiency, *Biotechnology Letters 25*, 1531-1535.
8. Liu, H., Ramnarayanan, R., and Logan, B. E. (2004) Production of electricity during wastewater treatment using a single chamber microbial fuel cell, *Environmental Science & Technology 38*, 2281-2285.
9. Tender, L. M., Reimers, C. E., Stecher, H. A., Holmes, D. E., Bond, D. R., Lowy, D. A., Pilobello, K., Fertig, S. J., and Lovley, D. R. (2002) Harnessing microbially generated power on the seafloor, *Nature Biotechnology 20*, 821-825.
10. Huang, Y. L., He, Z., Kan, J. J., Manohar, A. K., Nealson, K. H., and Mansfeld, F. (2012) Electricity generation from a floating microbial fuel cell, *Bioresource Technology 114*, 308-313.
11. Oh, S. E., and Logan, B. E. (2005) Hydrogen and electricity production from a food processing wastewater using fermentation and microbial fuel cell technologies, *Water Research 39*, 4673-4682.
12. Fu, L., You, S. J., Yang, F. L., Gao, M. M., Fang, X. H., and Zhang, G. Q. (2010) Synthesis of hydrogen peroxide in microbial fuel cell, *Journal of Chemical Technology and Biotechnology 85*, 715-719.
13. Inglesby, A. E., and Fisher, A. C. (2012) Enhanced methane yields from anaerobic digestion of Arthrospira maxima biomass in an advanced flow-through reactor with an integrated recirculation loop microbial fuel cell, *Energy & Environmental Science 5*, 7996-8006.
14. Lindblad, P., Lindberg, P., Oliveira, P., Stensjo, K., and Heidorn, T. (2012) Design, Engineering, and Construction of Photosynthetic Microbial Cell Factories for Renewable Solar Fuel Production, *Ambio*

*41*, 163-168.

15. Kim, M., Park, H. S., Jin, G. J., Cho, W. H., Lee, D. K., Hyun, M. S., Choi, C. H., and Kim, H. J. (2006) A novel combined biomonitoring system for BOD measurement and toxicity detection using microbial fuel cells, *2006 Ieee Sensors, Vols 1-3*, 1251-1252.
16. Cao, X. X., Huang, X., Liang, P., Xiao, K., Zhou, Y. J., Zhang, X. Y., and Logan, B. E. (2009) A New Method for Water Desalination Using Microbial Desalination Cells, *Environmental Science & Technology 43*, 7148-7152.
17. Kim, B. H., Chang, I. S., and Gadd, G. M. (2007) Challenges in microbial fuel cell development and operation, *Applied Microbiology and Biotechnology 76*, 485-494.
18. Logan, B. E. (2010) Scaling up microbial fuel cells and other bioelectrochemical systems, *Applied Microbiology and Biotechnology 85*, 1665-1671.
19. Balat, M. (2010) Microbial Fuel Cells as an Alternative Energy Option, *Energy Sources Part a-Recovery Utilization and Environmental Effects 32*, 26-35.
20. Tang, X., Li, H., Du, Z., Wang, W., and Ng, H. Y. (2015) Conductive polypyrrole hydrogels and carbon nanotubes composite as an anode for microbial fuel cells, *Rsc Advances 5*, 50968-50974.
21. Tang, X. H., Li, H. R., Wang, W. D., Du, Z. W., and Ng, H. Y. (2014) A high-performance electrocatalytic air cathode derived from aniline and iron for use in microbial fuel cells, *Rsc Advances 4*, 12789-12794.
22. Park, H. S., Kim, B. H., Kim, H. S., Kim, H. J., Kim, G. T., Kim, M., Chang, I. S., Park, Y. K., and Chang, H. I. (2001) A novel electrochemically active and Fe(III)-reducing bacterium phylogenetically related to Clostridium butyricum isolated from a microbial fuel cell, *Anaerobe 7*, 297-306.

23. Kim, H. J., Park, H. S., Hyun, M. S., Chang, I. S., Kim, M., and Kim, B. H. (2002) A mediator-less microbial fuel cell using a metal reducing bacterium, Shewanella putrefaciense, *Enzyme and Microbial Technology 30*, 145-152.

24. Chaudhuri, S. K., and Lovley, D. R. (2003) Electricity generation by direct oxidation of glucose in mediatorless microbial fuel cells, *Nature Biotechnology 21*, 1229-1232.

25. Rozendal, R. A., Hamelers, H. V. M., Rabaey, K., Keller, J., and Buisman, C. J. N. (2008) Towards practical implementation of bioelectrochemical wastewater treatment, *Trends in Biotechnology 26*, 450-459.

26. Potter, M. C. (1911) Electrical effects accompanying the decomposition of organic compounds, *Proceedings of the Royal Society of London Series B-Containing Papers of a Biological Character 84*, 260-276.

27. Lovley, D. R., and Phillips, E. J. P. (1988) Novel Mode of Microbial Energy-Metabolism - Organic-Carbon Oxidation Coupled to Dissimilatory Reduction of Iron or Manganese, *Applied and Environmental Microbiology 54*, 1472-1480.

28. Schroder, U. (2007) Anodic electron transfer mechanisms in microbial fuel cells and their energy efficiency, *Physical Chemistry Chemical Physics 9*, 2619-2629.

29. Rabaey, K., Boon, N., Denet, V., Verhaege, M., Hofte, M., and Verstraete, W. (2004) Bacteria produce and use redox mediators for electron transfer in microbial fuel cells., *Abstracts of Papers of the American Chemical Society 228*, U622-U622.

30. Tanaka, K., and Tamamushi, R. (1987) Effect of Hydrophobic Layers on the Electrochemical Electron-Transfer Reaction of Some Mediators in Microbial Fuel-Cells, *Journal of Electroanalytical Chemistry 236*,

305-307.

31. Du, Z. W., Li, H. R., and Gu, T. Y. (2007) A state of the art review on microbial fuel cells: A promising technology for wastewater treatment and bioenergy, *Biotechnology Advances 25*, 464-482.

32. Kim, H. J., Hyun, M. S., Chang, I. S., and Kim, B. H. (1999) A microbial fuel cell type lactate biosensor using a metal-reducing bacterium, Shewanella putrefaciens, *Journal of Microbiology and Biotechnology 9*, 365-367.

33. Chang, I. S., Moon, H., Jang, J. K., and Kim, B. H. (2005) Improvement of a microbial fuel cell performance as a BOD sensor using respiratory inhibitors, *Biosensors & Bioelectronics 20*, 1856-1859.

34. Rozendal, R. A., Leone, E., Keller, J., and Rabaey, K. (2009) Efficient hydrogen peroxide generation from organic matter in a bioelectrochemical system, *Electrochemistry Communications 11*, 1752-1755.

35. Gregory, K. B., and Lovley, D. R. (2005) Remediation and recovery of uranium from contaminated subsurface environments with electrodes, *Environmental Science & Technology 39*, 8943-8947.

36. Zhang, F., Ge, Z., Grimaud, J., Hurst, J., and He, Z. (2013) Long-Term Performance of Liter-Scale Microbial Fuel Cells Treating Primary Effluent Installed in a Municipal Wastewater Treatment Facility, *Environmental Science & Technology 47*, 4941-4948.

37. Rosenbaum, M., Schroder, U., and Scholz, F. (2006) Investigation of the electrocatalytic oxidation of formate and ethanol at platinum black under microbial fuel cell conditions, *Journal of Solid State Electrochemistry 10*, 872-878.

38. Shantaram, A., Beyenal, H., Raajan, R., Veluchamy, A., and Lewandowski, Z. (2005) Wireless sensors powered by microbial fuel

cells, *Environmental Science & Technology 39*, 5037-5042.

39. Tender, L. M., Gray, S. A., Groveman, E., Lowy, D. A., Kauffman, P., Melhado, J., Tyce, R. C., Flynn, D., Petrecca, R., and Dobarro, J. (2008) The first demonstration of a microbial fuel cell as a viable power supply: Powering a meteorological buoy, *Journal of Power Sources 179*, 571-575.

40. Pant, D., Van Bogaert, G., Diels, L., and Vanbroekhoven, K. (2010) A review of the substrates used in microbial fuel cells (MFCs) for sustainable energy production, *Bioresource Technology 101*, 1533-1543.

41. Puig, S., Serra, M., Coma, M., Balaguer, M. D., and Colprim, J. (2011) Simultaneous domestic wastewater treatment and renewable energy production using microbial fuel cells (MFCs), *Water Science and Technology 64*, 904-909.

42. Ghasemi, M., Daud, W. R. W., Ismail, A. F., Jafari, Y., Ismail, M., Mayahi, A., and Othman, J. (2013) Simultaneous wastewater treatment and electricity generation by microbial fuel cell: Performance comparison and cost investigation of using Nafion 117 and SPEEK as separators, *Desalination 325*, 1-6.

43. Lee, D. J., Lee, C. Y., and Chang, J. S. (2012) Treatment and electricity harvesting from sulfate/sulfide-containing wastewaters using microbial fuel cell with enriched sulfate-reducing mixed culture, *Journal of Hazardous Materials 243*, 67-72.

44. Virdis, B., Rabaey, K., Rozendal, R. A., Yuan, Z. G., and Keller, J. (2010) Simultaneous nitrification, denitrification and carbon removal in microbial fuel cells, *Water Research 44*, 2970-2980.

45. Fang, C., Min, B., and Angelidaki, I. (2011) Nitrate as an Oxidant in the Cathode Chamber of a Microbial Fuel Cell for Both Power Generation and Nutrient Removal Purposes, *Applied Biochemistry and*

*Biotechnology 164*, 464-474.

46. Ter Heijne, A., Liu, F., van der Weijden, R., Weijma, J., Buisman, C. J. N., and Hamelers, H. V. M. (2010) Copper Recovery Combined with Electricity Production in a Microbial Fuel Cell, *Environmental Science & Technology 44*, 4376-4381.
47. Wang, Z., Lim, B., and Choi, C. (2011) Removal of Hg2+ as an electron acceptor coupled with power generation using a microbial fuel cell, *Bioresource Technology 102*, 6304-6307.
48. Karube, I., Matsunga, T., Mitsuda, S., Suzuki, S. (1977) Microbial electrode BOD sensors, *Biotechnology & Bioengineering 19*, 1535–1547.
49. Kim, B. H., Chang, I. S., Gil, G. C., Park, H. S., and Kim, H. J. (2003) Novel BOD (biological oxygen demand) sensor using mediator-less microbial fuel cell, *Biotechnology Letters 25*, 541-545.
50. Kang, K. H., Jang, J. K., Pham, T. H., Moon, H., Chang, I. S., and Kim, B. H. (2003) A microbial fuel cell with improved cathode reaction as a low biochemical oxygen demand sensor, *Biotechnology Letters 25*, 1357-1361.
51. Chang, I. S., Jang, J. K., Gil, G. C., Kim, M., Kim, H. J., Cho, B. W., and Kim, B. H. (2004) Continuous determination of biochemical oxygen demand using microbial fuel cell type biosensor, *Biosensors & Bioelectronics 19*, 607-613.
52. Moon, H., Chang, I. S., Kang, K. H., Jang, J. K., and Kim, B. H. (2004) Improving the dynamic response of a mediator-less microbial fuel cell as a biochemical oxygen demand (BOD) sensor, *Biotechnology Letters 26*, 1717-1721.
53. Davila, D., Esquivel, J. P., Sabate, N., and Mas, J. (2011) Silicon-based microfabricated microbial fuel cell toxicity sensor, *Biosensors & Bioelectronics 26*, 2426-2430.

54. Stein, N. E., Keesman, K. J., Hamelers, H. V. M., and van Straten, G. (2011) Kinetic models for detection of toxicity in a microbial fuel cell based biosensor, *Biosensors & Bioelectronics 26*, 3115-3120.

55. Kim, M., Hyun, M. S., Gadd, G. M., and Kim, H. J. (2007) A novel biomonitoring system using microbial fuel cells, *Journal of Environmental Monitoring 9*, 1323-1328.

56. Liu, H., Grot, S., and Logan, B. E. (2005) Electrochemically assisted microbial production of hydrogen from acetate, *Environmental Science & Technology 39*, 4317-4320.

57. Sun, M., Sheng, G. P., Mu, Z. X., Liu, X. W., Chen, Y. Z., Wang, H. L., and Yu, H. Q. (2009) Manipulating the hydrogen production from acetate in a microbial electrolysis cell-microbial fuel cell-coupled system, *Journal of Power Sources 191*, 338-343.

58. Logan, B. E., Liu, H., Heilmann, J., Oh, S. E., Cheng, S., and Grot, S. (2005) Electricity and hydrogen production using different types of microbial fuel cell technologies, *Abstracts of Papers of the American Chemical Society 230*, U1680-U1680.

59. Booth, B. (2005) Hydrogen from a microbial fuel cell, *Environmental Science & Technology 39*, 235a-235a.

60. Sasaki, K., Sasaki, D., Morita, M., Hirano, S., Matsumoto, N., Ohmura, N., and Igarashi, Y. (2010) Bioelectrochemical system stabilizes methane fermentation from garbage slurry, *Bioresource Technology 101*, 3415-3422.

61. Rabaey, K., Butzer, S., Brown, S., Keller, J., and Rozendal, R. A. (2010) High Current Generation Coupled to Caustic Production Using a Lamellar Bioelectrochemical System, *Environmental Science & Technology 44*, 4315-4321.

62. Steinbusch, K. J. J., Hamelers, H. V. M., Schaap, J. D., Kampman, C., and Buisman, C. J. N. (2010) Bioelectrochemical Ethanol Production

through Mediated Acetate Reduction by Mixed Cultures, *Environmental Science & Technology 44*, 513-517.

63. Rabaey, K., Wise, A., Johnstone, A. J., Virdis, B., Freguia, S., and Rozendal, R. A. (2011) Bioelectrochemical conversion of glycerol to 1,3-propanediol, *Abstracts of Papers of the American Chemical Society 241*.

64. Logan, B. E. (2009) Exoelectrogenic bacteria that power microbial fuel cells, *Nature Reviews Microbiology 7*, 375-381.

65. Ringeisen, B. R., Henderson, E., Wu, P. K., Pietron, J., Ray, R., Little, B., Biffinger, J. C., and Jones-Meehan, J. M. (2006) High Power Density from a Miniature Microbial Fuel Cell Using Shewanella oneidensis DSP10, *Environmental Science & Technology 40*, 2629-2634.

66. Rabaey, K., Boon, N., Siciliano, S. D., Verhaege, M., and Verstraete, W. (2004) Biofuel cells select for microbial consortia that self-mediate electron transfer, *Applied and Environmental Microbiology 70*, 5373-5382.

67. Rabaey, K., Boon, N., Hofte, M., and Verstraete, W. (2005) Microbial phenazine production enhances electron transfer in biofuel cells, *Environmental Science & Technology 39*, 3401-3408.

68. Bond, D. R., and Lovley, D. R. (2003) Electricity production by Geobacter sulfurreducens attached to electrodes, *Applied and Environmental Microbiology 69*, 1548-1555.

69. Gorby, Y. A., Yanina, S. V., Moyles, D., McLean, J. S., Rosso, K. M., Beveridge, T. J., Kennedy, D. W., Marshall, M. J., Dohnalkova, A., Beliaev, A., Fredrickson, J. K., and Nealson, K. (2006) NUCL 74-Bacterial nanowires: Electrically conductive, redox-reactive appendages produced by dissimilatory metal reducing bacteria, *Abstracts of Papers of the American Chemical Society 232*.

70. Logan, B. E., and Regan, J. M. (2006) Electricity-producing bacterial communities in microbial fuel cells, *Trends in Microbiology 14*, 512-518.

71. Zuo, Y., Xing, D. F., Regan, J. M., and Logan, B. E. (2008) Isolation of the exoelectrogenic bacterium Ochrobactrum anthropi YZ-1 by using a U-tube microbial fuel cell, *Applied and Environmental Microbiology 74*, 3130-3137.

72. Biffinger, J. C., Pietron, J., Ray, R., Little, B., and Ringeisen, B. R. (2007) A biofilm enhanced miniature microbial fuel cell using Shewanella oneidensis DSP10 and oxygen reduction cathodes, *Biosensors & Bioelectronics 22*, 1672-1679.

73. Reguera, G., Nevin, K. P., Nicoll, J. S., Covalla, S. F., Woodard, T. L., and Lovley, D. R. (2006) Biofilm and nanowire production leads to increased current in Geobacter sulfurreducens fuel cells, *Applied and Environmental Microbiology 72*, 7345-7348.

74. Park, D. H., Laivenieks, M., Guettler, M. V., Jain, M. K., and Zeikus, J. G. (1999) Microbial utilization of electrically reduced neutral red as the sole electron donor for growth and metabolite production, *Applied and Environmental Microbiology 65*, 2912-2917.

75. Park, D. H., and Zeikus, J. G. (2000) Electricity generation in microbial fuel cells using neutral red as an electronophore, *Applied and Environmental Microbiology 66*, 1292-1297.

76. Pham, C. A., Jung, S. J., Phung, N. T., Lee, J., Chang, I. S., Kim, B. H., Yi, H., and Chun, J. (2003) A novel electrochemically active and Fe(III)-reducing bacterium phylogenetically related to Aeromonas hydrophila, isolated from a microbial fuel cell, *FEMS Microbiology Letters 223*, 129-134.

77. Niessen, J., Schroder, U., and Scholz, F. (2004) Exploiting complex carbohydrates for microbial electricity generation - a bacterial fuel cell

operating on starch, *Electrochemistry Communications 6*, 955-958.

78. Ieropoulos, I. A., Greenman, J., Melhuish, C., and Hart, J. (2005) Comparative study of three types of microbial fuel cell, *Enzyme and Microbial Technology 37*, 238-245.

79. Park, D. H., Kim, B. H., Moore, B., Hill, H. A. O., Song, M. K., and Rhee, H. W. (1997) Electrode reaction of Desulfovibrio desulfuricans modified with organic conductive compounds, *Biotechnology Techniques 11*, 145-148.

80. Vega, C. A., and Fernandez, I. (1987) Mediating Effect of Ferric Chelate Compounds in Microbial Fuel-Cells with Lactobacillus-Plantarum, Streptococcus-Lactis, and Erwinia Dissolvens, *Bioelectrochemistry and Bioenergetics 17*, 217-222.

81. Schroder, U., Niessen, J., and Scholz, F. (2003) A generation of microbial fuel cells with current outputs boosted by more than one order of magnitude, *Angewandte Chemie-International Edition 42*, 2880-2883.

82. Grzebyk, M., and Pozniak, G. (2005) Microbial fuel cells (MFCs) with interpolymer cation exchange membranes, *Separation and Purification Technology 41*, 321-328.

83. Min, B. K., Cheng, S. A., and Logan, B. E. (2005) Electricity generation using membrane and salt bridge microbial fuel cells, *Water Research 39*, 1675-1686.

84. Bond, D. R., Holmes, D. E., Tender, L. M., and Lovley, D. R. (2002) Electrode-reducing microorganisms that harvest energy from marine sediments, *Science 295*, 483-485.

85. Lee, S. A., Choi, Y., Jung, S. H., and Kim, S. (2002) Effect of initial carbon sources on the electrochemical detection of glucose by Gluconobacter oxydans, *Bioelectrochemistry 57*, 173-178.

86. Rhoads, A., Beyenal, H., and Lewandowski, Z. (2005) Microbial fuel

cell using anaerobic respiration as an anodic reaction and biomineralized manganese as a cathodic reactant, *Environmental Science & Technology 39*, 4666-4671.

87. Menicucci, J., Beyenal, H., Marsili, E., Veluchamy, R. A., Demir, G., and Lewandowski, Z. (2006) Procedure for determining maximum sustainable power generated by microbial fuel cells, *Environmental Science & Technology 40*, 1062-1068.

88. Choi, M.-J., Chae, K.-J., Ajayi, F. F., Kim, K.-Y., Yu, H.-W., Kim, C.-w., and Kim, I. S. (2011) Effects of biofouling on ion transport through cation exchange membranes and microbial fuel cell performance, *Bioresource Technology 102*, 298-303.

89. Thurston, C. F., Bennetto, H. P., Delaney, G. M., Mason, J. R., Roller, S. D., and Stirling, J. L. (1985) Glucose-Metabolism in a Microbial Fuel-Cell - Stoichiometry of Product Formation in a Thionine-Mediated Proteus-Vulgaris Fuel-Cell and Its Relation to Coulombic Yields, *Journal of General Microbiology 131*, 1393-1401.

90. Kim, B. H., Kim, H. J., Hyun, M. S., and Park, D. H. (1999) Direct electrode reaction of Fe(III)-reducing bacterium, Shewanella putrefaciens, *Journal of Microbiology and Biotechnology 9*, 127-131.

91. Logan, B. E., Hamelers, B., Rozendal, R. A., Schrorder, U., Keller, J., Freguia, S., Aelterman, P., Verstraete, W., and Rabaey, K. (2006) Microbial fuel cells: Methodology and technology, *Environmental Science & Technology 40*, 5181-5192.

92. Li, F. X., Sharma, Y., Lei, Y., Li, B. K., and Zhou, Q. X. (2010) Microbial Fuel Cells: The Effects of Configurations, Electrolyte Solutions, and Electrode Materials on Power Generation, *Applied Biochemistry and Biotechnology 160*, 168-181.

93. Qiao, Y., Li, C. M., Bao, S. J., and Bao, Q. L. (2007) Carbon nanotube/polyaniline composite as anode material for microbial fuel

cells, *Journal of Power Sources 170*, 79-84.

94. ter Heijne, A., Hamelers, H. V. M., Saakes, M., and Buisman, C. J. N. (2008) Performance of non-porous graphite and titanium-based anodes in microbial fuel cells, *Electrochimica Acta 53*, 5697-5703.

95. Dumas, C., Mollica, A., Feron, D., Basseguy, R., Etcheverry, L., and Bergel, A. (2007) Marine microbial fuel cell: Use of stainless steel electrodes as anode and cathode materials, *Electrochimica Acta 53*, 468-473.

96. Sun, M., Zhang, F., Tong, Z. H., Sheng, G. P., Chen, Y. Z., Zhao, Y., Chen, Y. P., Zhou, S. Y., Liu, G., Tian, Y. C., and Yu, H. Q. (2010) A gold-sputtered carbon paper as an anode for improved electricity generation from a microbial fuel cell inoculated with Shewanella oneidensis MR-1, *Biosensors & Bioelectronics 26*, 338-343.

97. Richter, H., Mccarthy, K., Nevin, K. P., Johnson, J. P., Rotello, V. M., and Lovley, D. R. (2008) Electricity Generation by Geobacter sulfurreducens Attached to Gold Electrodes, *Langmuir the Acs Journal of Surfaces & Colloids*.

98. Guo, K., Freguia, S., Dennis, P. G., Chen, X., Donose, B. C., Keller, J., Gooding, J. J., and Rabaey, K. (2013) The effects of surface charge and hydrophobicity on anodic biofilm formation, community composition and current generation in bioelectrochemical systems, *Environmental Science & Technology 47*, 7563-7570.

99. Kumar, G. G., Sarathi, V. G. S., and Nahm, K. S. (2013) Recent advances and challenges in the anode architecture and their modifications for the applications of microbial fuel cells, *Biosensors & Bioelectronics 43*, 461-475.

100. Fan, Y., Xu, S., Schaller, R., Jiao, J., Chaplen, F., and Liu, H. (2011) Nanoparticle decorated anodes for enhanced current generation in microbial electrochemical cells, *Biosensors and Bioelectronics 26*,

1908-1912.

101. Wang, P., Li, H. R., and Du, Z. W. (2013) Deposition of Iron on Graphite Felts by Thermal Decomposition of Fe(CO)(5) for Anodic Modification of Microbial Fuel Cells, *International Journal of Electrochemical Science 8*, 4712-4722.

102. Lai, B., Tang, X. H., Li, H. R., Du, Z. W., Liu, X. W., and Zhang, Q. (2011) Power production enhancement with a polyaniline modified anode in microbial fuel cells, *Biosensors & Bioelectronics 28*, 373-377.

103. Zou, Y. J., Pisciotta, J., and Baskakov, I. V. (2010) Nanostructured polypyrrole-coated anode for sun-powered microbial fuel cells, *Bioelectrochemistry 79*, 50-56.

104. Sun, J. J., Zhao, H. Z., Yang, Q. Z., Song, J., and Xue, A. (2010) A novel layer-by-layer self-assembled carbon nanotube-based anode: Preparation, characterization, and application in microbial fuel cell, *Electrochimica Acta 55*, 3041-3047.

105. Xie, X., Ye, M., Hu, L. B., Liu, N., McDonough, J. R., Chen, W., Alshareef, H. N., Criddle, C. S., and Cui, Y. (2012) Carbon nanotube-coated macroporous sponge for microbial fuel cell electrodes, *Energy & Environmental Science 5*, 5265-5270.

106. Tsai, H. Y., Wu, C. C., Lee, C. Y., and Shih, E. P. (2009) Microbial fuel cell performance of multiwall carbon nanotubes on carbon cloth as electrodes, *Journal of Power Sources 194*, 199-205.

107. Xie, X., Hu, L. B., Pasta, M., Wells, G. F., Kong, D. S., Criddle, C. S., and Cui, Y. (2011) Three-Dimensional Carbon Nanotube-Textile Anode for High-Performance Microbial Fuel Cells, *Nano Letters 11*, 291-296.

108. Lowy, D. A., Tender, L. M., Zeikus, J. G., Park, D. H., and Lovley, D. R. (2006) Harvesting energy from the marine sediment-water interface

II - Kinetic activity of anode materials, *Biosensors & Bioelectronics 21*, 2058-2063.

109. Lowy, D. A., and Tender, L. M. (2008) Harvesting energy from the marine sediment-water interface III. Kinetic activity of quinone- and antimony-based anode materials, *Journal of Power Sources 185*, 70-75.

110. Wei, J. C., Liang, P., and Huang, X. (2011) Recent progress in electrodes for microbial fuel cells, *Bioresource Technology 102*, 9335-9344.

111. Cheng, S. A., and Logan, B. E. (2007) Ammonia treatment of carbon cloth anodes to enhance power generation of microbial fuel cells, *Electrochemistry Communications 9*, 492-496.

112. Feng, Y. J., Yang, Q., Wang, X., and Logan, B. E. (2010) Treatment of carbon fiber brush anodes for improving power generation in air-cathode microbial fuel cells, *Journal of Power Sources 195*, 1841-1844.

113. Scott, K., Rimbu, G. A., Katuri, K. P., Prasad, K. K., and Head, I. M. (2007) Application of modified carbon anodes in microbial fuel cells, *Process Safety and Environmental Protection 85*, 481-488.

114. Zhu, N. W., Chen, X., Zhang, T., Wu, P. X., Li, P., and Wu, J. H. (2011) Improved performance of membrane free single-chamber air-cathode microbial fuel cells with nitric acid and ethylenediamine surface modified activated carbon fiber felt anodes, *Bioresource Technology 102*, 422-426.

115. Tang, X. H., Guo, K., Li, H. R., Du, Z. W., and Tian, J. L. (2011) Electrochemical treatment of graphite to enhance electron transfer from bacteria to electrodes, *Bioresource Technology 102*, 3558-3560.

116. Park, D. H., and Zeikus, J. G. (2003) Improved fuel cell and electrode designs for producing electricity from microbial degradation,

*Biotechnology and Bioengineering 81*, 348-355.

117. Harnisch, F., and Schroder, U. (2010) From MFC to MXC: chemical and biological cathodes and their potential for microbial bioelectrochemical systems, *Chemical Society Reviews 39*, 4433-4448.

118. Lu, M., and Li, S. F. Y. (2012) Cathode Reactions and Applications in Microbial Fuel Cells: A Review, *Critical Reviews in Environmental Science and Technology 42*, 2504-2525.

119. Zhao, F., Harnisch, F., Schrorder, U., Scholz, F., Bogdanoff, P., and Herrmann, I. (2006) Challenges and constraints of using oxygen cathodes in microbial fuel cells, *Environmental Science & Technology 40*, 5193-5199.

120. Freguia, S., Rabaey, K., Yuan, Z., and Keller, J. (2007) Non-catalyzed cathodic oxygen reduction at graphite granules in microbial fuel cells, *Electrochimica Acta 53*, 598-603.

121. Fornero, J. J., Rosenbaum, M., Cotta, M. A., and Angenent, L. T. (2008) Microbial Fuel Cell Performance with a Pressurized Cathode Chamber, *Environmental Science & Technology 42*, 8578-8584.

122. Li, S. Z., Hu, Y. Y., Xu, Q., Sun, J., Hou, B., and Zhang, Y. P. (2012) Iron- and nitrogen-functionalized graphene as a non-precious metal catalyst for enhanced oxygen reduction in an air-cathode microbial fuel cell, *Journal of Power Sources 213*, 265-269.

123. Pham, T. H., Jang, J. K., Chang, I. S., and Kim, B. H. (2004) Improvement of cathode reaction of a mediatorless microbial fuel cell, *Journal of Microbiology and Biotechnology 14*, 324-329.

124. Cheng, S., Liu, H., and Logan, B. E. (2006) Power densities using different cathode catalysts (Pt and CoTMPP) and polymer binders (Nafion and PTFE) in single chamber microbial fuel cells, *Environmental Science & Technology 40*, 364-369.

125. Zhao, F., Harnisch, F., Schroder, U., Scholz, F., Bogdanoff, P., and

Herrmann, I. (2005) Application of pyrolysed iron(II) phthalocyanine and CoTMPP based oxygen reduction catalysts as cathode materials in microbial fuel cells, *Electrochemistry Communications 7*, 1405-1410.

126. Harnisch, F., Wirth, S., and Schroder, U. (2009) Effects of substrate and metabolite crossover on the cathodic oxygen reduction reaction in microbial fuel cells: Platinum vs. iron(II) phthalocyanine based electrodes, *Electrochemistry Communications 11*, 2253-2256.
127. Zhang, L. X., Liu, C. S., Zhuang, L., Li, W. S., Zhou, S. G., and Zhang, J. T. (2009) Manganese dioxide as an alternative cathodic catalyst to platinum in microbial fuel cells, *Biosensors & Bioelectronics 24*, 2825-2829.
128. Zhang, Y. P., Hu, Y. Y., Li, S. Z., Sun, J., and Hou, B. (2011) Manganese dioxide-coated carbon nanotubes as an improved cathodic catalyst for oxygen reduction in a microbial fuel cell, *Journal of Power Sources 196*, 9284-9289.
129. Morris, J. M., Jin, S., Wang, J. Q., Zhu, C. Z., and Urynowicz, M. A. (2007) Lead dioxide as an alternative catalyst to platinum in microbial fuel cells, *Electrochemistry Communications 9*, 1730-1734.
130. Bergel, A., Feron, D., and Mollica, A. (2005) Catalysis of oxygen reduction in PEM fuel cell by seawater biofilm, *Electrochemistry Communications 7*, 900-904.
131. Clauwaert, P., Rabaey, K., Aelterman, P., De Schamphelaire, L., Ham, T. H., Boeckx, P., Boon, N., and Verstraete, W. (2007) Biological denitrification in microbial fuel cells, *Environmental Science & Technology 41*, 3354-3360.
132. Schaetzle, O., Barriere, F., and Schroder, U. (2009) An improved microbial fuel cell with laccase as the oxygen reduction catalyst, *Energy & Environmental Science 2*, 96-99.

# Chapter 2 Conductive polypyrrole hydrogels and carbon nanotubes composite anode for MFCs

## 2.1 Introduction

In the past decade, great progress has been made in MFCs and this technology has demonstrated its potential for various kinds of applications, such as wastewater treatment, biochemical oxygen demand detection, energy production, chemical and fuel synthesis and bioremediation (1-6). However, the practical applications of MFCs are still in the fancy due to the very small power density. The extracellular electron transfer from bacteria to electrode, a key process that defines the theoretical boundary of energy conversion, is currently a major limiting factor for power production in MFCs (7-8). Therefore, facilitating the extracellular electron transfer provides a promising approach to boost the power generation of MFCs.

Anode material plays a key role in determining the power production of MFCs as described previously. The surface properties of the anode not only affect the biofim formation on electrode surface, but also have an impact on the extracellular electron transfer between microorganisms and the electrode. Currently, carbon materials such as carbon paper, carbon cloth and graphite felt are the most commonly used anodes in MFCs due to their high specific surface area, excellent biocompatibility, high conductivity and strong stability in a microbial inoculum mixture (9). However, these materials demonstrate very low electrocatalytic activity for the anode microbial reactions and the electron transfer rate is slow, which significantly limits the power production in MFCs

(10). As a result, development of anode material with high electrocatalytic activity and excellent biocompatibility is expected to be an efficient method to enhance the biofilm formation, accelerate the electron transfer and enhance the power production in MFCs.

Recently, these has been a growing interest in conducting polymers electrode in chemical fuel cell and MFC studies (10). For example, some conducting polymers have been used in MFCs due to their high electrocatalytic activity, conductivity and chemical stability, and these materials have been demonstrated to be effective in increasing the power density (11-13). On the other hand, carbon nanotubes have been coated on carbon cloth, carbon paper or sponge to increase the power generation in MFCs due to their high specific surface area and excellent conductivity (14-16). In addition, anode materials with porous structure results in internal colonization, which improves the interaction between biofilm and electrode and accordingly accelerates the direct electron transfer from bacteria to electrode (17). However, these materials are typically physically adsorbed on electrode surface with weak interaction which could easily be desorbed under normal experimental conditions, or they are coated on electrode surface by binders such as Nafion and polytetrafluoroethylene, which are prohibitively expensive (10, 12, 16).

Conducting polymer hydrogels, a subclass of conducting polymers, have the advantageous qualities of both hydrogels and organic conductors. These materials exhibit excellent electrochemical properties due to their intrinsic porous structure and good conductivity (18). Conducting polymer hydrogels showed excellent electrochemical activity and superior electrode performance in different electrochemical devices (19-20). When CNTs were embedded into

conducting polymer hydrogels as conductive backbones, the composite exhibited much higher conductivity and electrochemical activity as an anode in lithium ion battery (21). However, CNTs doped conducting polymer hydrogels without the addition of binders for enhanced electrocatalytic activity in MFCs have so far not been reported.

In this chapter, a facile and scalable method was employed to synthesize conductive polypyrrole hydrogels and carbon nanotubes composite (CPHs/CNTs), which were directly coated on graphite felt without any binders. This composite was investigated as an anode in two-chambered MFCs for electricity production. The electrocatalytic activity and biocompatibility of CPHs/CNTs were comprehensively investigated.

## 2.2 Experimental section

### 2.2.1 Preparation of the CPHs/CNTs

Phytic acid (an abundant natural product from plants) was utilized as the gelator and dopant to synthesize the CPHs/CNTs composite. The CNTs were pretreated by sonication in a 1:3 mixture of 70% nitric acid and 97% sulfuric acid for 4 h, followed by precipitation and rinsing with deionized (DI) water (10). Graphite felt was pretreated by immersing sequentially in 1 M NaOH for 12 h and then 1 M $H_2SO_4$ for 12 h, followed by rinsing with DI water.

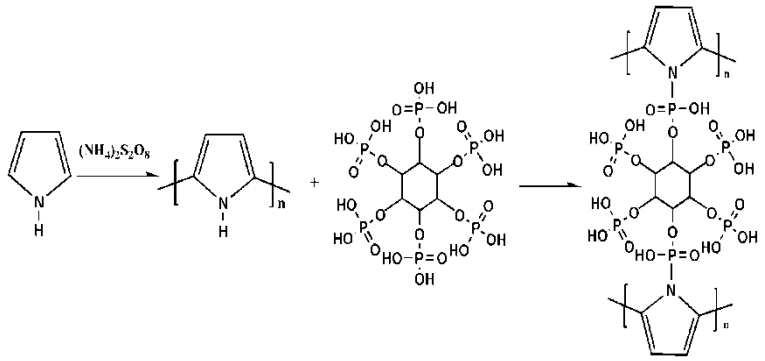

Figure 2. 1 The preparation mechanism and chemical structure of the polypyrrole hydrogel where phytic acid served as a dopant and a crosslinker.

The composite was synthesized *via* a liquid phase reaction in a solution-based method modified from the approach as previously described (21). The preparation mechanism and chemical structure of the polypyrrole hydrogel were illustrated in Figure 2.1. In particular, the synthesis process of CPHs/CNTs was carried out *via* the following process. First, 0.084 mL pyrrole monomer (98%, Sigma Aldrich) and 0.184 mL phytic acid solution ( 50%, wt% in water, Sigma Aldrich) was mixed with 2 mL isopropanol alcohol, marked as solution A, while 0.274 g ammonium persulfate (98%, Sigma Aldrich) was dissolved into 2 mL DI water with 5 mg dispersed CNTs, taken as solution B. Then, the two solutions were thoroughly mixed and sonicated for 5 min to form a CPHs/CNTs liquid product. After that, the CPHs/CNTs liquid product was uniformly coated onto graphite felt to obtain the CPHs/CNTs anode. Lastly, the anode was dried in a vacuum oven and then immersed in DI water and isopropanol alcohol for 12 h to thoroughly remove excess phytic acid and inorganic salts from its surface.

### 2.2.2 Characterization of the CPHs/CNTs

When the CPHs/CNTs anode was dried in air, its morphology was imaged by a field emission scanning electron microscopy (FESEM) (JSM-6701F, JEOL). The chemical structure of the CPHs/CNTs was analyzed by Fourier transform infrared spectroscopy (FT-IR).

The electrochemical properties of CPHs/CNTs anode was investigated by cyclic voltammetry (CV) in a conventional three-electrode system (CHI660D, Chenhua Instrument Co., China). The CPHs/CNTs anode was used as the working electrode, whereas a Pt foil electrode was used as the counter electrode and a saturated calomel electrode (SCE) was used as the reference electrode. The CV test was conducted in 0.5 mM $K_3[Fe(CN)_6]$ with 0.2 M KCl in MilliQ water, at a scanning rate of 50 mV/s and in the range of -0.2 V to 0.7 V (vs. SCE) at room temperature (22).

In order to investigate the anodic resistance, electrochemical impedance spectroscopy (EIS) measurements were conducted over a frequency range of 0.1 Hz to 100 kHz at the working potential with a perturbation signal of 10 mV when the MFCs were stably running with an external resistance of 200 Ω. The MFC anode was used as the working electrode, whereas the cathode was the counter electrode and an SCE placed in the anode chamber was used as the reference electrode.

### 2.2.3 MFC construction and operation

Two-chambered MFCs (Figure 2.2) separated by Proton exchange membranes (Nafion, 117, Dupont, 4 cm×4 cm) were constructed. The membrane was sequentially boiled in $H_2O_2$ (30%), DI water, 0.5 M $H_2SO_4$, and DI water for 1 h. Each chamber (4 cm×2 cm×4 cm) had a total volume of about 32 mL. CPHs/CNTs (4 cm×0.3 cm×4 cm) was placed in the anode chamber while graphite felt (4 cm×0.3 cm×4 cm) coated by Pt/C was placed in the cathode chamber. For comparison, bare graphite felt was used as the anode in another MFC as the control. Titanium wire was utilized to connect the anodes and cathodes with an external resistance of 200 Ω.

Cathodes used for MFCs were prepared by uniformly coating Pt/C catalyst onto the graphite felt surface (0.5 $mg_{Pt}/cm^2$) using 5% Nafion solutions as the binder (23). Briefly, Pt/C catalyst was initially mixed and dispersed well in the Nafion and ethanol solution by ultrasonication for 5 min. Then, the dispersion was uniformly brushed onto the graphite felt followed by drying at room temperature.

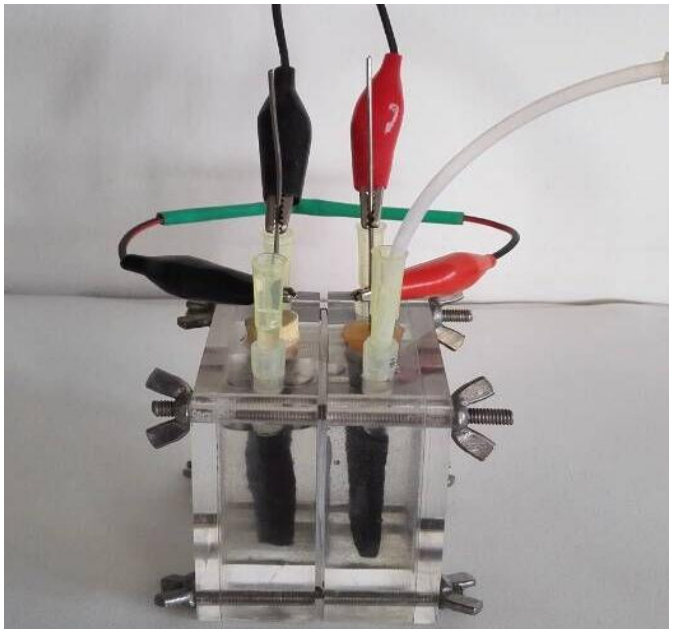

Figure 2. 2 Photograph of the two-chamber MFC reactor.

MFCs were inoculated using a mixed bacterial culture from another MFC which was originally started up with primary clarifier overflow from a wastewater treatment plant. A medium containing 10 mM Sodium acetate, 50 mM phosphate buffer solution ($Na_2HPO_4$, 4.09 g/L and $NaH_2PO_4$ $H_2O$, 2.93 g/L), $NH_4Cl$ (0.31 g/L), KCl (0.13 g/L), NaCl (2.9 g/L) metal salt (12.5 mL/L) and vitamin (5 mL/L) solutions was used as anolyte to feed the MFCs (24). The catholyte was composed of 50 mM phosphate buffer solution, $NH_4Cl$ (0.31 g/L), KCl (0.13 g/L) and NaCl (2.9 g/L).

The feeding solution had been sparged with high purity nitrogen gas for 30 min to remove the dissolved oxygen which were harmful for electrochemically active bacteria in MFCs. The anode chamber was maintained under anaerobic condition, while the cathode chamber was purged with sterile air (10 mL/min). MFCs were operated in a temperature-controlled incubator at 30 ℃ in a fed batch mode and the feeding solutions were refreshed when the voltage

dropped below 30 mV, which was considered as the end of one electricity production cycle.

### 2.2.4 Analyses and calculations

Cell voltages (U) across the external resistance were recorded and stored by a data acquisition system (AD8201H, Ribohua Co., Ltd). Polarization and power density curves were obtained by varying the external resistance (R) from 10 Ω to 2000 Ω. Polarization was tested when the MFCs became stable and reproducible in power production. For each test, it took about 20 min to reach a stable voltage output. Current (I) was calculated by $I = U/R$, and power density (P) was normalized to the projected area of anode surface, calculated as $P = U \times I/S$, where S was the projected area of anode surface (16 $cm^2$).

Biomass on electrodes was evaluated by measuring cell protein using Bradford protein assay method (25). At the end of the test, the anodes were removed from the MFCs and the washed biomass was treated in 1 M NaOH for 10 min at 100 ℃ to solubilize the attached cell protein. Then the protein was measured by Bradford protein assay at 595 nm. All the experiments were carried out in duplicate and the average values with standard deviation were obtained.

## 2.3 Results and discussion

### 2.3.1 FT-IR and morphology characterization of the CPHs/CNTs composite

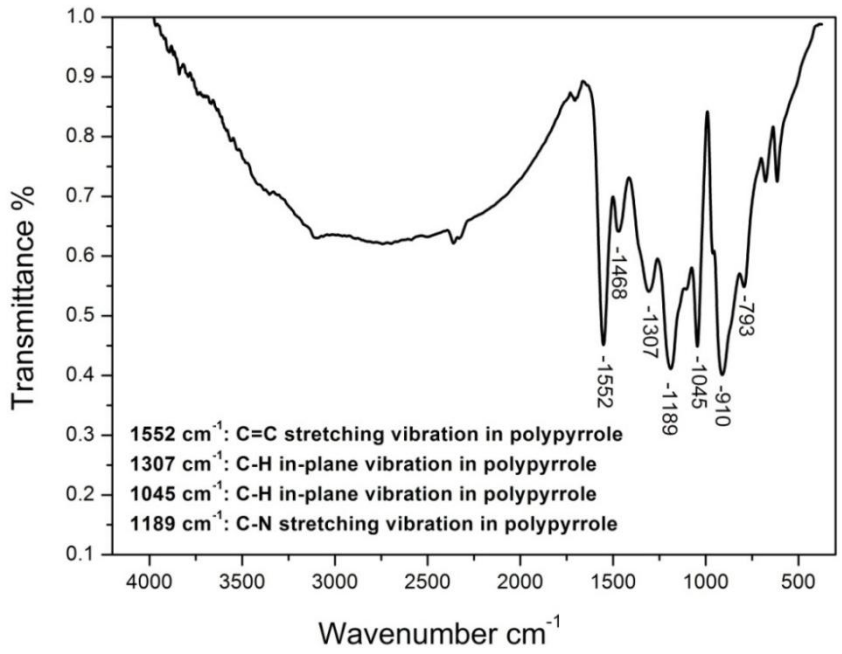


Figure 2. 3 FT-IR spectrum of the CPHs/CNTs composite with peaks labeled.

The chemical structure of the as-synthesized CPHs/CNTs was analyzed by the FT-IR spectrum. As shown in Figure 2.3, the absorption peak at 1552 $cm^{-1}$ was attributed to the in-ring stretching of C=C bonds in the pyrrole rings. The peaks at 1307 $cm^{-1}$ and 1045 $cm^{-1}$ were due to the C-H in-plane vibration and the peak at 1189 $cm^{-1}$ was assigned to the C-N stretching vibration. These characteristic peaks demonstrated that polypyrrole hydrogels were formed through the chemical oxidation method (19, 26).

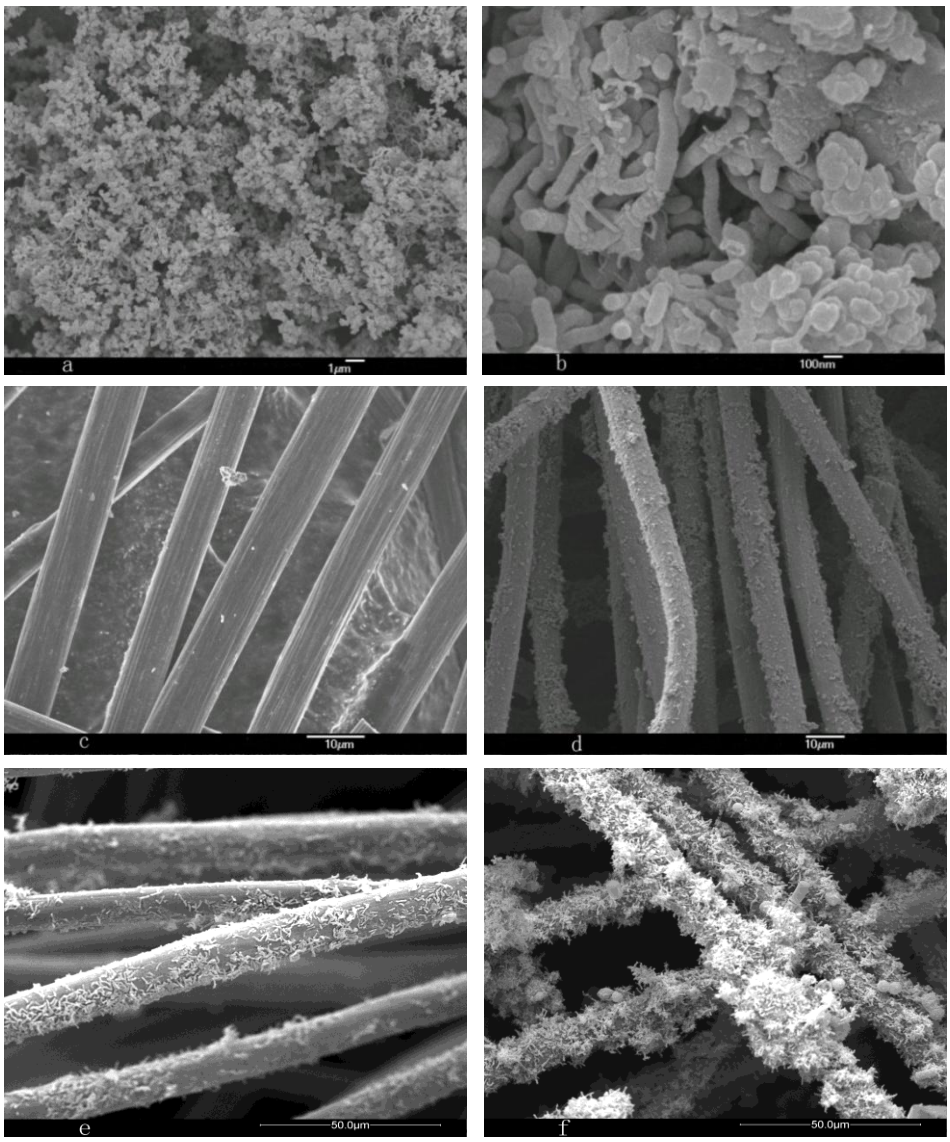


Figure 2. 4 SEM images of the CPHs/CNTs composite (a and b), bare graphite felt (c) and graphite felt coated by CPHs/CNTs, and biofilm formation on bare graphite felt (e) and graphite felt coated by CPHs/CNTs (f) after MFC operation.

SEM images (Figure 2.4) of the as-synthesized CPHs/CNTs revealed that the composite had a three-dimensional porous nanostructure with CNTs as the fortifier. The nanostructured polypyrrole hydrogels exhibited nanoscale and micrometer sized pores, which significantly enhanced the interfacial area between electrochemically active microorganisms and the electrodes. The highly conductive CNTs were embedded and intertwined within the hydrogel bulk, which effectively improved the electronic conductivity of the composite.

Phytic acid was the key for the synthesis of the CPHs/CNTs composite, as it served as both the dopant and the gelator during the formation of the porous structure (20). Phytic acid could crosslink the polypyrrole by protonating the nitrogens in the polypyrrole chains (Figure 2.1). Each phytic acid molecule could interact with more than one polypyrrole chains. As a result, a highly crosslinked structure was formed. The polypyrrole hydrogels were hydrophilic because there was an excess of phosphorous groups in the phytic acid. These phosphorous groups could improve the biofilm formation because it was proved that hydrophilic surface was favorable for the electroactive biofilm formation (27). Thus, the three dimensional porous structure and the hydrophilicity of this CPHs/CNTs composite was expected to exhibit excellent biocompatibility and enhance the biofilm formation.

### 2.3.2 Electrochemical analysis of the CPHs/CNTs composite

Conductivity was a very important parameter for anode material in MFCs. The bare graphite felt showed a high conductivity of 138 S/m, while the graphite felt coated by CPHs/CNTs exhibited a conductivity of 130 S/m. This result demonstrated that CPHs/CNTs composite had excellent conductivity. The electron transfer kinetic on the CPHs/CNTs surface was studied by CV using $K_3[Fe(CN)_6]$ as the redox probe. CVs using $K_3[Fe(CN)_6]$ showed a characteristic of a typical quasi-reversible electron transfer process (Figure 2.5). Compared with the peak current of the bare graphite felt ($1.12 \pm 0.08$

mA/cm$^2$), the peak current of the CPHs/CNTs (3.29 ± 0.16 mA/cm$^2$) increased by approximately 194%. The peak potential separation for the bare graphite felt was about 278 mV, while the value was decreased to 159 mV for the CPHs/CNTs material. The much higher peak current and the smaller peak potential separation indicated the kinetic of the chemical reaction on the CPHs/CNTs surface was enhanced. These results demonstrated that CPHs/CNTs significantly facilitated the electron transfer on the electrode surface and reduced the resistance of the anodic reaction.

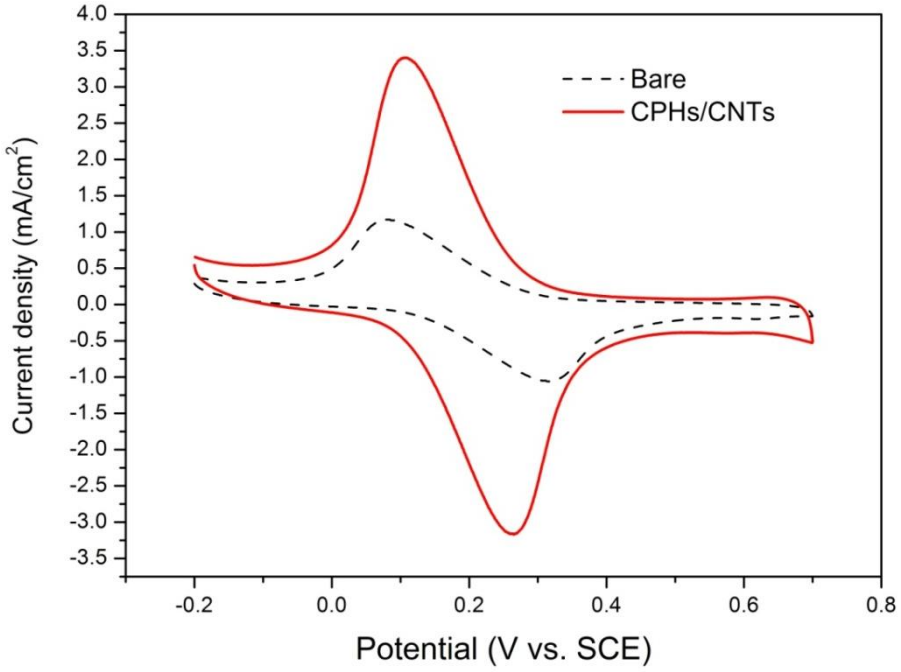


Figure 2. 5 CVs of CPHs/CNTs and bare graphite felt in 0.5 mM $K_3[Fe(CN)_6]$ with 0.2 M KCl at a scanning rate of 50 mV/s.

EIS of the electrode offered important information for the analysis of the electrochemical reactions on electrode surface and bacterial metabolism in MFCs. In this study, EIS of the anodes were carried out to measure the anode resistance of the MFCs under working cell condition. The Nyquist curves were recorded when a steady-state current was generated (Figure 2.6). These plots

exhibited semicircles over the high-frequency range and straight lines in the lower-frequency range. The solution resistance, resulting from the ionic resistance of electrolyte, was found at the high frequency where the plot intersected the Z' axis. The diameter of the semicircle stood for the charge transfer resistance, originated from the resistance of electrochemical reactions on the electrode surface. For the diffusion resistance, it could be obtained from the straight line in the lower-frequency range.

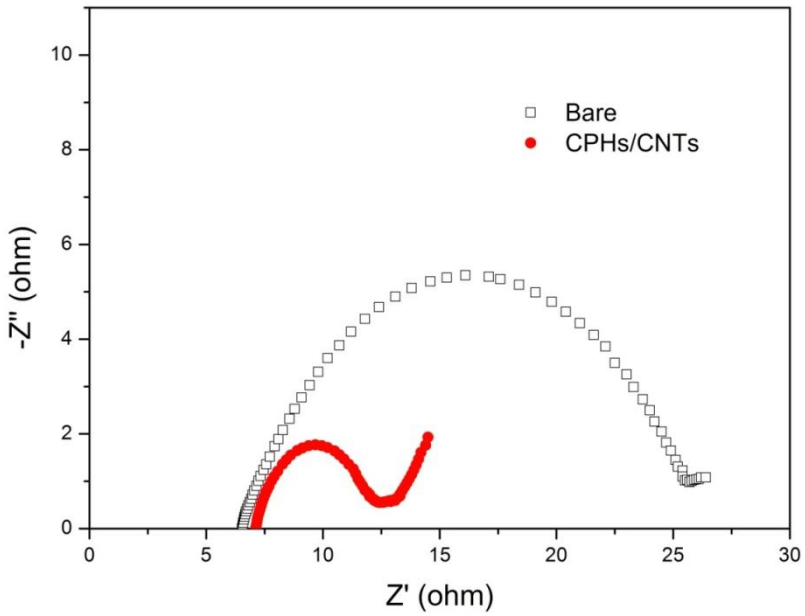


Figure 2. 6 EIS (Nyquist plots) of CPHs/CNTs anode and bare graphite felt anode at working potential with a perturbation signal of 10 mV in MFCs.

CPHs/CNTs and bare graphite felt had similar diffusion resistance and solution resistance in Nyquist plots. However, the charge transfer resistance of the two materials was considerably different. The charge transfer resistance of the bare graphite felt was approximately 19.2 Ω. However, CPHs/CNTs only had a charge transfer resistance of about 5.3 Ω. The much smaller charge transfer resistance of CPHs/CNTs demonstrated that resistance of the anodic

reactions was greatly reduced and the direct electron transfer from bacteria to anode surface was facilitated. This result demonstrated that CPHs/CNTs exhibited high electrocalytic activity towards the anodic reaction in MFCs.

### 2.3.3 CPHs/CNTs anode for electricity production in MFCs

Anodic degradation of acetate in MFCs is a type of respiration, in which the terminal electron acceptor is the anode. The oxidation of acetate availed itself through the tricarboxylic acid (TCA) cycle and the membrane bound electron transfer chain. Acetate firstly enters the TCA cycle through acetyl-CoA, and then NADH, NADPH and $FADH_2$ are produced in the TCA cycle. The electrons released by these compounds transfer through flavoproteins, iron-sulfur proteins, quinone pool and a series of cytochromes to form the electron transfer chain within the cell, and finally they are accepted by the anode *via* the extracellular electron transfer (28-29).

CPHs/CNTs composite was used as an anode in a two-chambered MFC for electricity production study. Bare graphite felt was also studied in an MFC as the control. When the power generation was stable and reproducible after the start-up time, a current density of about 0.16 mA /$cm^2$ in the MFC with the CPHs/CNTs anode and a current density of about 0.12 mA /$cm^2$ in the MFC with bare anode were obtained with an external resistance of 200 Ω. The higher current density of CPHs/CNTs anode in this study demonstrated that this material enhanced the current production in the MFC.

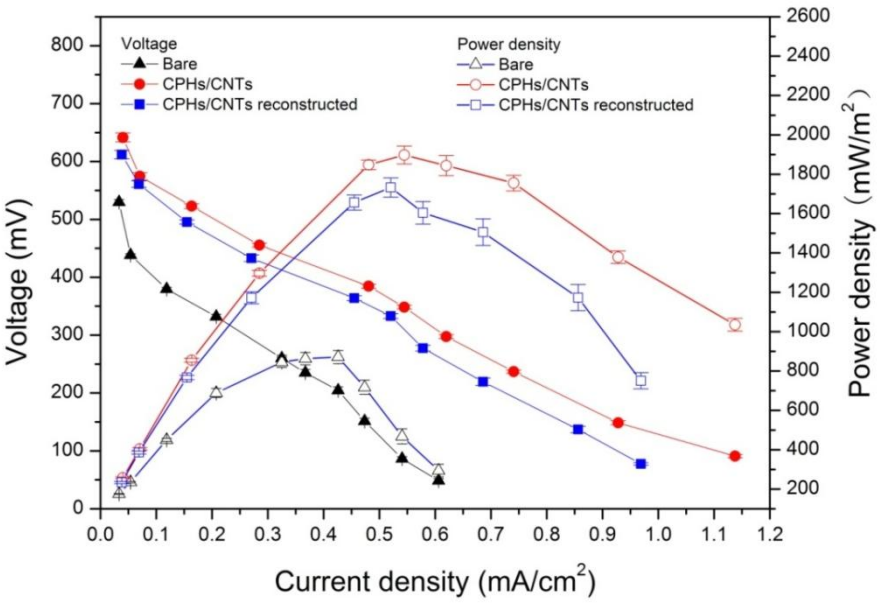


Figure 2. 7 Polarization and power density curves of the MFCs with CPHs/CNTs anode and bare graphite felt anode.

Polarization and power density curves (Figure 2.7) were acquired by varying the external resistance from 10 Ω to 1000 Ω. It took about 20 min to for the MFC to reach a stable voltage output for each of the external resistance. The internal resistance of MFCs could be obtained from the slope of the polarization curve, which indicated that CPHs/CNTs anode reduced the internal resistance from 48 Ω to 30 Ω. This result was consistent with the previous EIS study. The MFC with CPHs/CNTs anode presented a maximum power density of 1898±46 mW/m$^2$, while the MFC with bare graphite felt only had a maximum power density of 871±33 mW/m$^2$. The greatly enhanced power density showed that CPHs/CNTs composite was an ideal anode to facilitate the extracellular electron transfer from bacteria to anode in MFCs.

Anode material is of great significance to the power production in MFCs because anode surface property has great impact on the electrochemically active biofilm formation. The bacteria formed on anode surface was measured

by Bradford protein assay, and the results showed that the protein density on CPHs/CNTs anode was about 376 μg/cm$^2$, higher than the 324 μg/cm$^2$ on bare graphite felt anode. This result indicated that biofilm formation was enhanced on CPHs/CNTs anode surface, which was due to the three dimensional porous structures and the hydrophilicity of the CPHs/CNTs. On the one hand, the porous structures would allow the internal bacterial colonization, which would increase the interfacial area between the bacteria and the electrode. On the other hand, the hydrophilicity resulting from the phosphorous groups in the phytic acid was conducive to electrochemically active bacteria attachment (17, 27). Consequently, CPHs/CNTs anode enhanced the biofilm formation on its surface and helped to increase the power production from MFCs.

Anode properties not only have great impact on the electrochemically active biofilm formation, but also have significant effect on the extracellular electron transfer from bacteria to anode. The CPHs/CNTs in this study exhibited high electrocatalytic activity in the CV and EIS tests, indicated by the high current density, narrow peak potential separation and small charge transfer resistance. The high electrocatalytic activity facilitated the extracellular electron transfer and enhanced the kinetic of the anodic reactions on anode surface. As a result, CPHs/CNTs anode considerably enhanced the power production in MFCs by 118%.

Table 2. 1 Anode modification methods in MFCs.

| Modification method | MFC performance | Reference |
|---|---|---|
| Heat treatment of | Increased power density from | (30) |

| | | |
|---|---|---|
| carbon mesh | 893 mW/m$^2$ to 922 mW/m$^2$ | |
| Quinone grafted on graphite felt | Increased power density from 967 mW/m$^2$ to 1872 mW/m$^2$ | (31) |
| CNT/polyaniline coating on nickel foam | The power density reached 42 mW/m$^2$ | (10) |
| Polypyrrole coated CNTs | The maximum power density was 228 mW/m$^2$ | (26) |
| CPHs/CNTs coating on graphite felt | Enhanced power density from 871 mW/m$^2$ to 1898 mW/m$^2$ | This study |

The long term stability of the CPHs/CNTs anode in MFC reactor was further studied. After a period of three months, the CPHs/CNTs anode was taken away from the MFC reactor and autoclaved. Then the MFC was reconstructed using the autoclaved CPHs/CNTs anode and operated following the same procedures described above. Polarization and power density curves of the reconstructed MFC were also acquired when electricity production was stable and reproducible. Figure 2.7 showed that the maximum power density of the reconstructed MFC with CPHs/CNTs anode was $1733 \pm 46$ mW/m$^2$, which was only slightly dropped (about 8.7%). This test demonstrated that CPHs/CNTs had excellent stability and thus had the potential to be used for long term applications in MFCs.

Anode modification was an efficient strategy to enhance the electricity production in MFCs. Table 2.1 summarized some of the modification approaches that were used in MFC studies. Heat treatment improved the electrochemically active surface area. However, this method was energy

intensive and the power density only increased by 3% (30). Quinone modified on anode surface enhanced the mediated electron transfer and accordingly the power production in MFCs, but the modification method was complex and the quinine was expensive (31). CNT/polyaniline coating and polypyrrole coated CNTs required binders such as Nafion and polytetrafluoroethylene, which were prohibitively expensive (10, 26).

CPHs/CNTs composite exhibits excellent prosperities in MFCs: high elerocatalyic activity, excellent biocompatibility, strong chemical stability and high conductivity. In addition, the preparation is simple and scalable. More importantly, CPHs/CNTs composite itself presents strong adhesion on carbon materials. As a result, binders are not needed anymore to attach this material on carbon surface. All of these advantages make CPHs/CNTs composite an ideal anode for MFCs. Thus, CPHs/CNTs composite holds an exciting potential for application in MFCs to enhance the power density.

## 2.4 Conclusion

A facile and scalable approach was utilized in this chapter to prepare conductive polypyrrole hydrogels/carbon nanotubes (CPHs/CNTs) composite anode that possessed the advantageous features of both hydrogels and organic conductor. CV and EIS tests demonstrated that CPHs/CNTs reduced the interfacial charge transfer resistance and enhanced direct electron transfer from bacteria to anode. Further, the porous structure and hydrophilicity of

CPHs/CNTs improved the biofilm formation on anode surface. As a result, CPHs/CNTs anode increased the maximum power density by 118%. A three months investigation of this novel anode showed that the maximum power density only declined by 8.7%, which indicated that CPHs/CNTs anode had a high stability in long term operation of MFCs. This study demonstrates that this simple and scalable synthesis of CPHs/CNTs offers an effective method to enhance the power density in MFCs.

**2.5 References**


1. Huang, Y. L., He, Z., Kan, J. J., Manohar, A. K., Nealson, K. H., and Mansfeld, F. (2012) Electricity generation from a floating microbial fuel cell, *Bioresource Technology 114*, 308-313.
2. Chang, I. S., Moon, H., Jang, J. K., and Kim, B. H. (2005) Improvement of a microbial fuel cell performance as a BOD sensor using respiratory inhibitors, *Biosensors & Bioelectronics 20*, 1856-1859.
3. Rozendal, R. A., Leone, E., Keller, J., and Rabaey, K. (2009) Efficient hydrogen peroxide generation from organic matter in a bioelectrochemical system, *Electrochemistry Communications 11*, 1752-1755.
4. Gregory, K. B., and Lovley, D. R. (2005) Remediation and recovery of uranium from contaminated subsurface environments with electrodes, *Environmental Science & Technology 39*, 8943-8947.
5. Zhang, F., Ge, Z., Grimaud, J., Hurst, J., and He, Z. (2013) Long-Term Performance of Liter-Scale Microbial Fuel Cells Treating Primary Effluent Installed in a Municipal Wastewater Treatment Facility, *Environmental Science & Technology 47*, 4941-4948.

6. Oh, S. E., and Logan, B. E. (2005) Hydrogen and electricity production from a food processing wastewater using fermentation and microbial fuel cell technologies, *Water Research 39*, 4673-4682.
7. Rabaey, K., Boon, N., Hofte, M., and Verstraete, W. (2005) Microbial phenazine production enhances electron transfer in biofuel cells, *Environmental Science & Technology 39*, 3401-3408.
8. Srikanth, S., and Mohan, S. V. (2012) Influence of terminal electron acceptor availability to the anodic oxidation on the electrogenic activity of microbial fuel cell (MFC), *Bioresource Technology 123*, 480-487.
9. Zhou, M. H., Chi, M. L., Luo, J. M., He, H. H., and Jin, T. (2011) An overview of electrode materials in microbial fuel cells, *Journal of Power Sources 196*, 4427-4435.
10. Qiao, Y., Li, C. M., Bao, S. J., and Bao, Q. L. (2007) Carbon nanotube/polyaniline composite as anode material for microbial fuel cells, *Journal of Power Sources 170*, 79-84.
11. Lai, B., Tang, X. H., Li, H. R., Du, Z. W., Liu, X. W., and Zhang, Q. (2011) Power production enhancement with a polyaniline modified anode in microbial fuel cells, *Biosensors & Bioelectronics 28*, 373-377.
12. Zou, Y. J., Pisciotta, J., and Baskakov, I. V. (2010) Nanostructured polypyrrole-coated anode for sun-powered microbial fuel cells, *Bioelectrochemistry 79*, 50-56.
13. Qiao, Y., Bao, S. J., Li, C. M., Cui, X. Q., Lu, Z. S., and Guo, J. (2008) Nanostructured polyanifine/titanium dioxide composite anode for microbial fuel cells, *Acs Nano 2*, 113-119.
14. Sun, J. J., Zhao, H. Z., Yang, Q. Z., Song, J., and Xue, A. (2010) A novel layer-by-layer self-assembled carbon nanotube-based anode: Preparation, characterization, and application in microbial fuel cell, *Electrochimica Acta 55*, 3041-3047.

15. Xie, X., Ye, M., Hu, L. B., Liu, N., McDonough, J. R., Chen, W., Alshareef, H. N., Criddle, C. S., and Cui, Y. (2012) Carbon nanotube-coated macroporous sponge for microbial fuel cell electrodes, *Energy & Environmental Science 5*, 5265-5270.

16. Tsai, H. Y., Wu, C. C., Lee, C. Y., and Shih, E. P. (2009) Microbial fuel cell performance of multiwall carbon nanotubes on carbon cloth as electrodes, *Journal of Power Sources 194*, 199-205.

17. Xie, X., Hu, L. B., Pasta, M., Wells, G. F., Kong, D. S., Criddle, C. S., and Cui, Y. (2011) Three-Dimensional Carbon Nanotube-Textile Anode for High-Performance Microbial Fuel Cells, *Nano Letters 11*, 291-296.

18. Zhao, Y., Liu, B., Pan, L., and Yu, G. (2013) 3D nanostructured conductive polymer hydrogels for high-performance electrochemical devices, *Energy & Environmental Science 6*, 2856-2870.

19. Shi, Y., Pan, L., Liu, B., Wang, Y., Cui, Y., Bao, Z., and Yu, G. (2014) Nanostructured conductive polypyrrole hydrogels as high-performance, flexible supercapacitor electrodes, *Journal of Materials Chemistry A 2*, 6086-6091.

20. Pan, L., Yu, G., Zhai, D., Lee, H. R., Zhao, W., Liu, N., Wang, H., Tee, B. C. K., Cui, Y., and Bao, Z. (2012) Hierarchical nanostructured conducting polymer hydrogel with high electrochemical activity, *Proceedings of the National Academy of Sciences of the United States of America 109*, 9287-9292.

21. Liu, B., Soares, P., Checkles, C., Zhao, Y., and Yu, G. (2013) Three-Dimensional Hierarchical Ternary Nanostructures for High-Performance Li-Ion Battery Anodes, *Nano Letters 13*, 3414-3419.

22. Wang, P., Lai, B., Li, H. R., and Du, Z. W. (2013) Deposition of Fe on graphite felt by thermal decomposition of Fe(CO)(5) for effective cathodic preparation of microbial fuel cells, *Bioresource Technology*

*134*, 30-35.

23. Cheng, S., Liu, H., and Logan, B. E. (2006) Power densities using different cathode catalysts (Pt and CoTMPP) and polymer binders (Nafion and PTFE) in single chamber microbial fuel cells, *Environmental Science & Technology 40*, 364-369.
24. Lovley, D. R., and Phillips, E. J. P. (1988) Novel Mode of Microbial Energy-Metabolism - Organic-Carbon Oxidation Coupled to Dissimilatory Reduction of Iron or Manganese, *Applied and Environmental Microbiology 54*, 1472-1480.
25. Tang, X. H., Guo, K., Li, H. R., Du, Z. W., and Tian, J. L. (2011) Electrochemical treatment of graphite to enhance electron transfer from bacteria to electrodes, *Bioresource Technology 102*, 3558-3560.
26. Zou, Y. J., Xiang, C. L., Yang, L. N., Sun, L. X., Xu, F., and Cao, Z. (2008) A mediatorless microbial fuel cell using polypyrrole coated carbon nanotubes composite as anode material, *International Journal of Hydrogen Energy 33*, 4856-4862.
27. Guo, K., Freguia, S., Dennis, P. G., Chen, X., Donose, B. C., Keller, J., Gooding, J. J., and Rabaey, K. (2013) The effects of surface charge and hydrophobicity on anodic biofilm formation, community composition and current generation in bioelectrochemical systems, *Environmental Science & Technology 47*, 7563-7570.
28. Bond, D. R., and Lovley, D. R. (2003) Electricity production by Geobacter sulfurreducens attached to electrodes, *Applied and Environmental Microbiology 69*, 1548-1555.
29. Kim, B. H., Kim, H. J., Hyun, M. S., and Park, D. H. (1999) Direct electrode reaction of Fe(III)-reducing bacterium, Shewanella putrefaciens, *Journal of Microbiology and Biotechnology 9*, 127-131.
30. Wang, X., Cheng, S. A., Feng, Y. J., Merrill, M. D., Saito, T., and Logan, B. E. (2009) Use of Carbon Mesh Anodes and the Effect of Different Pretreatment Methods on Power Production in Microbial

Fuel Cells, *Environmental Science & Technology 43*, 6870-6874.

31. Tang, X. H., Li, H. R., Du, Z. W., and Ng, H. Y. (2014) Spontaneous modification of graphite anode by anthraquinone-2-sulfonic acid for microbial fuel cells, *Bioresource Technology 164*, 184-188.

# Chapter 3 Spontaneous modification of graphite anode by anthraquinone-2-sulfonic acid for MFCs

## 3.1 Introduction

Currently, the low power density generation is still one of the greatest challenges for MFC technology for various applications (1-6). This bottleneck is mainly due to the low rate of extracellular electron transfer from bacteria to anode surface, a key factor that defines the theoretical limits of energy conversion (7-8).

So far, it has been confirmed that there are two ways for electron transfer from bacteria to anode surface in MFCs, namely direct electron transfer and mediated electron transfer (9). In direct electron transfer pathway, bacteria can transfer the electron to electrode surface directly *via* bacterial cell outer membrane cytochromes or *via* biological conducting nanowire (10-13). For this type of extracellular electron transfer, enhancing the physical contact between bacteria and anode provides an efficient method to facilitate the electron transfer from bacteria to anode surface and ultimately improve the power generation in MFCs. In chapter 2, CPHs/CNTs anode enhanced the biofilm formation on anode surface and reduced the interfacial charge transfer resistance between bacteria and anode. As a result, CPHs/CNTs anode increased the maximum power density of MFCs by 118%.

The other extracellular electron transfer pathway relies on redox mediator and thus is known as mediated electron transfer. In this electron transfer pathway, electrons firstly transfer from bacteria to the redox mediator, and then to anode surface (7, 14-15). Thus, mediator plays a vital role during this type of extracellular electron transfer.

In fact, electron transfer mediators, such as quinone, thionine, new methylene blue, methyl viologen and neutral red, have been artificially added into the anode chamber to generate and enhance the electricity generation in the early stage of MFC study (9). Adding these mediators into the anode chamber, however, not only increased the operating cost, but also posed a potential environmental problem, as some of the mediators are toxic if they are discharged without proper treatment. As a result, immobilization of mediators onto anode surface offers an effective approach to enhance the electron transfer from bacteria to anode.

Currently, the immobilization methods of redox mediators include physical adsorption and covalently grafting. For physical adsorption method, anthraquinone-1, 6-disulfonic acid (AQDS) (16-17) and 1,4-naphthoquinone (NQ) (16) were physically adsorbed on graphite anodes by immersing the anodes in AQDS and NQ solutions respectively. AQDS and NQ physically adsorbed on anode surface functioned as the redox mediator to facilitate the mediated electron transfer and consequently increased the power production in MFCs. The power density of the MFCs, however, decreased significantly over

time because the mediators physically adsorbed on anode surface with weak force could easily be desorbed under normal operating conditions. The desorption of the mediator not only deteriorates the power production of MFCs during long term operation, but also causes environmental problems.

These two problems brought by physical adsorption, however, can be easily solved by covalently grafting, as covalently grafting of mediator can significantly enhances the force between the anode and the mediator. For instance, neutral red was covalently grafted on graphite anode *via* amidation reaction, which reached a power density of 845 $mW/m^2$ in an MFC using a sewage sludge inoculums, while the control MFC only had a power density of 0.65 $mW/m^2$ (18). However, this method consumes large quantity of organic solvents and acids and the operating is very complex. As a result, there is an urgent need to develop more environmentally friendly and simpler methods to effectively immobilize redox mediators on anode surface to enhance the electricity production in MFCs.

It has been reported that compounds can be grafted onto gold or carbon material surface *via* covalent bonding from spontaneous reduction of the *in situ* generated aryl diazonium cations (19-21); the grafting is simply conducted in aqueous solutions and a long term strong bonding of compounds onto the gold or carbon material surface has been demonstrated. This method offers a simple, environmentally friendly and effective way for immobilize compounds on electrode surface. In fact, aryl diazonium salts has already become a

popular coupling agents in many chemistry and biology studies.

The standard redox potential of anthraquinone-2-sulfonic acid(AQS) is -0.225 V (vs. normal hydrogen electrode, NHE), while the standard redox potential of NADH is -0.325 V (vs. NHE); these slightly higher potential of AQS indicates that it can be an ideal redox mediator as electron and most of the energy in NADH can be easily transferred into AQS (22). In addition, graphite anodes are commonly utilized in MFCs because they have good biocompatibility for biofilm formation, high conductivity, well stability and low price (23). Based on these studies, it was expected that covalently grafting AQS onto graphite anode surface *via* spontaneous reduction of the *in situ* generated AQS diazonium cations would be an effective approach to enhance the mediated electron transfer from electrochemically active bacteria to anode in MFCs. In this chapter, it shows that AQS can be easily grafted onto graphite anode *via* spontaneous reduction of its diazonium cation. This study also demonstrates that AQS covalently grafted onto graphite anode serves as the redox mediator to facilitate the extracellular electron transfer and significantly increases the power generation in MFCs.

## 3.2 Experimental section

### 3.2.1 Electrode preparation

Graphite felt (4 cm×0.4 cm×4 cm) was utilized as both the anodes and the cathodes in MFCs. Graphite felt was purified by immersing in 1 M NaOH for

12 h and then it was thoroughly washed by deionised (DI) water.

The grafting processof AQS onto graphite surface was described in Figure 3.1. In particular, AQS diazonium cations were *in situ* generated by diazonation of 1- aminoanthraquinone-2-sulfonic acid (1 mM) with $NaNO_2$ (1.5 mM) in HCl (0.5 M) solution (24). Covalently grafting of AQS to graphite anode was carried out below 5 ℃ *via* spontaneous reduction of AQS diazonium cations by immersing the graphite felt in the solution containing AQS diazonium cations for 3 hours. The spontaneous reduction of AQS diazonium cation would firstly generate the extremely active radical which covalently grafted onto anode surface immediately. During the grafting process, the solution was continuously stirred to facilitate the mass transfer. 3 hours later, the modified graphite felt was consecutively sonicated in acetonitrile and DI water for 30 min each to thoroughly remove the physically adsorbed species.

Cathodes used for MFCs were prepared by uniformly coating the commercially available Pt/C catalyst onto the graphite felt surface using 5% Nafion solutions as the binder (25). Briefly, the catalyst was mixed and dispersed well in the Nafion and ethanol solution by ultrasonication. After that, the dispersion was brushed onto the graphite felt surface and then the coated graphite felt was dried at room temperature. The Pt/C coated cathode had a loading of 0.5 $mg_{Pt}/cm^2$.

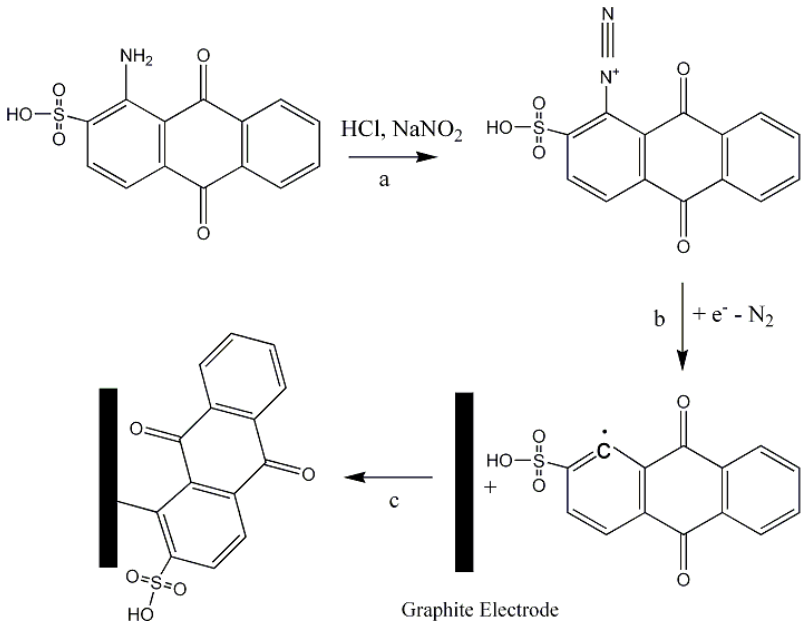


Figure 3. 1 Covalently grafting of graphite anode with AQS via spontaneous reduction of its diazonium cation: a. generation of AQS diazonium cation; b. spontaneous reduction of AQS diazonium cation to a radical; c. C-C bond formation on graphite surface.

### 3.2.2 MFC setup and operation

Two-chambered MFCs separated by proton exchange membranes (Nafion, 117, Dupont, 4 cm×4 cm) were constructed as described in chapter 2. The proton exchange membrane was successively boiled in $H_2O_2$ (30%), DI water, 0.5 M $H_2SO_4$, and deionized water (each for 1 h) to activate the membrane. Each chamber (anode or cathode, 4 cm×2 cm×4 cm) had a total volume of about 32 mL. AQS modified graphite felt or bare graphite felt were placed in the anode chamber while graphite felt coated by Pt/C catalyst was placed in the cathode chamber. The anode and cathode was connected by a titanium wire across an external resistance of 510 Ω.

MFCs were inoculated using a mixed bacterial culture from another MFC

which was originally started up with primary clarifier overflow from a wastewater treatment plant. A medium containing 10 mM Sodium acetate, 50 mM phosphate buffer solution ($Na_2HPO_4$, 4.09 g/L and $NaH_2PO_4$ $H_2O$, 2.93 g/L), $NH_4Cl$ (0.31 g/L), KCl (0.13 g/L), NaCl (2.9 g/L) metal salt (12.5 mL/L) and vitamin (5 mL/L) solutions was used as anolyte to feed the MFCs (26). While a medium containing 50 mM phosphate buffer solution, $NH_4Cl$ (0.31 g/L), KCl (0.13 g/L) and NaCl (2.9 g/L) was utilized as the catholyte.

The feeding solution had been sparged with high purity nitrogen gas for 30 min before the feeding. This was to remove the dissolved oxygen which would deteriorate the electricity generation of the electrochemically active bacteria in MFCs. The anode chamber was strictly maintained under anaerobic condition, while the cathode chamber was purged with sterile air (10 mL/min). MFCs were operated in a temperature-controlled incubator at 30 ℃ in a fed batch mode and the feeding solutions were refreshed when the voltage dropped below 30 mV, which was considered as the end of one electricity production cycle. MFCs were considered to be stable when the maximum voltage output was stable and reproducible. All the tests were performed in duplicate and the average values with standard deviation were acquired.

### 3.2.3 Analyses and calculations

Energy dispersive spectrometry (EDS) (INCA X-MAX, Oxford Instruments)

was utilized to examine the chemical elements on the modified graphite surface. Cyclic voltammetry (CV) was carried out to investigate the electrochemical properties of the AQS modified graphite felt. This test was performed in an oxygen-free phosphate buffer solution (50 mM, pH 7.0) at a scan rate of 50 mV/s in a conventional three-electrode system. AQS modified graphite felt (1 cm×1 cm) or bare graphite felt (1 cm×1 cm) was utilized as the working electrode, while a Pt foil electrode was utilized as the counter electrode and a saturated calomel electrode (SCE) was utilized as the reference electrode. Before the test, high purity nitrogen gas had been sparged into the solution for 30 min to remove the dissolved oxygen in the solution. During the test, the oxygen-free environment was continuously maintained by flowing nitrogen in the headspace of the test cell. A potential range from -0.9 V to 0.1 V (vs. SCE) was selected for the CV tests at room temperature.

The surface concentration of the covalently grafted AQS ($\Gamma_{AQS}$ ) on graphite felt was determined by the following equation: $\Gamma_{AQS}$ = Q/nFA, in which Q was the charge integrated from the reduction peak of the CV curve, n was the number of electrons exchanged in one AQS molecule (n = 2), F was the Faraday constant (96485 C/mol), and A was the geometric electrode area (nominal) (19).

CV was also employed to study the stability of the AQS grafted graphite felt anode. The stability was examined by comparing the peak current of the newly grafted graphite felt and the grafted graphite which had been used as the anode

in MFCs for two months. In addition, the stability of the grafted anode was also tested by operating the MFCs over a period of two months for electricity production.

Cell voltages (U) across the external resistance were recorded and stored by a data acquisition system (AD8201H, Ribohua Co., Ltd). Polarization and power density curves were obtained by varying the external resistance (R) from 10 Ω to 2000 Ω. Polarization was measured when the MFCs became stable and reproducible in power production. For each test, it took about 20 min to reach a stable voltage output. Current (I) was calculated by $I = U/R$, and power density (P) was normalized to the projected area of anode surface, calculated as $P = U \times I/S$, where S was the projected area of anode surface (16 $cm^2$).

### 3.3 Results and discussion

#### 3.3.1 Electrochemical test and EDS spectra

CV measurements were carried out in phosphate buffer solution without dissolved oxygen to investigate whether AQS was covalently immobilized onto the graphite felt surface. CV tests were also performed to study the electrochemical property and the stability of the AQS grafted on graphite felt. Figure 3.2 presented the CV results of the AQS modified anode and the bare

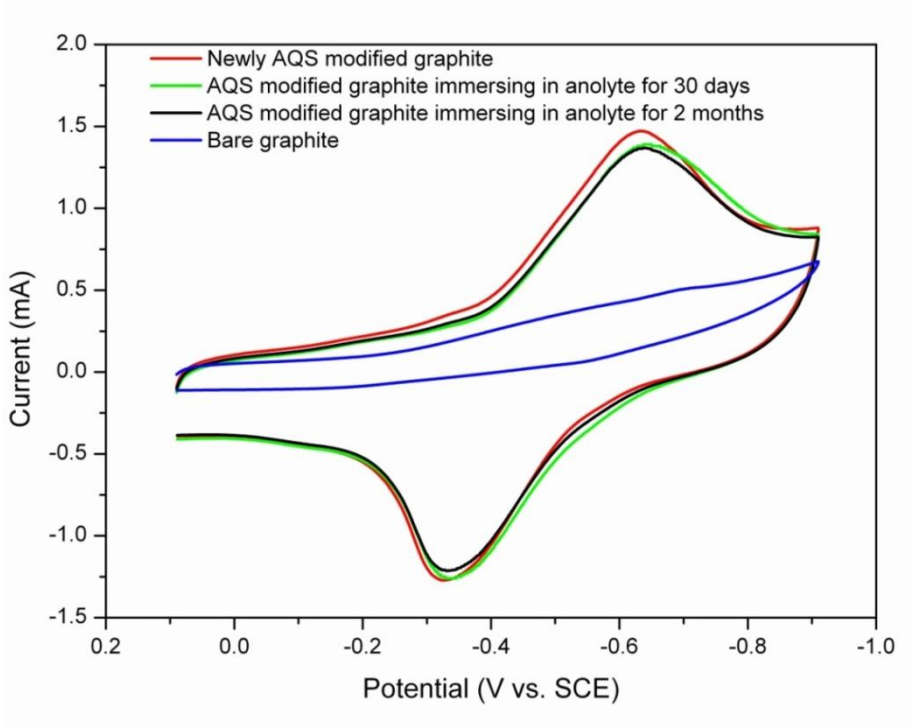


Figure 3. 2 Cyclic voltammograms of AQS modified graphite felt and bare graphite felt in an oxygen-free phosphate buffer solution (50 mM, pH 7.0) at a scan rate of 50 mV/s.

graphite felt anode. The CV of the bare graphite felt anode shown in Figure 3.2 was featureless and the current was quite small. However, the CV of the AQS modified graphite felt anode displayed a well-defined couple of redox peaks. The average of the anodic peak potential and the cathodic peak potential (the midpoint potential) was approximately -0.489 V (vs. SCE), which was about -0.248 V (vs. NHE). These redox peaks were attributing to the AQS covalently grafted onto the surface of the graphite felt, as this anode had been sequentially sonicated in acetonitrile and DI water for 30 min each to thoroughly remove the physically adsorbed species. EDS spectrum (Figure 3.3) showed that sulfur element was present on the modified graphite felt, while sulfur element was absent on the bare graphite felt. This result further confirmed that AQS was successfully grafted on the surface of the graphite felt

*via* strong covalent bonding.

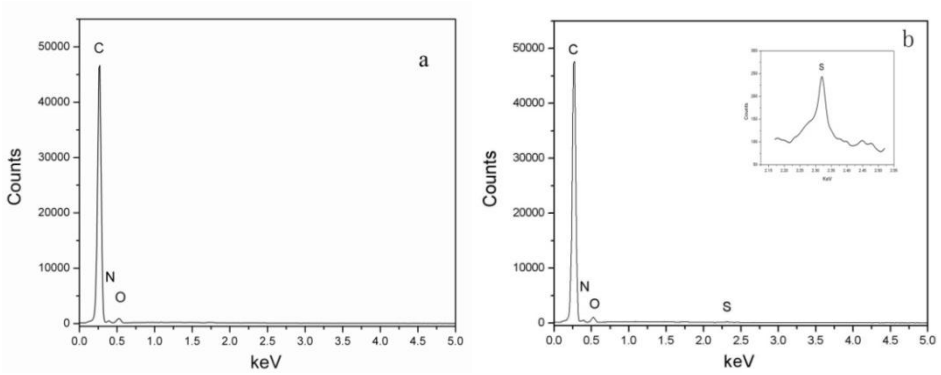


Figure 3. 3 EDS spectra of bare graphite (a) and AQS grafted graphite (b).

The surface concentration of the covalently grafted AQS on graphite felt surface was obtained from the above equation; the result showed that the concentration was approximately $5.37 \pm 1.15 \times 10^{-9}$ mol/cm$^2$. Previous study reported that anthraquinone derivatives physically adsorbed on carbon fiber surface usually had a surface concentration of about $3.7 \pm 1.7 \times 10^{-9}$ mol/cm$^2$ (27). Compared with the physical adsorption, the surface concentration of the AQS in this study was increased by about 45.1%. More importantly, the strong covalent bonding could effectively solve the problem of desorption of physical immobilization (16-17). Compared with other immobilization methods, another benefit of this method, was that the modification process was very simple, versatile and environmentally friendly. For instance, immobilization of mediator *via* amidation reaction typically consumes very large amount of nitric acids and organic solvents, while the electropolymerization immobilization requires complex electrochemical devices such as a potentiostat, a power source and a three-electrode system (28).

The redox potential of the AQS grafted on graphite felt surface obtained in this

study was a little higher than the redox potential of NADH. This result indicated that it had the potential to be an ideal mediator for electron transfer from NADH to the anode surface in MFCs. Figure 3.2 also showed that the current density of the AQS modified graphite felt anode increased significantly compared with the control, which demonstrated that the AQS could enhance the kinetic of the electrode reaction. Therefore, this novel anode was expected to have high performance in MFCs for electricity production.

### 3.3.2 AQS modified anode for power production in MFCs

AQS modified graphite felt was utilized as anode in two-chambered MFCs to study its performance for electricity generation. Bare graphite felt was also investigated as the control in MFCs. When the voltage output across an external resistance of 510 Ω was stable and reproducible after a short start-up time, a current of approximately 1.12 mA was produced in the MFC with modified anode while a current of about 0.83 mA was generated in the MFC with bare graphite felt anode. This result demonstrated that this novel anode enhanced the current production in MFCs by about 34.9%.

Figure 3.4 showed the polarization and power density plots that were obtained by varying the external resistance from 10 Ω to 2000 Ω. For the control anode, it displayed a maximum power density of $967 \pm 33$ mW/m$^2$. However, the AQS modified graphite felt anode exhibited a maximum power density of about $1872 \pm 42$ mW/m$^2$, which was 93.6% higher than the control.

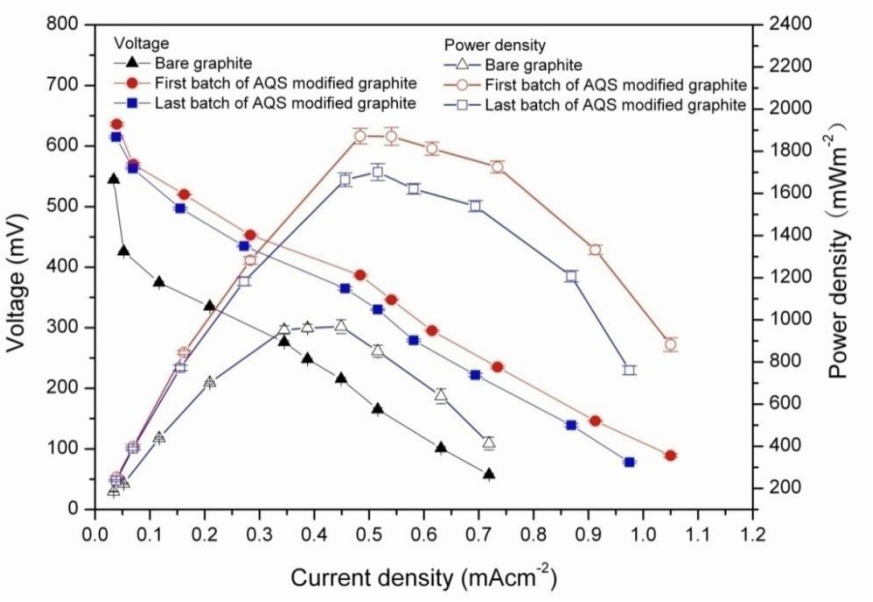


Figure 3. 4 Polarization and power density curves of the MFCs with bare graphite and AQS grafted graphite over a period of two months.

The biofilm formed on both anode surfaces was measured, as an enhanced biofilm formation could also improve the power production in MFCs. Bradford protein assay method indicated that the bacterial protein concentration in both anode surfaces was almost the same. The result ruled out the possibility that the power production enhancement was ascribe to the enhanced biofilm formation on the AQS modified anode, as this novel anode did not increase the bacteria attachment on its surface. Therefore, the power production enhancement was attributing to the AQS covalently grafted on graphite felt surface, which served as the electron transfer mediator to enhance the extracellular electron transfer from bacteria to anode in MFCs. The possible mechanism was illustrated in Figure 3.5. AQS might receive the electron from outer cell membrane cytochrome *via* physical contact or electron hopping, and then delivered the electron to the anode.

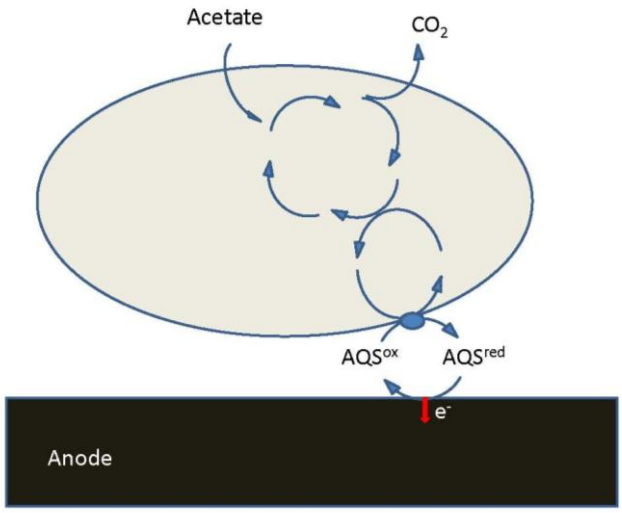


Figure 3. 5 Scheme of mediated electron transfer *via* AQS in MFCs (9).

As stated in chapter 1, anode material is of great significance to the electricity production in MFCs, as anode surface property has considerable impact on the extracellular electron transfer from bacteria to anode. $NAD^+$/NADH is one of the key enzymes in cellular electron transfer pathway. This enzyme lies in the end of the electron transfer chain during microbial respiration with a standard redox potential of -0.325 V (vs. NHE) (29). Electrons accepted by NADH initially transfer into a cell terminal membrane enzyme and then to an electron acceptor outside of the cell. In order to facilitate the electron transfer and at the same time reduce the energy loss during the transfer process, the redox potential of the mediator should be as low as possible but should be higher than the redox potential of $NAD^+$/NADH (30-31). On the one hand, an ideal electron mediator is expected to have a higher redox potential than NADH, which makes it possible to accept the electron from NADH. On the other hand, this ideal mediator should have a low redox potential, as a low potential of the mediator in the anode can increase the potential difference between the

electron donor (anode potential) and the electron acceptor (cathode potential) in MFCs. The redox potential of the AQS grafted on electrode surface in this study (-0.248 V vs. NHE) was a little higher than $NAD^+$/NADH redox potential, which indicated that it was an ideal mediator for electron transfer from NADH to the anode surface. As a result, this novel anode facilitated the extracellular electron transfer and accordingly enhanced the power production in MFCs.

### 3.3.3 Stability of the AQS modified anode in MFCs

The stability of anode material is also significant for MFCs, especially for the long term operation. Therefore, the stability of this modified anode was investigated by two approaches.

First, the stability was examined by operating the MFCs over a period of two months. In the last batch of this period, the maximum power density of the MFCs with AQS modified anode was still as high as $1701 \pm 47$ mW/m$^2$ (Figure 3.4). Compared with the power density in the first batch, this value was only approximately 9.1% drop compared with the first batch of this period. The open circuit potential of this AQS modified anode in the MFCs at the beginning, day 30 and 2 months was -0.237 V, -0.228 V and -0.215 V (vs. NHE) respectively, while the corresponding value of the cathode was 0.472 V, 0.466 V and 0.458 V (vs. NHE) respectively. These results demonstrated that the maximum power density drop was because of the joint effects of both

anode and cathode. The fouling of the cathode catalyst decreased the cathode potential while the anode potential increased due to the instability of the anode material. However, the total 9.1% decrease of the maximum power density over the period of 2 months demonstrated that AQS modified anode had good stability and the novel anode could be used for long term operation in MFCs.

The stability of the AQS modified graphite was further studied by CV. The peak current of the newly AQS modified graphite and the AQS modified graphite utilized as anode in MFCs for 30 days and 2 months was compared (Figure 3.2). Prior to the CV test, the anode was removed from the MFCs and then it was sonicated for 30 min and followed by rinsing with 1 M NaOH and DI water to thoroughly remove the biofiom formed on anode surface. After immersing in anolyte of the MFCs for 30 days, the anodic peak current maintained 90.6±3.3% of the initial value and the cathodic peak current preserved 94.4±2.7% of the initial value. After 2 months, the anodic peak current still maintained 90.1±2.4% of the initial values while the cathodic peak current preserved 90.4±2.9% of the initial value. These results further showed that AQS modified graphite felt anode was very stable during the long term operation of MFCs.

### 3.4 Conclusion

AQS, an electron transfer mediator, was covalently grafted onto graphite felt surface *via* spontaneous reduction of the *in situ* generated AQS diazonium

cations. The AQS grafted on graphite felt had a surface concentration of 5.37 $\pm 1.15\times10^{-9}$ mol/cm$^2$. This AQS modified graphite felt displayed good electrochemical activity during CV tests. AQS modified graphite felt anode used in MFCs considerably increased the maximum power density from $967\pm33$ mW/m$^2$ to $1872\pm42$ mW/m$^2$. Stability tests demonstrated that the AQS modified graphite felt anode had good stability in long term operation in MFCs. This study demonstrates that graphite felt anode covalently grafted with AQS *via* spontaneous reduction of its diazonium cation is a simple, effective and environmentally friendly strategy to facilitate extracellular electron transfer and consequently to enhance the power production in MFCs.

### 3.5 References


1. Nimje, V. R., Chen, C. Y., Chen, H. R., Chen, C. C., Huang, Y. M., Tseng, M. J., Cheng, K. C., and Chang, Y. F. (2012) Comparative bioelectricity production from various wastewaters in microbial fuel cells using mixed cultures and a pure strain of Shewanella oneidensis, *Bioresource Technology 104*, 315-323.
2. Zhuang, L., Yuan, Y., Wang, Y. Q., and Zhou, S. G. (2012) Long-term evaluation of a 10-liter serpentine-type microbial fuel cell stack treating brewery wastewater, *Bioresource Technology 123*, 406-412.
3. Chang, I. S., Moon, H., Jang, J. K., and Kim, B. H. (2005) Improvement of a microbial fuel cell performance as a BOD sensor using respiratory inhibitors, *Biosensors & Bioelectronics 20*, 1856-1859.
4. Zhang, Y. F., and Angelidaki, I. (2012) Self-stacked submersible microbial fuel cell (SSMFC) for improved remote power generation

from lake sediments, *Biosensors & Bioelectronics 35*, 265-270.

5. Dong, K., Jia, B. Y., Yu, C. L., Dong, W. B., Du, F. Z., and Liu, H. (2013) Microbial fuel cell as power supply for implantable medical devices: A novel configuration design for simulating colonic environment, *Biosensors & Bioelectronics 41*, 916-919.
6. Oh, S. E., and Logan, B. E. (2005) Hydrogen and electricity production from a food processing wastewater using fermentation and microbial fuel cell technologies, *Water Research 39*, 4673-4682.
7. Rabaey, K., Boon, N., Hofte, M., and Verstraete, W. (2005) Microbial phenazine production enhances electron transfer in biofuel cells, *Environmental Science & Technology 39*, 3401-3408.
8. Srikanth, S., and Mohan, S. V. (2012) Influence of terminal electron acceptor availability to the anodic oxidation on the electrogenic activity of microbial fuel cell (MFC), *Bioresource Technology 123*, 480-487.
9. Schroder, U. (2007) Anodic electron transfer mechanisms in microbial fuel cells and their energy efficiency, *Physical Chemistry Chemical Physics 9*, 2619-2629.
10. Chaudhuri, S. K., and Lovley, D. R. (2003) Electricity generation by direct oxidation of glucose in mediatorless microbial fuel cells, *Nature Biotechnology 21*, 1229-1232.
11. Bond, D. R., and Lovley, D. R. (2003) Electricity production by Geobacter sulfurreducens attached to electrodes, *Applied and Environmental Microbiology 69*, 1548-1555.
12. Kim, H. J., Park, H. S., Hyun, M. S., Chang, I. S., Kim, M., and Kim, B. H. (2002) A mediator-less microbial fuel cell using a metal reducing bacterium, Shewanella putrefaciense, *Enzyme and Microbial Technology 30*, 145-152.
13. Gorby, Y. A., Yanina, S. V., Moyles, D., McLean, J. S., Rosso, K. M.,

Beveridge, T. J., Kennedy, D. W., Marshall, M. J., Dohnalkova, A., Beliaev, A., Fredrickson, J. K., and Nealson, K. (2006) NUCL 74-Bacterial nanowires: Electrically conductive, redox-reactive appendages produced by dissimilatory metal reducing bacteria, *Abstracts of Papers of the American Chemical Society 232*.

14. Ringeisen, B. R., Henderson, E., Wu, P. K., Pietron, J., Ray, R., Little, B., Biffinger, J. C., and Jones-Meehan, J. M. (2006) High Power Density from a Miniature Microbial Fuel Cell Using Shewanella oneidensis DSP10, *Environmental Science & Technology 40*, 2629-2634.
15. Rabaey, K., Boon, N., Siciliano, S. D., Verhaege, M., and Verstraete, W. (2004) Biofuel cells select for microbial consortia that self-mediate electron transfer, *Applied and Environmental Microbiology 70*, 5373-5382.
16. Lowy, D. A., Tender, L. M., Zeikus, J. G., Park, D. H., and Lovley, D. R. (2006) Harvesting energy from the marine sediment-water interface II - Kinetic activity of anode materials, *Biosensors & Bioelectronics 21*, 2058-2063.
17. Lowy, D. A., and Tender, L. M. (2008) Harvesting energy from the marine sediment-water interface III. Kinetic activity of quinone- and antimony-based anode materials, *Journal of Power Sources 185*, 70-75.
18. Park, D. H., and Zeikus, J. G. (2003) Improved fuel cell and electrode designs for producing electricity from microbial degradation, *Biotechnology and Bioengineering 81*, 348-355.
19. Seinberg, J. M., Kullapere, M., Maeorg, U., Maschion, F. C., Maia, G., Schiffrin, D. J., and Tammeveski, K. (2008) Spontaneous modification of glassy carbon surface with anthraquinone from the solutions of its diazonium derivative: An oxygen reduction study, *Journal of*

*Electroanalytical Chemistry 624*, 151-160.

20. Kullapere, M., Marandi, M., Sammelselg, V., Menezes, H. A., Maia, G., and Tammeveski, K. (2009) Surface modification of gold electrodes with anthraquinone diazonium cations, *Electrochemistry Communications 11*, 405-408.
21. Mahouche-Chergui, S., Gam-Derouich, S., Mangeney, C., and Chehimi, M. M. (2011) Aryl diazonium salts: a new class of coupling agents for bonding polymers, biomacromolecules and nanoparticles to surfaces, *Chemical Society Reviews 40*, 4143-4166.
22. Rau, J., Knackmuss, H. J., and Stolz, A. (2002) Effects of different quinoid redox mediators on the anaerobic reduction of azo dyes by bacteria, *Environmental Science & Technology 36*, 1497-1504.
23. Crittenden, S. R., Sund, C. J., and Sumner, J. J. (2006) Mediating electron transfer from bacteria to a gold electrode via a self-assembled monolayer, *Langmuir 22*, 9473-9476.
24. Aulenta, F., Ferri, T., Nicastro, D., Majone, M., and Papini, M. P. (2011) Improved electrical wiring of microbes: anthraquinone-modified electrodes for biosensing of chlorinated hydrocarbons, *New Biotechnology 29*, 126-131.
25. Cheng, S., Liu, H., and Logan, B. E. (2006) Power densities using different cathode catalysts (Pt and CoTMPP) and polymer binders (Nafion and PTFE) in single chamber microbial fuel cells, *Environmental Science & Technology 40*, 364-369.
26. Lovley, D. R., and Phillips, E. J. P. (1988) Novel Mode of Microbial Energy-Metabolism - Organic-Carbon Oxidation Coupled to Dissimilatory Reduction of Iron or Manganese, *Applied and Environmental Microbiology 54*, 1472-1480.
27. Abdelwahab, A. A., Jung, O. S., and Shim, Y. B. (2009) Enhanced electrocatalytic reduction of oxygen with a molecule having

multi-quinone moieties adsorbed in the nanofiber film, *Journal of Electroanalytical Chemistry 632*, 102-108.

28. Guo, K., Chen, X., Freguia, S., and Donose, B. C. (2013) Spontaneous modification of carbon surface with neutral red from its diazonium salts for bioelectrochemical systems, *Biosensors & Bioelectronics 47*, 184-189.

29. Park, D. H., and Zeikus, J. G. (1999) Utilization of electrically reduced neutral red by Actinobacillus succinogenes: Physiological function of neutral red in membrane-driven fumarate reduction and energy conservation, *Journal of Bacteriology 181*, 2403-2410.

30. Park, D. H., and Zeikus, J. G. (2000) Electricity generation in microbial fuel cells using neutral red as an electronophore, *Applied and Environmental Microbiology 66*, 1292-1297.

31. Adachi, M., Shimomura, T., Komatsu, M., Yakuwa, H., and Miya, A. (2008) A novel mediator-polymer-modified anode for microbial fuel cells, *Chemical Communications*, 2055-2057.

# Chapter 4 Polyaniline and iron based catalysts as air cathodes for enhanced oxygen reduction in microbial fuel cells

## 4.1 Introduction

As a novel environmental biotechnology, MFCs have expanded the applications from wastewater treatment to biochemical oxygen demand detection, toxicity detection, sea water desalination, power supply, and chemical synthesis (1-7). In order to improve these applications, most of the studies focus on the electrochemically active bacteria, the extracellular electron transfer mechanisms from bacteria to anode surface, anode material design and MFC configuration (8-11). However, the cathode research was almost neglected in the early study of MFCs.

Although ferricyanide, $MnO_4^-$, $NO_3^-$, $ClO_4^-$, $Cu^{2+}$, $Cr_2O_7^{2-}$ and $Ag^+$ have also been used as electron acceptor in MFCs (12-13). These electron acceptors are not sustainable and they should be routinely supplied during the operation. Currently, oxygen has become the dominant electron acceptor in MFCs due to its positive redox potential, the harmlessness of the reduction product ($H_2O$), the virtually inexhaustible availability and the low cost. As a result, oxygen reduction reaction (ORR) is the only cathode reaction practically feasible for electricity production in MFCs.

ORR rate, however, is now a bottleneck for power production in MFCs due to the unfavorable reaction condition: ambient temperature, almost neutral pH and small concentration of supporting electrolytes (14). Just as stated in chapter 1, the cathode overpotential of ORR resulting from kinetic loss and

side reaction loss in MFCs is very large, which considerably brings down the cell voltage and the power production. The use of high-performance catalyst is the best solution to solve this problem (14).

So far, platinum-based catalysts have been widely used in MFCs due to their high catalytic activity towards oxygen reduction reaction. These noble catalysts, however, can amount to almost half of the total construction cost of the MFC reactor (15). The cost of MFC reactor has to be reduced to enhance its competition for other wastewater treatment technology such as aerobic treatment and fermentation (15-16). In addition, the scarcity of platinum also requires the development of novel alternatives. As a result, the exploration of non-precious metal catalyst with high catalytic activity towards oxygen reduction reaction is currently a major issue in MFC research.

Recently, transition metal-nitrogen-carbon catalysts (M/N/C) prepared under high temperature have attracted lots of attention due to their excellent catalytic activity and remarkable stability towards oxygen reduction in fuel cells (17-19). For M/N/C catalyst, surface nitrogen, transition metal and micropores are considered to be critical for the active catalytic sites formation on catalyst surface (18). Consequently, the catalytic activities of these materials strongly depend on the carbon and nitrogen sources and the synthesis condition. These catalysts have exhibited good electrocatalytic activity for oxygen reduction in fuel cells, such as the high selectivity of the four-electron reaction pathway and the very positive onset potential (17, 19). A more positive onset potential means a smaller overpotential and a larger cell voltage output, which improves the cathode performance in a cell system. Further, the two-electron reaction competes with the four-electron reaction in oxygen reduction, which not only

lowers the theoretical cathode potential, but also generates hydrogen peroxide, which causes damages to electrode material, membrane and even electrochemically active bacteria (20). Therefore, a catalyst with excellent selectivity for four-electron reaction is desirable for enhanced cathode performance in MFCs. As a result, this type of catalyst may find its application as an ideal cathode catalyst for MFCs to bring down the construction cost and improve the cathode performance.

In this report, non-precious metal catalysts were prepared by pyrolyzing iron containing polyaniline (PANI) under high temperature in $NH_3$ atmosphere. PANI was employed as both nitrogen and carbon precursor because it offered a uniform and enhanced distribution of nitrogen on the surface. These catalysts were comprehensively examined by field emission scanning electron microscope (FESEM), nitrogen physisorption, elemental analysis, X-ray photoelectron spectroscopy (XPS), and electrochemical measurement. These catalysts were further used as air cathodes to study their performance for electricity production in MFCs. Besides, an explanation for the high catalytic activity toward oxygen reduction was proposed. This study demonstrated that these catalysts are excellent cathode for MFCs.

## 4.2 Experimental section

### 4.2.1 Catalysts preparation

Two catalysts, labeled as PANI-$Fe_{900}$ and PANI-$Fe_{700}$, were synthesized by heat treatment of iron incorporated polyaniline in $NH_3$ under 900℃ and 700 ℃ respectively. In short, distilled aniline (4.5 mL) and $Fe_2SO_4$ (0.15 g) were dispersed in $H_2SO_4$ solution (300 mL, 0.5 M) *via* stirring and then the

suspension was ice cooled below 5℃. After that, $(NH_4)_2S_2O_8$ was trickled into the suspension to initiate the polymerization of aniline. When polymerization was finished, this dark green sample was leached in $H_2SO_4$ solution, rinsed completely with deionized (DI) water, and then dried in air. Finally, the sample was heat-treated in $NH_3$ atomosphere under high temperature (900℃ and 700 ℃ respectively) for 30 min and the catalysts were obtained. Another catalyst, labeled as $PANI_{900}$, was also synthesized using the same pyrolysis method under 900℃, but without the incorporation of iron.

### 4.2.2 Electrode preparation

The catalytic activity of these catalysts was measured by a glassy rotating ring disk electrode (RRDE). The RRDE was first polished by aluminas to obtain a smooth surface, and then sonicated in Milli-Q water, and finally dried in the air. Coating of catalysts onto RRDE and MFC cathodes (graphite felt) was carried out as previously described (21). In brief, catalyst powder was first dispersed well in a mixture solution of Nafion and ethanol. Next, this ink solution was uniformly coated onto the RRDE or the graphite felt surface and then dried in the air. For comparison, commercially available platinum supported on carbon black (Pt/C) was also uniformly coated onto RRDE and cathode surface. The loading of non-precious metal catalyst and Pt/C on RRDE were 0.6 $mg/cm^2$ and 20$\mu g_{Pt}/cm^2$, respectively.

### 4.2.3 Air cathode MFC construction and operation

Single-chambered MFC reactors (empty bed volume of approximately 100 mL) were used in this study (22). Graphite felt worked as anode at the bottom of the

reactor, while graphite felt coated with catalysts served as air cathode at the top of the reactor. The as-prepared catalyst and the Pt/C catalyst had a loading of 2 $mg/cm^2$ and 0.5 $mg_{Pt}/cm^2$, respectively. A bare cathode without any coating was also utilized for control. The anode and cathode were connected *via* titanium wire across an external resistance of 500 Ω.

MFCs were inoculated with mixed bacteria from another stably running MFC in the laboratory (23). The electrolyte contained KCl (0.13 g/L), NaCl (2.9 g/L), $NH_4Cl$ (0.31g/L), metal salt (12.5 mL/L), vitamin (5 mL/L) and phosphate buffer (50 mM, pH 7) (24). Sodium acetate (10 mM), a widely used substrate, was added into MFC reactors as electron donor.

MFCs were operated in a fed-batch mode at 30 ℃ and the feeding solutions were replaced once the voltage output fell below 40 mV, which was considered as the ending of a cycle for electricity generation.

### 4.2.4 Calculation and analysis

Field emission scanning electron microscopy (FESEM) (JSM-6701F, JEOL) was used to examine the morphology of the catalysts. Specific surface area and micropore area were investigated by nitrogen physisorption (ASAP 2010, Micromeritics). Eelectron probe microanalyzer (JXA-8100, JEOL) was applied to measure the iron content. Element analyzer (Vario EL cube) was utilized to examine the nitrogen content in these catalysts. The electronic states of the nitrogen were studied by XPS (ESCALab, 220i-XL).

Linear sweep voltammograms (LSV) using RRDE (PINE, 5.61 mm of disk diameter) was applied to investigate the catalytic activity of these catalysts

towards oxygen reduction at room temperature. The LSV tests were carried out by an electrochemical workstation (CHI, 760B) in a conventional three-electrode system in oxygen saturated $H_2SO_4$ solution (0.5 M). LSV was performed at a potential scan rate of 10mV/s with the disk rotating speed of 900 rpm. RRDE electrode coated with catalyst worked as the working electrode, whereas an Ag/AgCl electrode (KCl saturated) was used as the reference electrode and a platinum foil electrode was utilized as the counter electrode. The ring potential was set at 1.0 V (vs. Ag/AgCl) during the tests. All the potentials were later converted into the reversible hydrogen electrode (RHE) scale.

RRDE experiment was also used to investigate the selectivity of these catalysts towards oxygen reduction reaction. The four-electron selectivity was evaluated by the percentage of the hydrogen peroxide yield during oxygen reduction, which was calculated by the equation: $H_2O_2\%=200\times I_R/(I_R+NI_D)$, in which $I_D$ was the disk current, $I_R$ was the ring current, and N was collection efficiency of the ring (37%) (17, 25).

A data acquisition system was used to measure and store the cell voltage output (U). The maximum power densities were acquired by varying the external resistance (R) from 10 to 2000 Ω, when MFCs became steady and reproducible in electricity generation. Power density (P) was measured by the equation on the basis of the total volume (V) of the reactor: $P = U^2/(R\times V)$.

## 4.3 Results and Discussion

### 4.3.1 Electrochemical characterization of the catalysts

LSV measurements were carried out to study the catalytic activity as well as the associated reduction pathways of these catalysts towards oxygen reduction in comparison with Pt/C.

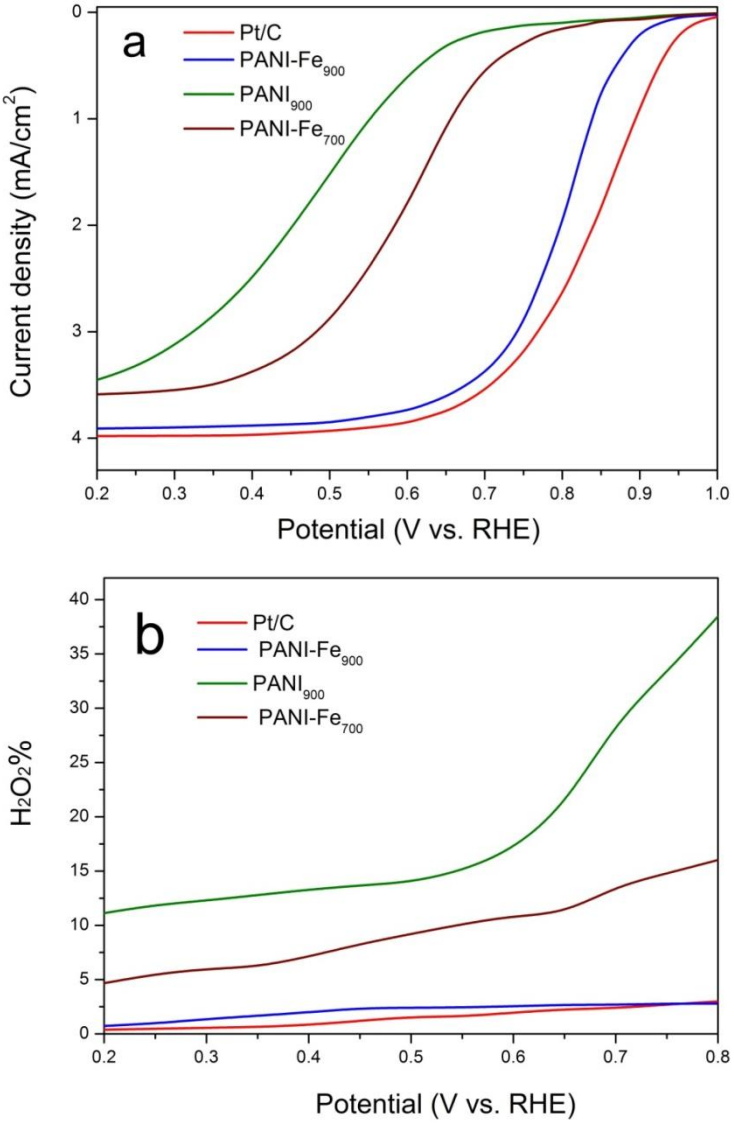


Figure 4. 1 Disk current (a) and $H_2O_2$ yield (b) plots during oxygen reduction reaction in oxygen saturated $H_2SO_4$ solution (0.5 M) (scan rate: 10 mV/s; rotating speed: 900 rpm).

The onset potential was a key criterion to evaluate the catalytic activity of

these catalysts toward ORR. The results of the LSV with a RRDE showed in Figure 4.1a indicated that the onset potential increased in the following order: $PANI_{900}$＜PANI-$Fe_{700}$＜PANI-$Fe_{900}$＜Pt/C. Specifically, the onset potential of PANI-$Fe_{900}$was as high as 0.92 V (vs. RHE), which was almost the same as the onset potential exhibited by the state-of-the-art Pt/C. The onset potential of the cathode determined cell performance once the anode was fixed. A more positive onset potential meant a smaller overpotential, a higher cathode potential, and consequently a larger cell voltage. In addition, the current density also increased in the above order. In fact, the current density of PANI-$Fe_{900}$ was very close to the value of Pt/C. This high current density indicated thatPANI-$Fe_{900}$ significantly enhanced the kinetic of the ORR. The very positive onset potential as well as the high current density of PANI-$Fe_{900}$ demonstrated that it had high catalytic activity towards oxygen reduction. As a result, it was expected to be a good alternative for Pt/C in MFCs.

As described in chapter 1, ORR proceeds either *via* a four-electron pathway to form water or *via* a two-electron pathway to generate hydrogen peroxide. The theoretical potential of the four-electron reaction of ORR is 1.229 V (vs. RHE) under standard condition, while the value is only 0.695 V (vs. RHE) for the two-electron reaction to produce hydrogen peroxide (14). Therefore, the four-electron reaction is the target reaction in MFCs for power production. However, the undesirable two-electron reaction competes with the target four-electron reaction, which also causes the formation of a mixed theoretical

potential lying between 0.695 V (vs. RHE) and 1.229 V (vs. RHE) and consequently reduces the cathode potential (26). In addition, $H_2O_2$ is a corrosive agent, which will be harmful to cathode catalyst, membrane and even electrochemically active bacteria (20). As such, cathode catalyst with high selectivity for the four-electron reaction is desired for MFCs. In this study, the selectivity for the desired four-electron reaction of ORR was investigated by the RRDE experiments.

The hydrogen peroxide yield percentage showed in Figure 4.1b indicated that it decreased in the following order: $PANI_{900}$ > PANI-$Fe_{700}$ > PANI-$Fe_{900}$ > Pt/C. For $PANI_{900}$ and PANI-$Fe_{700}$, the hydrogen peroxide yield percentage ranged from 5%-40%, indicating that the two-electron reaction of ORR occurred in a great extent. However, the hydrogen peroxide yield on the surface of PANI-$Fe_{900}$ and Pt/C was less than 3% in the full potential range. This study demonstrated that both PANI-$Fe_{900}$ and Pt/C had high selectivity for the four-electron reaction of ORR.

RRDE experiments also revealed that $H_2O_2$ production of PANI-$Fe_{900}$ was comparable to that of Pt/C. The less than 3% yield of hydrogen peroxide in the full potential range indicated that oxygen reduction reaction on PANI-$Fe_{900}$ proceeds predominantly via the four-electron pathway. Therefore, PANI-$Fe_{900}$ was an excellent alternative for Pt/C and was highly anticipated to enhance the cathode potential, the cell voltage and the overall performance of MFCs.

### 4.3.2 Performance of the catalysts in MFCs

After the electrochemical measurements, these catalysts were further utilized as cathodes in MFCs to study their performance for electricity production. For comparison, bare cathode without catalyst coating and the benchmark Pt/C catalyst were also investigated as controls in MFCs.

Figure 4.2 was the polarization curves and the power density curves. As shown in Figure 4.2 and Table 4.1, the maximum power density of the MFCs with $PANI_{900}$, $PANI\text{-}Fe_{700}$, and $PANI\text{-}Fe_{900}$were 3.00 $W/m^3$, 7.45 $W/m^3$, and 12.54 $W/m^3$, respectively. This result was consistent with their catalytic activity measured in RRDE tests. For comparison, the bare cathode MFC only produced a maximum power density of 1.32 $W/m^3$, while the Pt/C cathode MFC had a maximum power density of 10.03 $W/m^3$. These results demonstrate that these catalysts, especially $PANI\text{-}Fe_{900}$, significantly enhanced the power density of MFCs. The enhancement was attributed to the improved cell voltage and the reduced internal resistance (Table 4.1). Particularly, the open circuit voltage of the $PANI\text{-}Fe_{900}$ cathode MFC was 0.72 V, whereas the corresponding value was 0.43 V for the bare cathode MFC and 0.73 V for the Pt/C cathode MFC.

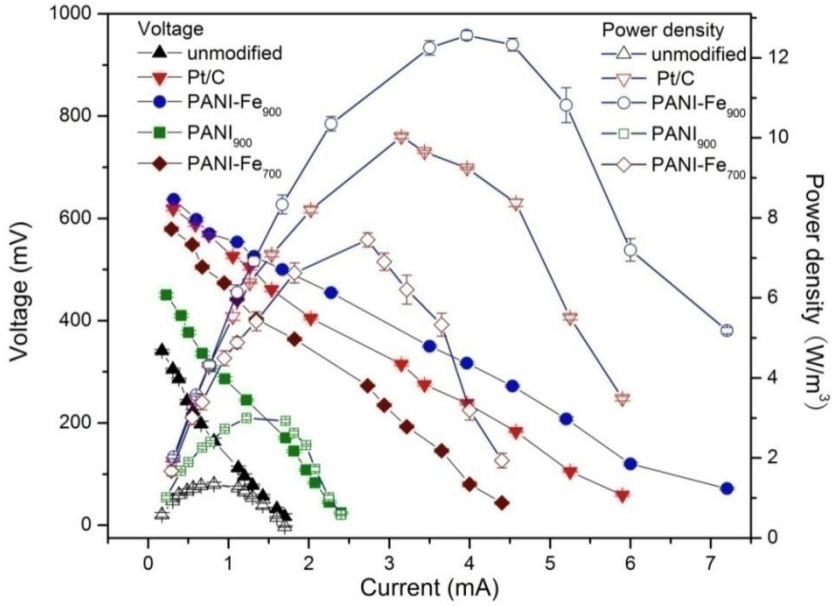


Figure 4. 2 Polarization (solid symbols) and power density (empty symbols) curves of the MFCs with different cathodes.

The internal resistance obtained from the slope of the polarization curves (Figure 4.2) was 84 Ω, 210 Ω and 99 Ω for the PANI-$Fe_{900}$ cathode MFC, bare cathode MFC and Pt/C cathode MFC, respectively. Compared with the bare cathode, the increased open circuit voltage, the reduced internal resistance and the enhanced power density suggested that PANI-$Fe_{900}$ significantly improved the cathode performance for electricity production in MFCs.

Table 4. 1 Performances of the air-cathode MFCs with different catalysts.

| Cathodes | Open circuit voltage (V) | Internal resistance (Ω) | Maximum power density ($W/m^3$) |
|---|---|---|---|
| PANI-$Fe_{900}$ | 0.72 | 84 | 12.54 |
| $PANI_{900}$ | 0.49 | 185 | 3.00 |
| PANI-$Fe_{700}$ | 0.65 | 126 | 7.45 |
| Bare | 0.43 | 210 | 1.32 |
| Pt/C | 0.73 | 99 | 10.03 |

The stability of the cathode catalyst is another key property that needs to be

seriously considered in MFCs. In this study, the stability of these catalysts was measured by running the MFCs over a period of four months. During this period, the maximum power density of the PANI-$Fe_{900}$ MFC declined from 12.54 $W/m^3$ to 11.63 $W/m^3$, approximately 7.3% deterioration. For comparison, the maximum power density of the Pt/C MFC decreased from 10.03 $W/m^3$ to 9.19 $W/m^3$, a drop of about 8.4%. This result demonstrated that PANI-$Fe_{900}$ possessed good stability for long term operation in MFCs.

Besides catalytic activity and stability, the cost is another criterion for the evaluation of the cathode in MFCs (26). The cost of PANI-$Fe_{900}$ prepared here is approximately 0.08 US dollar per gram, which is less than 1% of the commercially available Pt based catalyst (Table 4.2). Though the price of $Fe_2O_3$ is very close to PANI-$Fe_{900}$, its power density in MFCs is much smaller than PANI-$Fe_{900}$ (22). Compared with nitrogen doped grapheme and nitrogen doped carbon nanosheet, PANI-$Fe_{900}$ produced much higher power density (27-28). As mentioned above, Pt/C cathode accounts for nearly half of the construction cost of the MFC reactor, which limits the large-scale applications of this technology. Therefore, this low-cost and high-performance catalyst is an excellent candidate to replace the noble Pt/C to bring down the construction cost of MFCs.

Table 4. 2 Cost and power density of some cathode catalysts in MFCs.

| Cathode catalysts | Price (US dollar/g) | Power density($W/m^3$) | Reference |
|---|---|---|---|
| PANI-$Fe_{900}$ | 0.08 | 12.54 | This study |

| | | | |
|---|---|---|---|
| Pt | 35.6 | 10.03 | This study |
| $Fe_2O_3$ | 0.13 | 0.93 | (22) |
| Nitrogen doped graphene | N/A | 6.98 | (27) |
| Nitrogen doped carbon nanosheet | N/A | 5.13 | (28) |

### 4.3.3 Understanding of the high catalytic activity by physical and chemical characterization

Physical and chemical characterizations were carried out to explore the intrinsic properties of these catalysts, which helped to explain the high catalytic activity of these catalysts towards oxygen reduction reaction.

FESEM images of the as-prepared catalysts were showed in Figure 4.3, which demonstrated that these catalysts exhibited highly microporous structures, especially the catalysts pyrolyzed under 900℃. The specific surface area and the micropore area of these catalysts tested by the multiple point BET method were summarized in Table 4.3. PANI-$Fe_{900}$ and $PANI_{900}$ had quite high surface area and micropore area, while PANI-$Fe_{700}$ displayed relatively lower values. All of the catalysts, however, only had a specific surface area of 12.8 $m^2/g$ before the pyrolysis treatment. Therefore, pyrolysis treatment in $NH_3$ atmosphere under high temperature significantly enhanced the surface area of these catalysts.

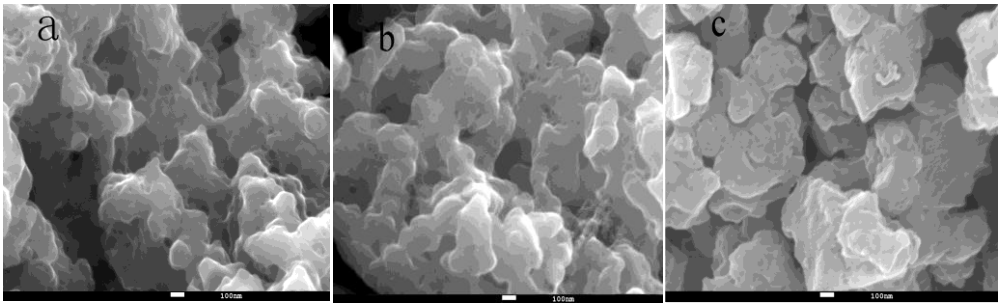


Figure 4. 3 FESEM images of the non-precious metal catalysts: a. PANI-$Fe_{900}$; b. $PANI_{900}$; and c. PANI-$Fe_{700}$.

The enhancement was the result of the etching effect of $NH_3$, which reacted with carbon to produce volatile compounds and create large number of micropores (19). On the one hand, a high surface area provided sufficient interface for the adsorption of oxygen, which would inevitably enhance the kinetic of the ORR on the catalyst surface. On the other hand, the active sites in these catalysts for oxygen reduction were considered to be hosted in micropores generated during the pyrolysis treatment (18, 29).Therefore, a higher surface area and micropore area indicated a higher catalytic activity. In this study, the specific surface area and micropore area of PANI-$Fe_{900}$ were higher than PANI-$Fe_{700}$, which elucidated the result that PANI-$Fe_{900}$ exhibited higher catalytic activity than PANI-$Fe_{700}$.

Table 4. 3 Specific surface area, micropore area, iron and nitrogen content in catalysts.

| Catalyst | Surface area ($m^2/g$) | Micropore area ($m^2/g$) | Iron content (wt%) | Nitrogen content (wt%) |
|---|---|---|---|---|
| PANI-$Fe_{900}$ | 769.8 | 570.5 | 0.72 | 5.26 |
| $PANI_{900}$ | 752.1 | 561.4 | 0 | 5.37 |
| PANI-$Fe_{700}$ | 541.5 | 388.6 | 0.68 | 5.92 |

Transition metal was also crucial for the catalytic activity of the catalysts

prepared in this study. Both PANI-$Fe_{900}$ and $PANI_{900}$ showed similar micropore area, specific surface area, nitrogen content and even the relative intensity of each nitrogen species (Table 4.3 and Table 4.4). PANI-$Fe_{900}$, however, exhibited considerably higher catalytic activity than $PANI_{900}$, as suggested by the more positive onset potential and the much higher current density in RRDE tests, the greatly higher selectivity for the four-electron reaction and the considerably enhanced higher power density in MFCs. One mechanism to explain the role of iron in Fe/N/C catalysts was that iron was coordinated with nitrogen in compounds such as $FeN_4$ and $FeN_2$ to form the active sites, which effectively facilitated oxygen reduction reaction (30-32). Therefore, iron served as active sites and played a critical role in enhancing oxygen reduction reaction in PANI-$Fe_{900}$.

Nitrogen content measured by elemental analysis was listed in Table 4.3 for the three catalysts. Nitrogen content in PANI was about 17%.The nitrogen content, however, decreased to about 5-6% after pyrolysis treatment. The decrease of nitrogen content was because of the gasification of nitrogen-containing fragments by $NH_3$ under high temperature pyrolysis.

Table 4. 4 Nitrogen species and their relative intensity in the catalysts

| Catalyst | N species | Binding energy (eV) | Relative Intensity (%) | Content (wt%) |
|---|---|---|---|---|
| PANI-$Fe_{900}$ | pyridinic N | 398.3 | 37.5 | 1.97 |
| | pyrrolic N | 400.7 | 46.7 | 2.46 |
| | oxidized N | 403.8 | 15.8 | 0.83 |
| $PANI_{900}$ | pyridinic N | 398.4 | 37.1 | 1.99 |

| | | | | |
|---|---|---|---|---|
| | pyrrolic N | 400.7 | 32.9 | 1.77 |
| | oxidized N | 403.2 | 30.0 | 1.61 |
| PANI-$Fe_{700}$ | pyridinic N | 398.4 | 22.8 | 1.35 |
| | pyrrolic N | 400.5 | 62.6 | 3.71 |
| | oxidized N | 403.5 | 14.6 | 0.86 |

The electronic states of the nitrogen on catalysts were examined by XPS. The deconvoluted N1s spectra showed in Figure 4.4 exhibited that three types of nitrogen species were present in these catalysts, namely pyridinic nitrogen, pyrrolic nitrogen and oxidized nitrogen. The binding energy, relative intensity and content of these nitrogen species were also summarized in Table 4.4. The relative intensity of pyridinic nitrogen in PANI-$Fe_{900}$ (37.5%) and $PANI_{900}$ (37.1%) was much higher than that in PANI-$Fe_{700}$ (22.8%), while the relative intensity of pyrrolic nitrogen in PANI-$Fe_{700}$ (62.6%) was much higher than the value in both PANI-$Fe_{900}$ (46.7%) and $PANI_{900}$ (32.9%).

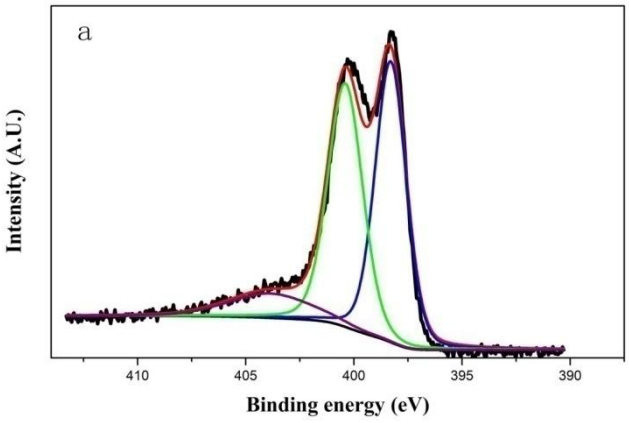

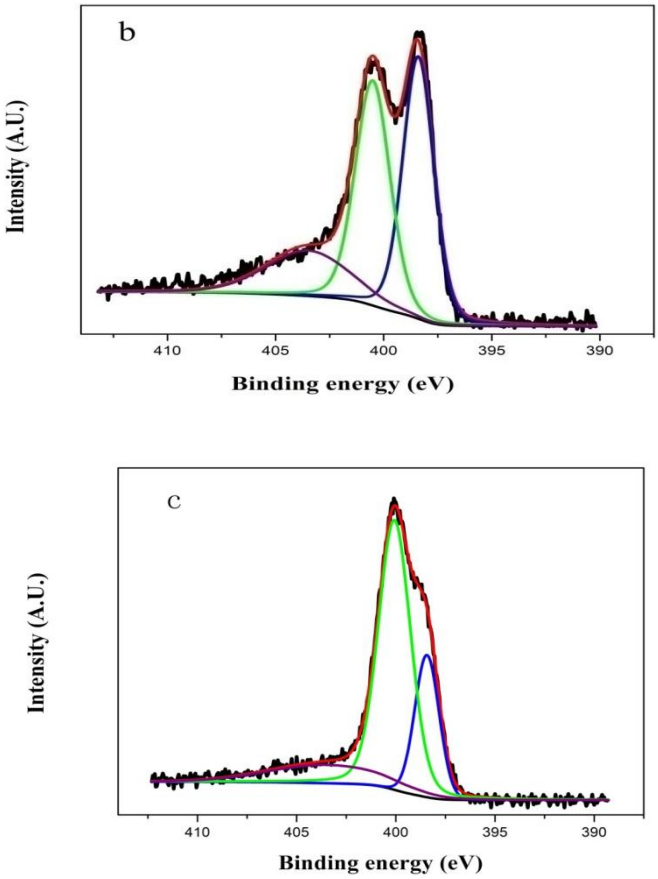


Figure 4. 4 The deconvoluted high resolution N1s X-ray photoelectron spectra for the catalysts: a. PANI-$Fe_{900}$; b. $PANI_{900}$; and c. PANI-$Fe_{700}$.

Nitrogen was essential for the catalysis of oxygen reduction reaction in M/N/C catalysts. As mentioned above, transition metal coordinated with nitrogen to form the catalytic active sites (18, 31). Jaouen et al. prepared 19 types of M/N/C catalysts with nitrogen content in the range of 0.3% to 2.5%, and they demonstrated that the catalytic activity increased in proportion to nitrogen content in these materials, as higher nitrogen content resulted in higher active site density (31). The highest onset potential was about 0.8 V (vs. RHE) in $H_2SO_4$ solution (0.5 M) in that report, while the onset potential reached 0.92 V (vs. RHE) in this study. The nitrogen content of the catalysts prepared here was about 5-6%, which explained their high performance of these catalysts for

oxygen reduction.

Previous studies of M/N/C catalysts revealed that the active sites were made of pyridinic nitrogen, rather than pyrrolic nitrogen or oxidized nitrogen hosted in micropores (18, 31, 33-34). Pyridinic nitrogen was able to coordinate the iron to form the active sites, which reduced the oxygen primarily via the four-electron pathway (17, 32). Besides, pyridinic nitrogen could impart a positive charge on neighboring carbon atoms, and this charge delocalization could alter oxygen adsorption from the typical end-on chemisorption (Pauling mode) to side-on chemisorption (Yeager model), which efficiently weakened the bonding of O-O and facilitated oxygen reduction rate (35). In this study, PANI-$Fe_{900}$displayed higher pyridinic nitrogen content and lower pyrrolic and oxidized nitrogen content than PANI-$Fe_{700}$. Therefore, the result that PANI-$Fe_{900}$ exhibited higher catalytic activity than PANI-$Fe_{700}$ was due to its higher pyridinic nitrogen content, because a higher pyrdinic N content meant a higher active site density.

The positive onset potential and the high current density in RRDE experiments, the excellent selectivity of the four-electron reaction and the high performance in MFCs demonstrate that these catalysts are highly active towards oxygen reduction. This high electrocatalytic activity was due to the active sites formed by iron coordinated with pyridinic nitrogen in micropores during pyrolysis at high temperature. Therefore, microporous structure, iron and pyridinic nitrogen are the key requirements for these catalysts.

## 4.4 Conclusion

In this chapter, high-performance and low-cost catalysts towards oxygen reduction reaction in the cathode of MFCs were prepared by pyrolyzing iron containing polyaniline at high temperature in $NH_3$ atmosphere. Electrochemical tests showed that these catalysts displayed very positive onset potential, high current density, and excellent selectivity for the four-electron reaction towards ORR. Particularly, PANI-$Fe_{900}$ exhibited a catalytic activity that was comparable to the benchmark Pt/C catalyst. PANI-$Fe_{900}$ significantly enhanced the power production in MFCs from 1.32 W/$m^3$ to 12.54 W/$m^3$, and PANI-$Fe_{900}$ showed excellent stability during the long term operation of the MFCs. Physical and chemical characterizations of the catalysts indicated that iron coordinated with pyridinic nitrogen hosted in micropores was responsible for the high catalytic activity. This study demonstrates that these high-performance but low-cost catalysts are excellent cathode for MFC applications.

## 4.5 References


1. Nimje, V. R., Chen, C. Y., Chen, H. R., Chen, C. C., Huang, Y. M., Tseng, M. J., Cheng, K. C., and Chang, Y. F. (2012) Comparative bioelectricity production from various wastewaters in microbial fuel cells using mixed cultures and a pure strain of Shewanella oneidensis, *Bioresource Technology 104*, 315-323.
2. Zhuang, L., Yuan, Y., Wang, Y. Q., and Zhou, S. G. (2012) Long-term evaluation of a 10-liter serpentine-type microbial fuel cell stack treating brewery wastewater, *Bioresource Technology 123*, 406-412.
3. Chang, I. S., Moon, H., Jang, J. K., and Kim, B. H. (2005)

Improvement of a microbial fuel cell performance as a BOD sensor using respiratory inhibitors, *Biosensors & Bioelectronics 20*, 1856-1859.

4. Zhang, Y. F., and Angelidaki, I. (2012) Self-stacked submersible microbial fuel cell (SSMFC) for improved remote power generation from lake sediments, *Biosensors & Bioelectronics 35*, 265-270.
5. Dong, K., Jia, B. Y., Yu, C. L., Dong, W. B., Du, F. Z., and Liu, H. (2013) Microbial fuel cell as power supply for implantable medical devices: A novel configuration design for simulating colonic environment, *Biosensors & Bioelectronics 41*, 916-919.
6. Oh, S. E., and Logan, B. E. (2005) Hydrogen and electricity production from a food processing wastewater using fermentation and microbial fuel cell technologies, *Water Research 39*, 4673-4682.
7. Cao, X. X., Huang, X., Liang, P., Xiao, K., Zhou, Y. J., Zhang, X. Y., and Logan, B. E. (2009) A New Method for Water Desalination Using Microbial Desalination Cells, *Environmental Science & Technology 43*, 7148-7152.
8. Schroder, U. (2007) Anodic electron transfer mechanisms in microbial fuel cells and their energy efficiency, *Physical Chemistry Chemical Physics 9*, 2619-2629.
9. Du, Z. W., Li, H. R., and Gu, T. Y. (2007) A state of the art review on microbial fuel cells: A promising technology for wastewater treatment and bioenergy, *Biotechnology Advances 25*, 464-482.
10. Bond, D. R., Holmes, D. E., Tender, L. M., and Lovley, D. R. (2002) Electrode-reducing microorganisms that harvest energy from marine sediments, *Science 295*, 483-485.
11. Zhou, M. H., Chi, M. L., Luo, J. M., He, H. H., and Jin, T. (2011) An overview of electrode materials in microbial fuel cells, *Journal of Power Sources 196*, 4427-4435.

12. Lu, M., and Li, S. F. Y. (2012) Cathode Reactions and Applications in Microbial Fuel Cells: A Review, *Critical Reviews in Environmental Science and Technology 42*, 2504-2525.
13. Xie, X., Ye, M., Hsu, P. C., Liu, N., Criddle, C. S., and Cui, Y. (2013) Microbial battery for efficient energy recovery, *Proceedings of the National Academy of Sciences of the United States of America 110*, 15925-15930.
14. Zhao, F., Harnisch, F., Schrorder, U., Scholz, F., Bogdanoff, P., and Herrmann, I. (2006) Challenges and constraints of using oxygen cathodes in microbial fuel cells, *Environmental Science & Technology 40*, 5193-5199.
15. Rozendal, R. A., Hamelers, H. V. M., Rabaey, K., Keller, J., and Buisman, C. J. N. (2008) Towards practical implementation of bioelectrochemical wastewater treatment, *Trends in Biotechnology 26*, 450-459.
16. McCarty, P. L., Bae, J., and Kim, J. (2011) Domestic Wastewater Treatment as a Net Energy Producer-Can This be Achieved?, *Environmental Science & Technology 45*, 7100-7106.
17. Wu, G., More, K. L., Johnston, C. M., and Zelenay, P. (2011) High-Performance Electrocatalysts for Oxygen Reduction Derived from Polyaniline, Iron, and Cobalt, *Science 332*, 443-447.
18. Lefevre, M., Proietti, E., Jaouen, F., and Dodelet, J. P. (2009) Iron-Based Catalysts with Improved Oxygen Reduction Activity in Polymer Electrolyte Fuel Cells, *Science 324*, 71-74.
19. Kim, S., Nahm, K., and Kim, P. (2012) High Electrocatalytic Performance of NH-Activated Iron-Adsorbed Polyaniline for Oxygen Reduction Reactions, *Catalysis Letters*, 1244-1250.
20. Li, S. Z., Hu, Y. Y., Xu, Q., Sun, J., Hou, B., and Zhang, Y. P. (2012) Iron- and nitrogen-functionalized graphene as a non-precious metal

catalyst for enhanced oxygen reduction in an air-cathode microbial fuel cell, *Journal of Power Sources 213*, 265-269.

21. Cheng, S., Liu, H., and Logan, B. E. (2006) Power densities using different cathode catalysts (Pt and CoTMPP) and polymer binders (Nafion and PTFE) in single chamber microbial fuel cells, *Environmental Science & Technology 40*, 364-369.
22. Wang, P., Lai, B., Li, H., and Du, Z. (2013) Deposition of Fe on Graphite Felt by Thermal Decomposition of Fe $(CO)_5$ for Effective Cathodic Preparation of Microbial Fuel Cells, *Bioresource Technology*.
23. Tang, X. H., Guo, K., Li, H. R., Du, Z. W., and Tian, J. L. (2011) Electrochemical treatment of graphite to enhance electron transfer from bacteria to electrodes, *Bioresource Technology 102*, 3558-3560.
24. Lovley, D. R., and Phillips, E. J. P. (1988) Novel Mode of Microbial Energy-Metabolism - Organic-Carbon Oxidation Coupled to Dissimilatory Reduction of Iron or Manganese, *Applied and Environmental Microbiology 54*, 1472-1480.
25. Vukmirovic, M. B., Zhang, J., Sasaki, K., Nilekar, A. U., Uribe, F., Mavrikakis, M., and Adzic, R. R. (2007) Platinum monolayer electrocatalysts for oxygen reduction, *Electrochimica Acta 52*, 2257-2263.
26. Harnisch, F., and Schroder, U. (2010) From MFC to MXC: chemical and biological cathodes and their potential for microbial bioelectrochemical systems, *Chemical Society Reviews 39*, 4433-4448.
27. Liu, Y., Liu, H., Wang, C., Hou, S. X., and Yang, N. (2013) Sustainable energy recovery in wastewater treatment by microbial fuel cells: stable power generation with nitrogen-doped graphene cathode, *Environmental Science & Technology 47*, 13889-13895.
28. Wen, Q., Wang, S., Yan, J., Cong, L., Chen, Y., and Xi, H. (2014) Porous nitrogen-doped carbon nanosheet on graphene as metal-free

catalyst for oxygen reduction reaction in air-cathode microbial fuel cells, *Bioelectrochemistry 95*, 23-28.

29. Matter, P. H., Zhang, L., and Ozkan, U. S. (2006) The role of nanostructure in nitrogen-containing carbon catalysts for the oxygen reduction reaction, *Journal of Catalysis 239*, 83-96.
30. Vanwingerden, B., Vanveen, J. A. R., and Mensch, C. T. J. (1988) An Extended X-Ray Absorption Fine-Structure Study of Heat-Treated Cobalt Porphyrin Catalysts Supported on Active-Carbon, *Journal of the Chemical Society-Faraday Transactions I 84*, 65-74.
31. Jaouen, F., Marcotte, S., Dodelet, J. P., and Lindbergh, G. (2003) Oxygen reduction catalysts for polymer electrolyte fuel cells from the pyrolysis of iron acetate adsorbed on various carbon supports, *Journal of Physical Chemistry B 107*, 1376-1386.
32. Koslowski, U. I., Abs-Wurmbach, I., Fiechter, S., and Bogdanoff, P. (2008) Nature of the catalytic centers of porphyrin-based electrocatalysts for the ORR: A correlation of kinetic current density with the site density of Fe-N-4 Centers, *Journal of Physical Chemistry C 112*, 15356-15366.
33. Bashyam, R., and Zelenay, P. (2006) A class of non-precious metal composite catalysts for fuel cells, *Nature 443*, 63-66.
34. Proietti, E., Jaouen, F., Lefevre, M., Larouche, N., Tian, J., Herranz, J., and Dodelet, J. P. (2011) Iron-based cathode catalyst with enhanced power density in polymer electrolyte membrane fuel cells, *Nature Communications 2*, 416-425.
35. Gong, K. P., Du, F., Xia, Z. H., Durstock, M., and Dai, L. M. (2009) Nitrogen-Doped Carbon Nanotube Arrays with High Electrocatalytic Activity for Oxygen Reduction, *Science 323*, 760-764.

## Chapter 5 Bicarbonate buffer to enhance coulombic efficiency of MFCs

### 5.1 Introduction

MFCs have exciting potentials for various kinds of applications (1-6). While electricity generation is the major objective for these applications of MFCs, it is also desired to recovery as much electrons stored in the substrate as possible to produce electricity, and to enhance the energy generation as much as possible (7). Coulombic efficiency (CE) is defined as the as the ratio of the amount of electrons transferred *via* the circuit to the amount of electrons theoretically delivered by the substrate.

CE is one of the most important criteria to evaluate the MFC applications. However, CE in MFCs is still too low, which limits the applications of this novel technology (7-11). Many factors have impact on the CE in MFCs. For example, two chamber MFC with a membrane typically has a larger CE compared with single chamber MFC, as the membrane can effectively reduce the oxygen diffusion from the cathode chamber to the anode chamber (12-13). The operation parameters also have influence on the CE, such as the external resistance and the concentration of the substrate (12). Besides the MFC configuration and the operation parameters, the CE is further affected by growth and reproduction of microorganisms, competitive degradation processes such as fermentation and aerobic respiration due to the diffusing of

oxygen into the anode chamber (7, 14). Since the enhancement of CE can greatly optimize the applications of MFCs, it is of great significance to address the above challenges to enhance the CE.

Previous studies have demonstrated that biofilm formed on the anode surface is primarily responsible for the electricity production while bacteria suspended in the anolyte contributes nothing or only a little to the electricity production in MFCs (15-18). Bacteria suspended in the electrolyte, however, compete with bacteria attached on anode surface to consume organics for fermentation and aerobic respiration, which consequently lowers the CE of MFCs. As a consequence, inhibiting the growth and reproduction of bacteria suspended in electrolyte can be an effective approach to improve the CE of MFCs.

As proton is generated in the anode while it is consumed in the cathode to generate water in MFCs, the pH in the anode chamber will drop while it will increase in the cathode (19). The pH difference between the anode and cathode solution will cause an electrochemical loss and thus lower the cell voltage output. In order to address this problem, phosphate buffer is prevalently used in electrolyte to stabilize the pH for electrochemically active bacteria and to enhance the power generation of MFCs (12, 20-21). Adding phosphate into MFCs, however, not only causes the eutrophication of water bodies if the effluents are discharged without effective removal of phosphates, but also contributes to the growth and reproduction of suspended bacteria as phosphorus is an essential element for bacteria to synthesize ATP,

phospholipids, DNA and RNA. Therefore, the strategy here was to utilize a phosphorus-free electrolyte by using bicarbonate buffer as an alternative of phosphate buffer to inhibit the growth and reproduction of suspended bacteria. This study demonstrates that electrolyte with bicarbonate buffer greatly reduces the suspended bacteria and considerably enhances the CE of MFCs.

## 5.2 Experimental section

### 5.2.1Two-chamber MFC construction and operation

The MFCs were constructed by joining two bottles (height 22 cm, diameter 3.8 cm) with the proton exchange membranes (Nafion 117, Dupont) held by a clamp in the tube (inner diameter 2 cm) separating the two chambers, as previously described (22). The proton exchange membranes were successively boiled in $H_2O_2$ (30%), deionized water, 0.5 M $H_2SO_4$, and deionized water. Graphite felts (3 cm×0.6 cm×8 cm) were placed in the anode and cathode chamber with an electrode spacing of 7 cm. Graphite felts were pretreated by immersing successively in 1 M NaOH for 12 h and then 1 M $H_2SO_4$ for 12 h, followed by rinsing with DI water. Cathode were prepared by uniformly coating Pt/C catalysts (0.5 mg/cm$^2$ Pt) onto the graphite felt surface using 5% Nafion solutions as the binder (23). In brief, Pt/C catalyst was firstly mixed and dispersed well in the Nafion and ethanol solution by ultrasonication. Next, the dispersion was evenly brushed onto the graphite felt followed by drying at room temperature. Titanium wire across an external resistance of 500 Ω was

used to connect the anode and cathode

The MFCs was inoculated using a mixed bacterial culture from another MFC in the laboratory (24). MFCs were fed media (a volume of 58 ml) containing 10 mM sodium acetate, $NH_4Cl$ (0.31 g/L), KCl (0.13 g/L), NaCl (2.9 g/L), 50 mM phosphate buffer (pH 7.0 and pH 8.3) metal salt (12.5 mL/L) and vitamin (5 mL/L) solutions (25). Another MFC was fed the same medium except that 50 mM bicarbonate (pH 8.3) was used as the substitute for phosphate buffer. The catholyte was composed of $NH_4Cl$ (0.31 g /L), KCl (0.13 g/L), NaCl (2.9 g/L) and 50 mM Tris-HCl buffer.

The anode chamber was kept under anaerobic condition, while the cathode chamber was purged with sterile air (40 mL/min). The MFCs were operated in a temperature-controlled incubator at 30 ℃ in a fed batch mode. Anolyte with different acetate concentration (2 mM-11 mM) was replaced at the end of each batch when the voltage dropped below 20 mV. The feeding solution had been sparged with high purity nitrogen gas for 30 min to remove the dissolved oxygen before adding into the anode chamber. All the tests were carried out in duplicate and the average values with standard deviation were acquired.

### 5.2.2 Analyses and calculation

Cell voltage (V) across an external resistance (R) was measured and stored by a data acquisition system (AD8201H, Ribohua Co., Ltd) while current (I) was calculated by I = V/R. Charge passing through the external circuit (Coulombs,

Cp) was acquired by integrating the current over time. The theoretical amount of charge (Ct) that could be produced from the substrate (acetate) degraded was calculated by Ct=Fbcv, where F was the Faraday's constant (96,500 C per mole of electrons), b was the number of mole of electrons produced per mole of acetate (b=8 for acetate), c was the consumed acetate concentration and v was the anolyte volume (200 mL). CE was obtained by the equation CE= Cp /Ct.

Acetate concentrations were analyzed using the standard method of potassium dichromate (26). The pH of the anolyte was measured by a pH meter (PHS-2F, INESA) and the conductivity of the anolyte was examined by a conductivity meter (S700, Mettler Toledo). Bacteria formed on graphite felt surface were imaged by environmental scanning electron microscopy (SEM) (Quanta 200, FEI). Suspended cell mass was evaluated by two methods at the end of each batch: the turbidimetric method using a spectrophotometer to measure the optical density at 600 nm ($OD_{600}$) (27), and Bradford protein assay to measure the absorbance at 595 nm.

## 5.3 Results and discussion

### 5.3.1 Electricity generation from MFCs

When MFCs became stable and reproducible in power generation, approximately 220 mV across an external resistance of 500 Ω was generated in the three MFCs (Figure 5.1). SEM images clearly showed that

microorganisms adhered on graphite felt anode surface to form biofilm, which was expected to generate electricity in MFCs (Figure 5.2). In order to confirm whether the biofilm was responsible for the electricity generation in these MFCs, the anolyte in the stably running MFCs was removed and replaced. After the replacement, voltage generation rapidly increased to a maximum (less than 30 min) and maintained at levels to those observed prior to anolyte replacement. The result that replacement of the anolyte surrounding the anode did not change the voltage output capacity confirmed that bacteria attached on the anode surface was responsible for electricity production in this study, which was consistent with the previous reports (16-18). This result also showed that bacteria suspended in the anolyte did not contribute to the power production in theses MFCs.

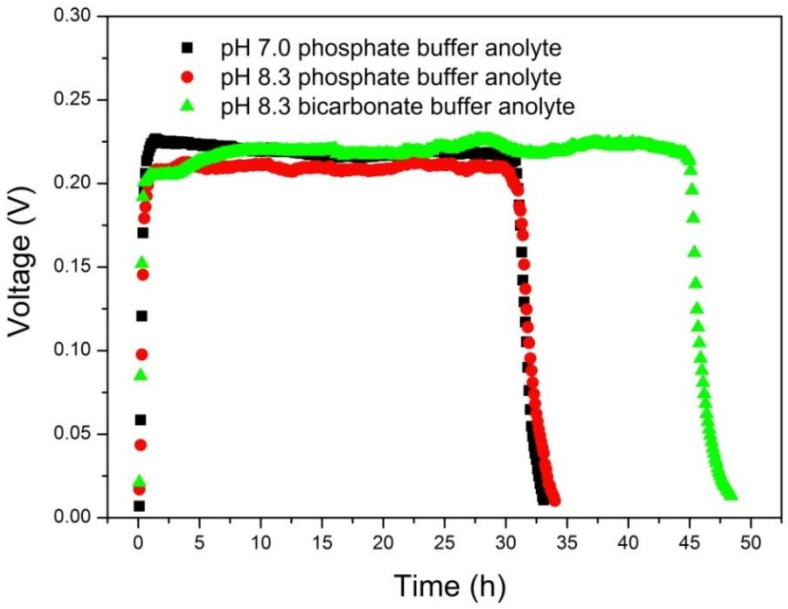


Figure 5. 1 Voltage generation from MFCs with the phosphorus-free anolyte and the phosphate-containing anolyte (acetate concentration: 2 mM).

These suspended microorganisms, however, would compete with the bacteria

attached on anode surface to consume substrate for fermentation and/or aerobic respiration, which accordingly decreased the CE of MFCs. As a consequence, inhibiting the growth and reproduction of bacteria suspended in the solution could be an effective approach to enhance the CE of these MFCs.

In each batch cycle, voltage generation from MFCs rapidly ascended to a maximum and sustained at a certain level (200-230 mV) (Figure 5.1). When acetate became a limiting factor for the electricity production, the voltage output began to decline and it dropped gradually. The stable voltage output was almost the same in the three MFCs except that voltage output with the bicarbonate buffer anolyte sustained much longer than that of the phosphate buffer anolyte. A longer time for electricity production meant a higher CE. Also, this result showed that biofilm on anode surface in all the anolytes was stable and could constantly produce electricity, even in the anolyte without phosphorus.

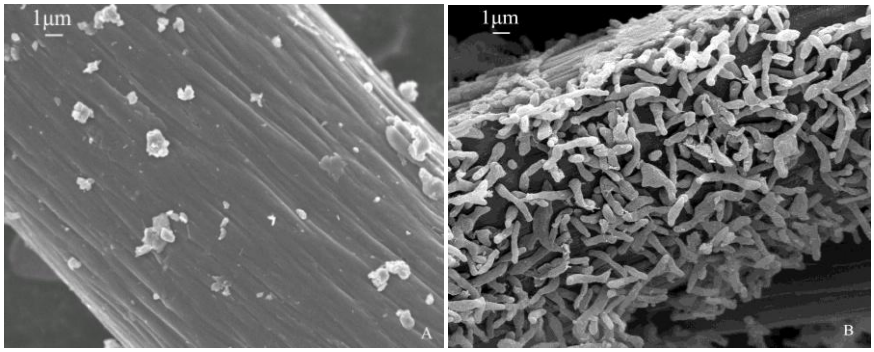


Figure 5. 2 SEM images of graphite felt anode before (A) and after (B) biofilm formation.

### 5.3.2 The pH and conductivity

The pH of the anolyte has great impact on the electricity production of MFCs.

when pH buffer is not used in MFCs, the pH can change widely, which deteriorates the electricity production of the electrochemically active bacteria (12). Because of this problem, buffer is popularly used in MFCs to maintain a suitable pH for electrochemically active bacteria.

The $pK_2$ of the phosphate buffer was 7.2 and the $pK_1$ of the bicarbonate buffer was 6.4. Therefore, both of them showed strong buffering capacity in the pH range of 6-8.5. In this study, the pH varied slightly (0.01-0.03 unit) when 10 mM acetate was added into the three anolyte (Table 5.1). After a batch cycle for electricity production using 10 mM acetate as the electron donor, the pH only decreased 0.24, 0.26 and 0.27 Unit in the pH 7.0 phosphate buffer anolyte, the pH 8.3 phosphate buffer anolyte and the bicarbonate buffer anolyte, respectively. These results demonstrated that all the three buffers exhibited strong capacity in stabilizing the pH of the anolyte.

Table 5. 1 pH and conductivity of the anolytes with different buffers.

| Anolyte | pH | pH (+acetate 10 mM) | Conductivity (mS/cm) | Conductivity (+acetate 10 mM) (mS/cm) |
|---|---|---|---|---|
| pH 7.0phosphate buffer anolyte | 7.01 | 7.02 | 10.76 | 11.29 |
| pH 8.3 phosphate buffer anolyte | 8.31 | 8.33 | 11.87 | 12.38 |
| pH 8.3 bicarbonate buffer anolyte | 8.30 | 8.33 | 9.25 | 9.79 |

In MFCs, a relatively higher conductivity is considered to be beneficial for power generation and CE because it facilitates proton transfer in the solution

and reduces the ohmic resistance of the solution (28). In this study, the conductivity of the bicarbonate buffer anolyte was 9.25 mS/cm, smaller than the 10.76 mS/cm of the pH 7.0 phosphate buffer anolyte and the 11.87 mS/cm of the pH 8.3 phosphate buffer anolyte (Table 5.1). Thus, the relatively smaller conductivity of the bicarbonate buffer anolyte was not favorable for the CE of MFCs.

### 5.3.3 Suspended bacteria and CE

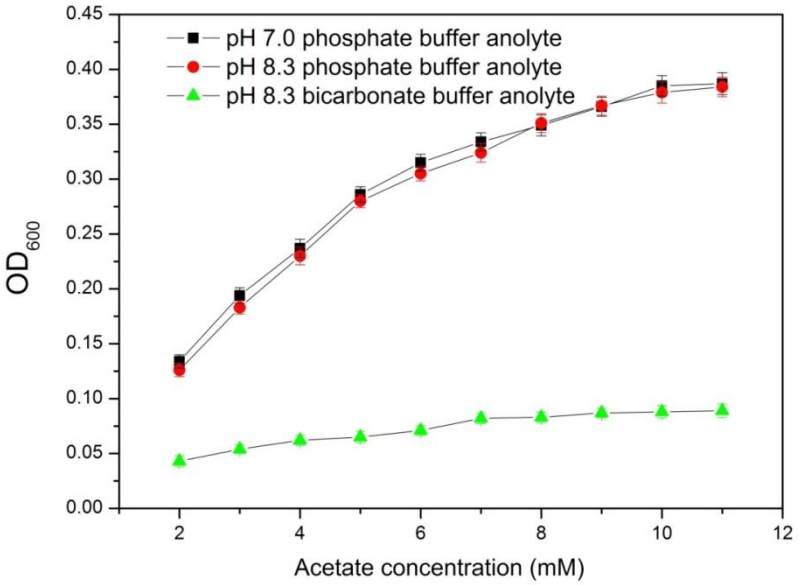


Figure 5. 3 The optical density ($OD_{600}$) of the suspended bacteria in MFCs fed with various acetate concentrations.

Suspended cell mass is widely evaluated by measuring the optical density at 600 nm ($OD_{600}$) as the optical density of a cell suspension is proportional to the biomass concentration (29-30). The $OD_{600}$ of the suspended bacteria in MFCs fed with various acetate concentrations was measured at the end of each batch cycle for electricity production (Figure 5.3). When acetate concentration increased from 2 mM to 11 mM, the $OD_{600}$ boosted sharply from 0.136 to

0.389 in the pH 7.0 phosphate buffer anolyte and increased from 0.126 to 0.384 in the pH 8.3 phosphate buffer anolyte. The $OD_{600}$ in the bicarbonate buffer anolyte, however, was quite steady, and the $OD_{600}$ only increased slightly from 0.042 to 0.091 when acetate concentration changed from 2 mM to 11 mM. Compared with the phosphate buffer anolyte, the $OD_{600}$ in the bicarbonate buffer anolyte was much smaller, which indicated that bacteria suspended in bicarbonate buffer anolyte were much smaller than that in phosphate buffer anolyte. Besides, larger suspended cell mass was detected in a higher acetate concentration which had a longer batch cycle time for these bacteria to grow and propagate. This finding demonstrated that suspended cell mass in MFCs increased considerably due to the growth and reproduction of suspended bacteria.

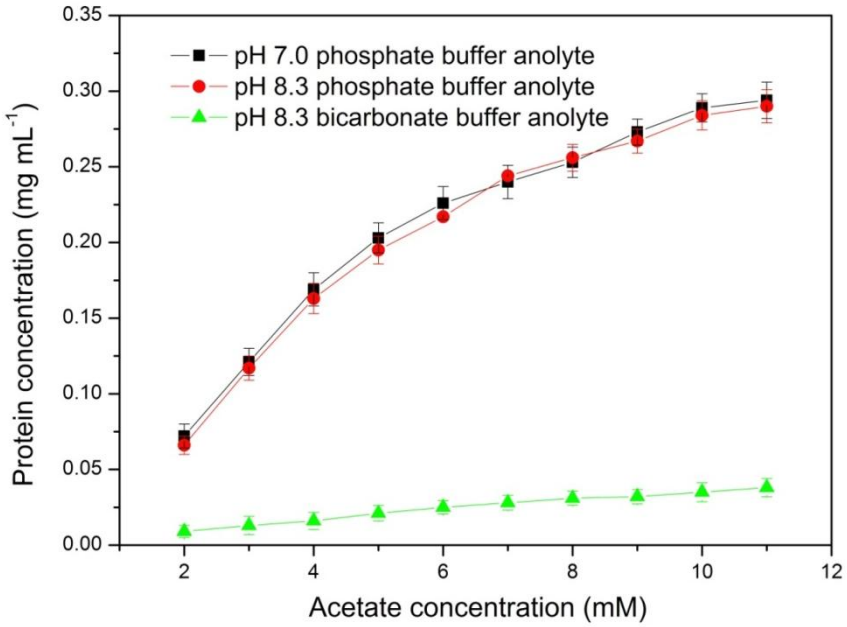


Figure 5. 4 The protein concentration of the suspended microorganisms in MFCs fed with different acetate concentration.

In order to measure the suspended biomass more precisely, the Bradford

protein assay of the bacteria in the solution was conducted. When acetate concentration varied from 2 mM to 11 mM, the protein concentration increased from 0.072 mg/mL to 0.294 mg/mL in the pH 7.0 phosphate buffer solution and increased from 0.066 mg/mL to 0.290 mg/mL in the pH 8.3 phosphate buffer solution (Figure 5.4). However, the corresponding protein concentration in the bicarbonate buffer anolyte only rose slightly from 0.012 mg/mL to 0.038 mg/mL.

These results exhibited that bicarbonate buffer anolyte effectively inhibited the growth and reproduction of suspended bacteria in MFCs, compared with the phosphate buffer anolyte. As a result, bicarbonate buffer anolyte greatly reduced the biomass suspended in the solution.

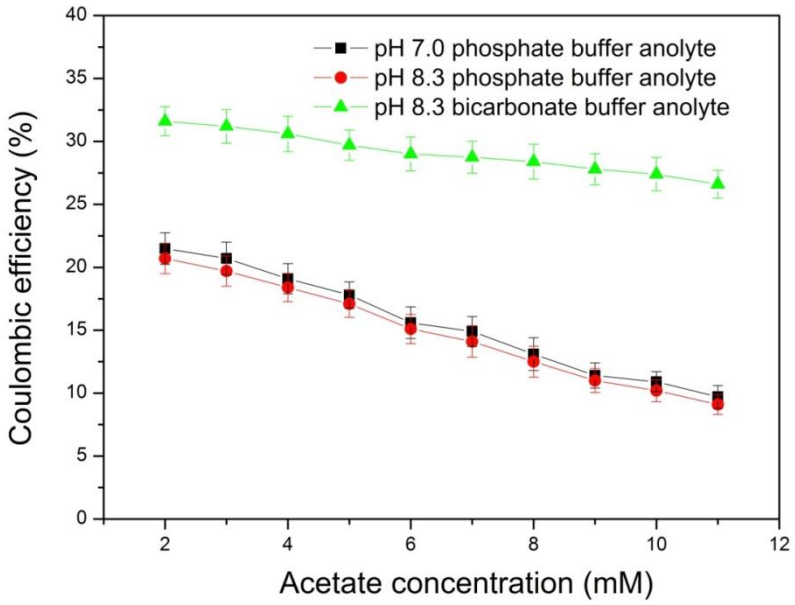


Figure 5. 5 Coulombic efficiency of MFCs fed with different acetate concentrations.

Figure 5.5 was the CE of MFCs fed with various acetate concentrations. When the acetate concentration increased from 2 mM to 11 mM, the CE of the MFC with pH 7.0 phosphate buffer anolyte dropped dramatically from 21.5% to 9.7%

and the CE of the MFC with the pH 8.3 phosphate buffer anolyte decreased from 20.7 to 9.1%. However, the corresponding CE of the MFC with bicarbonate anolyte only declined from 31.6% to 26.6%. These experiments demonstrated that the anolyte with bicarbonate buffer significantly increased the CE of MFCs, compared with the anolyte with phosphate buffer. Besides, the CE in MFCs with bicarbonate buffer anolyte was much more stable, as it only decreased by 15.8% while a drop of 56.0% was obtained in the phosphate buffer anolyte.

The greatly higher CE in the MFC with the bicarbonate buffer anolyte was due to the considerably reduced bacteria suspended in the solution which had no contribution to the electricity production in the MFCs. The reduction of bacteria suspended in the solution meant that less substrate was consumed by suspended bacteria and more substrate was available for bacteria formed on anode surface for power production.

The bicarbonate buffer anolyte effectively restrained the growth and reproduction of suspended bacteria. However, it did not affect the bacteria attached on anode surface for electricity production. The biofilm attached on anode surface maintained in the bicarbonate buffer anolyte generated electricity without any deterioration during the whole experiment period. One explanation could be that bacteria attached on the anode surface could take advantage of the phosphorus sources from the dead cells within the biofilm.

The enhanced CE can enhance the practical applications of MFCs. Traditional

aerobic wastewater treatment such as activated sludge is energy intensive and costly. For instance, about 3% of electricity produced in the U.S. is consumed by wastewater treatment plants and the annual cost for wastewater treatment is as high as $25 billion (2). Compared with aerobic treatment, the greatest benefit of MFC technology is that clean energy can be extracted from organics in wastewater. MFC has the potential to be a self sufficient technology for wastewater treatment if the CE is enhanced to recover sufficient amount of energy to compensate the energy demanded during wastewater treatment process. Besides, an enhanced CE can improve the applications of MFCs for environmental detection, such as the BOD measurement (31-32). For example, a higher and relatively more stable CE can enhance the accuracy, reliability and repeatability because more coulombs pass through the circuit, which are proportional to the BOD concentration in the solution (33). Another advantage of an enhanced CE is that it can enhance the applications of MFCs as batteries for power supply as a higher CE means that more energy is recovered and a longer time of electricity discharge is achieved (34-35). As a consequence, this bicarbonate buffer anolyte has an exciting potential to enhance the feasibility for various applications of MFCs.

### 5.4 Conclusions

In this chapter, bicarbonate buffer anolyte was used in MFCs to enhance the electricity production. Compared with phosphate buffer anolyte, bicarbonate

anolyte efficiently inhibited the growth and reproduction of suspended bacteria in the solution and consequently considerably reduced the suspended biomass in MFCs. The reduction of suspended bacteria allowed more substrate to be consumed by biofilm formed on anode surface for electricity production. As a consequence, bicarbonate buffer anolyte significantly enhanced the CE of MFCs. Further, a much more stable CE was obtained in this bicarbonate anolyte, as it only decreased by 15.8% while a drop of 56.0% was obtained in the phosphate buffer anolyte. This study demonstrated that bicarbonate buffer anolyte has an exciting potential to enhance the feasibility for various applications of MFCs.

### 5.5 References


1. Cao, X. X., Huang, X., Boon, N., Liang, P., and Fan, M. Z. (2008) Electricity generation by an enriched phototrophic consortium in a microbial fuel cell, *Electrochemistry Communications 10*, 1392-1395.
2. McCarty, P. L., Bae, J., and Kim, J. (2011) Domestic Wastewater Treatment as a Net Energy Producer-Can This be Achieved?, *Environmental Science & Technology 45*, 7100-7106.
3. Di Lorenzo, M., Curtis, T. P., Head, I. M., and Scott, K. (2009) A single-chamber microbial fuel cell as a biosensor for wastewaters, *Water Research 43*, 3145-3154.
4. Wan, D. J., Liu, H. J., Qu, J. H., Lei, P. J., Mao, S. H., and Hou, Y. N. (2009) Using the combined bioelectrochemical and sulfur autotrophic denitrification system for groundwater denitrification, *Bioresource Technology 100*, 142-148.
5. Zhou, M. H., Wang, H. Y., Hassett, D. J., and Gu, T. Y. (2013) Recent

advances in microbial fuel cells (MFCs) and microbial electrolysis cells (MECs) for wastewater treatment, bioenergy and bioproducts, *Journal of Chemical Technology and Biotechnology 88*, 508-518.

6. Cao, X. X., Huang, X., Liang, P., Xiao, K., Zhou, Y. J., Zhang, X. Y., and Logan, B. E. (2009) A New Method for Water Desalination Using Microbial Desalination Cells, *Environmental Science & Technology 43*, 7148-7152.
7. Logan, B. E., Hamelers, B., Rozendal, R. A., Schrorder, U., Keller, J., Freguia, S., Aelterman, P., Verstraete, W., and Rabaey, K. (2006) Microbial fuel cells: Methodology and technology, *Environmental Science & Technology 40*, 5181-5192.
8. Zhang, X. Y., Cheng, S. A., Liang, P., Huang, X., and Logan, B. E. (2011) Scalable air cathode microbial fuel cells using glass fiber separators, plastic mesh supporters, and graphite fiber brush anodes, *Bioresource Technology 102*, 372-375.
9. Ringeisen, B. R., Ray, R., and Little, B. (2007) A miniature microbial fuel cell operating with an aerobic anode chamber, *Journal of Power Sources 165*, 591-597.
10. He, Z., Wagner, N., Minteer, S. D., and Angenent, L. T. (2006) An upflow microbial fuel cell with an interior cathode: Assessment of the internal resistance by impedance Spectroscopy, *Environmental Science & Technology 40*, 5212-5217.
11. Cheng, S. A., Xing, D. F., and Logan, B. E. (2011) Electricity generation of single-chamber microbial fuel cells at low temperatures, *Biosensors & Bioelectronics 26*, 1913-1917.
12. Gil, G. C., Chang, I. S., Kim, B. H., Kim, M., Jang, J. K., Park, H. S., and Kim, H. J. (2003) Operational parameters affecting the performance of a mediator-less microbial fuel cell, *Biosensors & Bioelectronics 18*, 327-334.

13. Fan, Y. Z., Hu, H. Q., and Liu, H. (2007) Enhanced Coulombic efficiency and power density of air-cathode microbial fuel cells with an improved cell configuration, *Journal of Power Sources 171*, 348-354.
14. Fornero, J. J., Rosenbaum, M., and Angenent, L. T. (2010) Electric Power Generation from Municipal, Food, and Animal Wastewaters Using Microbial Fuel Cells, *Electroanalysis 22*, 832-843.
15. Biffinger, J. C., Pietron, J., Ray, R., Little, B., and Ringeisen, B. R. (2007) A biofilm enhanced miniature microbial fuel cell using Shewanella oneidensis DSP10 and oxygen reduction cathodes, *Biosensors & Bioelectronics 22*, 1672-1679.
16. Reguera, G., Nevin, K. P., Nicoll, J. S., Covalla, S. F., Woodard, T. L., and Lovley, D. R. (2006) Biofilm and nanowire production leads to increased current in Geobacter sulfurreducens fuel cells, *Applied and Environmental Microbiology 72*, 7345-7348.
17. Cheng, K. Y., Ho, G., and Cord-Ruwisch, R. (2008) Affinity of microbial fuel cell biofilm for the anodic potential, *Environmental Science & Technology 42*, 3828-3834.
18. Bond, D. R., and Lovley, D. R. (2003) Electricity production by Geobacter sulfurreducens attached to electrodes, *Applied and Environmental Microbiology 69*, 1548-1555.
19. Tang, X. H., Guo, K., Li, H. R., Du, Z. W., and Tian, J. L. (2010) Microfiltration membrane performance in two-chamber microbial fuel cells, *Biochemical Engineering Journal 52*, 194-198.
20. Tang, X. H., Du, Z. W., and Li, H. R. (2010) Anodic electron shuttle mechanism based on 1-hydroxy-4-aminoanthraquinone in microbial fuel cells, *Electrochemistry Communications 12*, 1140-1143.
21. Zhuang, L., Yuan, Y., Yang, G. Q., and Zhou, S. G. (2012) In situ formation of graphene/biofilm composites for enhanced oxygen reduction in biocathode microbial fuel cells, *Electrochemistry*

*Communications 21*, 69-72.

22. Liu, H., Grot, S., and Logan, B. E. (2005) Electrochemically assisted microbial production of hydrogen from acetate, *Environmental Science & Technology 39*, 4317-4320.
23. Cheng, S., Liu, H., and Logan, B. E. (2006) Power densities using different cathode catalysts (Pt and CoTMPP) and polymer binders (Nafion and PTFE) in single chamber microbial fuel cells, *Environmental Science & Technology 40*, 364-369.
24. Tang, X. H., Guo, K., Li, H. R., Du, Z. W., and Tian, J. L. (2011) Electrochemical treatment of graphite to enhance electron transfer from bacteria to electrodes, *Bioresource Technology 102*, 3558-3560.
25. Lovley, D. R., and Phillips, E. J. P. (1988) Novel Mode of Microbial Energy-Metabolism-Organic-Carbon Oxidation Coupled to Dissimilatory Reduction of Iron or Manganese, *Applied and Environmental Microbiology 54*, 1472-1480.
26. Rand, M., Greenberg, A. E., and Taras, M. J. (1976) Standard methods for the examination of water and wastewater, Prepared and published jointly by American Public Health Association, American Water Works Association, and Water Pollution Control Federation.
27. Walker, G. M., and Weatherley, L. R. (2000) Biodegradation and biosorption of acid anthraquinone dye, *Environmental Pollution 108*, 219-223.
28. Lefebvre, O., Tan, Z., Kharkwal, S., and Ng, H. Y. (2012) Effect of increasing anodic NaCl concentration on microbial fuel cell performance, *Bioresource Technology 112*, 336-340.
29. Biswas, S. R., Ray, P., Johnson, M. C., and Ray, B. (1991) Influence of Growth-Conditions on the Production of a Bacteriocin, Pediocin Ach, by Pediococcus-Acidilactici H, *Applied and Environmental Microbiology 57*, 1265-1267.

30. Podsiadlo, P., Paternel, S., Rouillard, J. M., Zhang, Z. F., Lee, J., Lee, J. W., Gulari, L., and Kotov, N. A. (2005) Layer-by-layer assembly of nacre-like nanostructured composites with antimicrobial properties, *Langmuir 21*, 11915-11921.

31. Moon, H., Chang, I. S., Jang, J. K., Kim, K. S., Lee, J., Lovitt, R. W., and Kim, B. H. (2005) On-line monitoring of low biochemical oxygen demand through continuous operation of a mediator-less microbial fuel cell, *Journal of Microbiology and Biotechnology 15*, 192-196.

32. Zhang, Y. F., and Angelidaki, I. (2011) Submersible Microbial Fuel Cell Sensor for Monitoring Microbial Activity and BOD in Groundwater: Focusing on Impact of Anodic Biofilm on Sensor Applicability, *Biotechnology and Bioengineering 108*, 2339-2347.

33. Kim, B. H., Park, H. S., Kim, H. J., Kim, G. T., Chang, I. S., Lee, J., and Phung, N. T. (2004) Enrichment of microbial community generating electricity using a fuel-cell-type electrochemical cell, *Applied Microbiology and Biotechnology 63*, 672-681.

34. Dewan, A., Donovan, C., Heo, D., and Beyenal, H. (2010) Evaluating the performance of microbial fuel cells powering electronic devices, *Journal of Power Sources 195*, 90-96.

35. Ren, H., Lee, H. S., and Chae, J. (2012) Miniaturizing microbial fuel cells for potential portable power sources: promises and challenges, *Microfluidics and Nanofluidics 13*, 353-381.

## Chapter 6 Energy production from wastewater by MFCs

### 6.1 Introduction

Approximately 80% of world energy consumption of 2012 came from fossil fuels (1). However, fossil fuels, such as petroleum, coal and natural gas, are being exhausted, which might result in an energy crisis in the near future. In order to mitigate this crisis, sustainable energy sources as alternatives to fossil fuels have to be developed and utilized. One untapped resource is the organic matters in wastewater theoretically sufficient to generate about $7.4 \times 10^{18}$ J per year, which is three to four times more energy than what is needed to treat the wastewater (2). Therefore, sustainable energy extraction from wastewater offers a promising solution to mitigate this energy crisis (2).

As a promising environmental biotechnology, MFC can directly convert the chemical energy stored in organic matters into electrical energy by the catalysis of electrochemically active bacteria (3-4). Compared with anaerobic digestion and combined combustion, direct electrical energy production is the greatest benefit of MFC technology (5-6). Therefore, MFCs provide a promising strategy for simultaneous electricity production and wastewater treatment (7-8).

Currently, the energy recovery efficiency is still too low. For instance, an electrical energy density of 0.14 kWh/kg COD was obtained by an MFC after 120 h of degradation (9). While in a cooperative MFC system consisted of a conventional MFC and a dual-cathode MFC, the energy recovery density was 0.1023 kWh/kg COD from the wastewater containing acetate (10). For

comparison, anaerobic digestion combined with combustion typically captured 0.6-1.1 kWh/kg COD (11). Therefore, energy recovery efficiency in MFCs has to be improved in order to enhance the competiveness of this technology (9).

Previous studies indicated that buffer solution had a great influence on energy production from MFCs as buffer could help maintain the solution pH for electrochemically active bacteria (12). In chapter 5, it was demonstrated that bicarbonate buffer solution could greatly enhance the CE of MFCs, as it considerably reduced the suspended bacteria and allowed more substrate to be consumed by biofilm formed on anode surface for electricity production. Therefore, bicarbonate buffer was employed for energy production study in this chapter.

Anode material plays a key role in energy production in MFCs. The surface properties of the anode material not only have a great effect on the biofim formation, but also have a considerable impact on the extracellular electron transfer from bacteria to anode surface. In chapter 2, it was exhibited that CPHs/CNTs composite anode could improve the biofilm formation on anode surface, reduce the interfacial charge transfer resistance and enhance extracellular electron transfer in MFCs. Thus, CPHs/CNTs anode was used in this study for energy production.

Cathode with noble metal catalyst can amount to almost half of the total construction cost of an MFC (13). In chapter 4, non precious metal catalyst PANI-$Fe_{900}$ showed very high catalytic activity towards ORR in the cathode of MFCs. It exhibited very positive onset potential, high current density, and excellent selectivity for the four-electron reaction towards ORR, which was comparable to the benchmark Pt/C catalyst. More importantly, the cost of

PANI-$Fe_{900}$ was less than 1% of the Pt/C catalyst. Therefore, PANI-$Fe_{900}$ was used as the cathode catalyst for energy production in this study.

Energy recovery efficiency between MFC and other traditional wastewater treatment methods, such as anaerobic digestion and activated sludge, was also discussed.

## 6.2 Experimental section

### 6.2.1 Electrode preparation

Graphite felt with a diameter of 4 cm was used as anode in this study. Graphite felt anode was modified by CPHs/CNTs composite as previously described (14). Graphite felt cathode with a diameter of 7 cm was prepared by coating PANI-$Fe_{900}$ catalyst using 5% Nafion solution as the binder (15-16). In brief, the catalyst powder was firstly mixed and dispersed well in the Nafion and ethanol solution *via* ultrasonication. Then, the dispersion was uniformly coated onto the graphite felt followed by drying at room temperature.

### 6.2.2 MFC setup and operation

Single chamber air-cathode MFC was constructed as previously described (17). The lower chamber was cylindrical with a diameter of 4.2 cm and a height of 6.0 cm, and the upper chamber exposed to air was also cylindrical with a diameter of 7 cm and a height of 0.5 cm. The graphite felt cathode was put at the upper chamber and the anode was placed at the lower chamber. Titanium wire with an external resistance was used to connect the anode and cathode. The MFC was inoculated using a mixed bacterial culture from another stably running MFC in the laboratory.

MFC was fed a medium (a volume of 58 mL) containing 10 mM sodium acetate, $NH_4Cl$ (0.31 g/L), KCl (0.13 g/L), NaCl (2.9 g/L), 50 mM bicarbonate buffer, metal salt (12.5 mL/L) and vitamin (5 mL/L) solutions. The feeding solution had been sparged with high purity nitrogen gas for 30 min to remove the dissolved oxygen. MFC was operated in a temperature-controlled room at 30 ℃ in a fed batch mode and the feeding solution was refreshed when the current dropped below 0.05 mA. MFC was considered to be stable when the maximum voltage output was reproducible.

### 6.2.3 Analyses and calculations

Cell voltage (U) across the external resistance (R) was recorded and stored by a data acquisition system (AD8201H, Ribohua Co., Ltd) every 3 min. The open circuit potentials of anode and cathode were measured by placing a saturated calomel electrode (SCE) in the electrolyte. Current (I) was calculated by $I = U/R$, and power (P) was calculated as $P = U \times I$. A data acquisition system was used to measure and store the cell voltage output (U). The maximum power densities were acquired by varying the external resistance (R) from 10 to 2000 Ω, when MFCs became steady and reproducible in electricity generation. Power density ($P_d$) was measured on the basis of the total volume (V) of the reactor: $P_d = U^2/(R \times V)$.

Charge passing through the external circuit (Coulombs, $C_p$) was calculated by integrating the generated current over time. The theoretical amount of charge ($C_t$) that could be generated from the degraded acetate was obtained by the equation $C_t$=Fbcv, where F was the Faraday's constant (96,500 C/mol of

electrons), b was the number of mole of electrons produced per mole of acetate (b=8 for acetate), c was the consumed substrate concentration and v was the liquid volume (58 ml). Coulombic efficiency (CE) could be obtained by the equation $CE= C_p /C_t$.

Electrical energy output (E) was calculated by integrating the power over time. The total chemical energy stored ($E_t$) in the acetate was assumed to be the combustion energy ($0.87 \times 10^6$ J/mol for acetate). Energy efficiency (EE) was obtained by $EE=E/E_t$ and energy density ($E_d$) was calculated by $E_d= E/COD$, where COD was the chemical oxygen demand removed. The COD concentration of the electrolyte was determined using the standard method of potassium dichromate (18).

## 6.3 Results and Discussion

### 6.3.1 Energy production from MFCs

Figure 6.1 showed the polarization and power density curves obtained by varying the external resistance from 10 Ω to 2000 Ω, when electricity generation in the air-cathode MFC was stable and reproducible. The result indicated that the maximum power density of this air-cathode MFC could reach 18.04 $W/m^3$. Compared with the MFC using bare anode and cathode in Chapter 4 with a maximum power density of 1.32 $W/m^3$, this MFC significantly improved the power production.

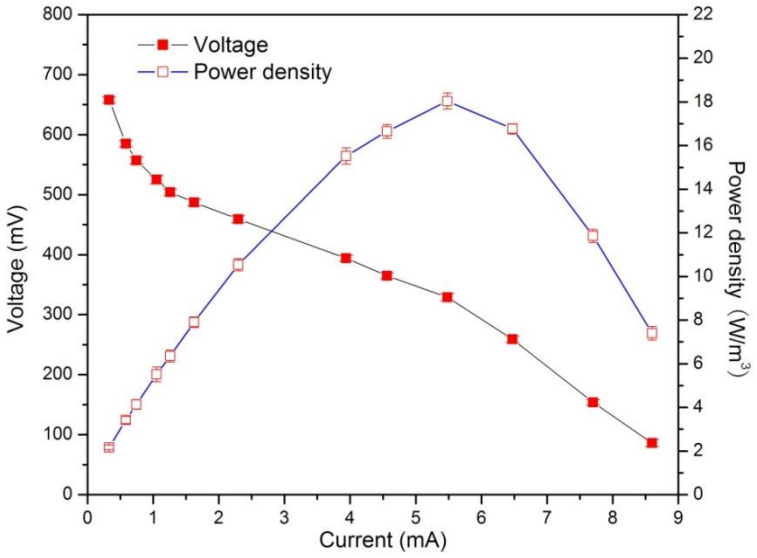


Figure 6. 1 Polarization and power density curves of the air-cathode MFC.

Figure 6.2 was the voltage output of a typical bath cycle of electricity production in this MFC. The voltage output was about 500 mV across an external resistance of 500 Ω. Voltage output in the MFC sustained for about 50 h before it declined due to the limit of acetate concentration.

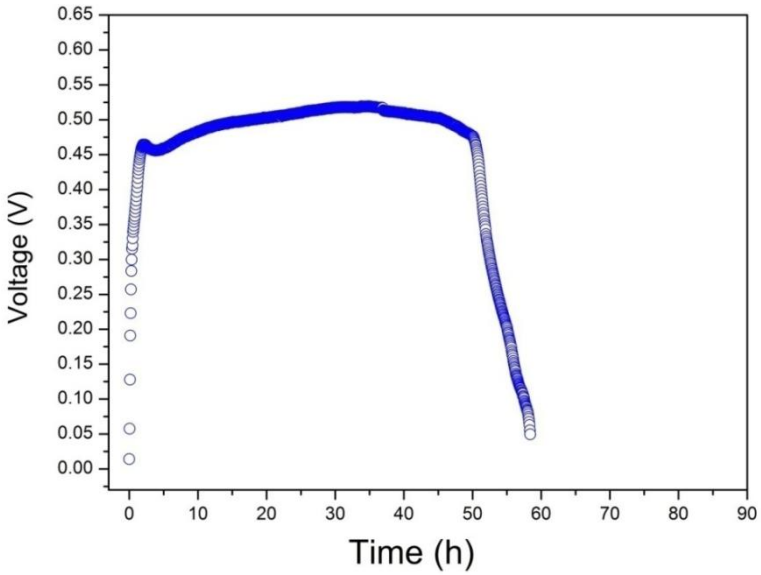


Figure 6. 2 Voltage generation in the air-cathode MFC.

Current generation and cumulative charge of the MFC with an external resistance of 500 Ω was shown in Figure 6.3. The Coulomb generated by the MFCs was approximately 192.4 C (Figure 6.3 and Table 6.1). The residual

COD concentration in the MFC after one batch of current generation 142 mg/L, indicating that the CE was about 55.2% (Table 6.1).

Table 6. 1 The air-cathode MFC performance

| Residual COD (mg/L) | $C_p$ (C) | CE (%) | E (J) | EE on total energy (%) | $E_d$ (kWh/kg COD) |
|---|---|---|---|---|---|
| 142 ±8 | 192.4 ±5.7 | 55.2 ±1.6 | 92.6 ±3.7 | 18.4 ±0.7 | 0.89 ±0.04 |

Power output and cumulative energy generated from the MFC was shown in Figure 6.4. The electrical energy recovered by the MFC was about 92.6 J, indicating that energy recovery efficiency based on the total chemical energy input was 18.4% (Table 6.1).

Energy density, a better link between COD contents and the produced electricity than CE, was also calculated. It was showed in Table 6.1 that the energy density of the MFC 0.89 kWh/kg COD based on the COD degraded from the electrolyte (Table 6.1), which was much higher than the previously reported energy density of 0.14 kWh/kg COD and 0.1023 kWh/kg COD in MFCs (9-10).

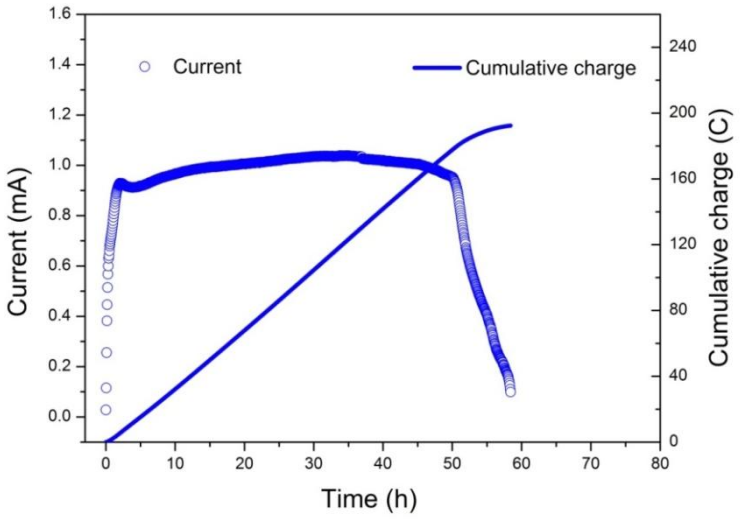


Figure 6. 3 Current generation and cumulative charge in the air-cathode MFC.

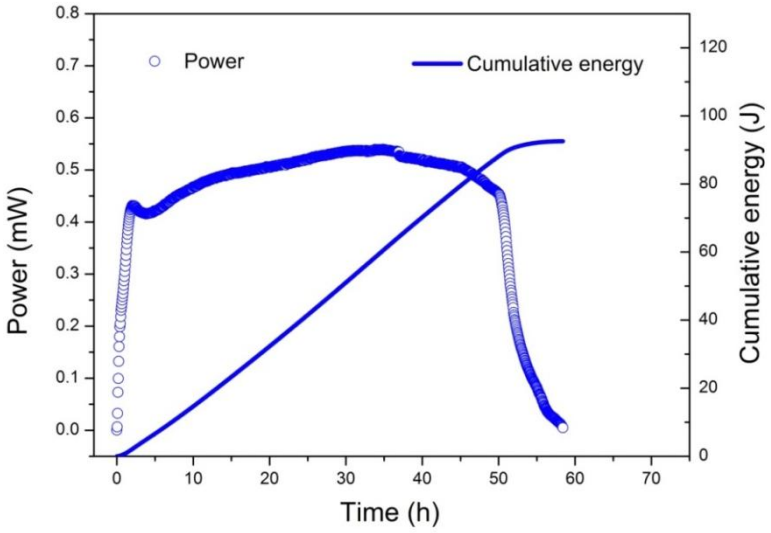


Figure 6. 4 Power output and cumulative energy generated in the air-cathode MFC.

### 6.3.2 Comparison with traditional wastewater treatment methods

The most important advantage of MFC technology is the simultaneous energy production during wastewater treatment. Actually, wastewater treatment using MFC technology has the potential be a net energy producer rather than an energy consumer if sufficient energy is produced (19). Therefore, it is of great significance to compare MFC with other traditional wastewater treatment technologies.

Aerobic treatment of wastewater such as activated sludge is an efficient technology for removing organic contaminants because aerobic heterotrophic microorganisms can degrade organic matters very fast due to their high metabolic kinetics (20). However, it is energy intensive and costly because of aeration and sludge treatment. Currently, about 0.4-1.0 kWh of energy is needed for removing one kilogram COD from wastewater by activated sludge treatment (21). In the U.S., about 3% of electricity produced is consumed by wastewater treatment plants and the annual cost for wastewater treatment is as high as $25

billion (19-20). Compared with aerobic treatment, the greatest benefit of MFC for wastewater treatment is energy recovery and energy saving. For this air-cathode MFC, about 0.89 kWh/kg COD was produced and further 0.4-1.0 kWh/kg COD was saved because aeration was not needed and less sludge was generated. The combined energy recovery and energy saving from this MFC resulted in a total energy benefit of 1.29-1.89 kWh/kg COD compared with aerobic treatment. Therefore, MFC has the potential to be a self-sufficient technology for wastewater treatment because MFC can be an energy exporter rather than an energy consumer.

Anaerobic digestion is a traditional technology to capture energy from dissolved organic matters in wastewater, which has the potential to achieve net energy production while meeting wastewater treatment objectives (22). The study of the wastewater treatment plant in North Toronto demonstrated that 46% of the energy entering the anaerobic digester was recovered in biogas production as methane, while the conversion efficiency of methane to electricity typically varied in the range from 30% to 40% for different combustion systems (23). Consequently, the overall energy efficiency of anaerobic digestion was 13.8% to 18.4%. Another study of anaerobic digestion indicated that 0.6-1.1 kWh was captured from 1 kg COD (11).

The energy recovery efficiency in this study was 18.4% and the energy density was 0.89 kWh/kg COD, which was comparable to anaerobic digestion combined with combustion. Methane produced by anaerobic digestion, however, must be efficiently collected and safely stored, because methane is a greenhouse gas which might cause explosion (24). In addition, anaerobic digestion normally requires a warm temperature higher than 20 ℃, while MFC

can function well over a wide range of temperature (2). Another advantage of MFC over anaerobic digestion is that the former can work over a large range of COD concentration and the latter is more suitable for high COD loading. Therefore, compared with anaerobic digestion, MFC technology is more environmentally friendly and more versatile because electricity is directly generated from organic matters.

Although the advantages of MFCs are obvious, their disadvantages cannot be neglected. The power density is still quite low while the construction cost is prohibitive (25-27). On the one side, the power density of MFCs is expected to reach approximately 400 $W/m^3$ for real-world application for wastewater treatment (21). However, the maximum power density in this thesis was only about 18 $W/m^3$. On the other side, the construction cost of MFC bioreactor is much higher than anaerobic digester and active sludge. Another problem is the scale-up of MFCs. So far, the volume of most of the MFC bioreactor is in the level of less than 10 L, while pilot plant of large scale MFCs (larger than 100 L) is rarely reported. Therefore, quite a lot of challenges still need to be overcome before the real-world applications of MFC technology.

Further energy recovery enhancement could be focused on the energy loss due to microbial cell synthesis, aerobic respiration and anaerobic fermentation. Diffusion of oxygen dissolved into the anode chamber could inhibit the electrochemically active bacteria for electricity production, led to the growth of aerobic bacteria and oxidation of organic matters without electricity production. Anaerobic fermentation could also contribute to this part of energy loss, because methanogens were known to compete with exoelectrogens for electrons available and methane production had been demonstrated in MFCs in

some studies (28-29). This part of energy could be decreased by reducing or eliminating the dissolved oxygen in the anode chamber or inhibiting the growth and reproduction of methanogens. For example, two chamber MFC separated by an ion exchange membrane, or other oxidants such as potassium ferricyanide and silver oxide could be useful options to decrease this part of energy loss.

### 6.4 Conclusion

In this chapter, electrical energy production from wastewater by an air-cathode MFC was investigated. It was demonstrated that this air-cathode MFC achieved an energy recovery efficiency of 18.4% and an energy density of 0.89 kWh/kg COD, which was comparable to anaerobic digestion combined with combustion. These results demonstrated that MFC has the potential to be a self-sufficient technology for wastewater treatment because MFC can be an energy exporter rather than an energy consumer. Further energy recovery enhancement should focus on energy loss due to microbial cell synthesis, aerobic respiration and anaerobic fermentation.

### 6.5 References


1. International Energy Agency. (2012) Key World Energy Statistics, *International Energy Agency, Paris*.
2. Logan, B. E., and Rabaey, K. (2012) Conversion of Wastes into Bioelectricity and Chemicals by Using Microbial Electrochemical Technologies, *Science 337*, 686-690.
3. Rabaey, K., Lissens, G., Siciliano, S. D., and Verstraete, W. (2003) A microbial fuel cell capable of converting glucose to electricity at high rate and efficiency, *Biotechnology Letters 25*, 1531-1535.

4. Liu, H., Ramnarayanan, R., and Logan, B. E. (2004) Production of electricity during wastewater treatment using a single chamber microbial fuel cell, *Environmental Science & Technology 38*, 2281-2285.
5. Tender, L. M., Reimers, C. E., Stecher, H. A., Holmes, D. E., Bond, D. R., Lowy, D. A., Pilobello, K., Fertig, S. J., and Lovley, D. R. (2002) Harnessing microbially generated power on the seafloor, *Nature Biotechnology 20*, 821-825.
6. Huang, Y. L., He, Z., Kan, J. J., Manohar, A. K., Nealson, K. H., and Mansfeld, F. (2012) Electricity generation from a floating microbial fuel cell, *Bioresource Technology 114*, 308-313.
7. Puig, S., Serra, M., Coma, M., Balaguer, M. D., and Colprim, J. (2011) Simultaneous domestic wastewater treatment and renewable energy production using microbial fuel cells (MFCs), *Water Science and Technology 64*, 904-909.
8. Ghangrekar, M. M., and Shinde, V. B. (2008) Simultaneous sewage treatment and electricity generation in membrane-less microbial fuel cell, *Water Science and Technology 58*, 37-43.
9. Wang, H., Lu, L., Cui, F. Y., Liu, D. M., Zhao, Z. W., and Xu, Y. P. (2012) Simultaneous bioelectrochemical degradation of algae sludge and energy recovery in microbial fuel cells, *Rsc Advances 2*, 7228-7234.
10. Zhang, F., and He, Z. (2013) A cooperative microbial fuel cell system for waste treatment and energy recovery, *Environmental Technology 34*, 1905-1913.
11. Pham, T. H., Rabaey, K., Aelterman, P., Clauwaert, P., De Schamphelaire, L., Boon, N., and Verstraete, W. (2006) Microbial fuel cells in relation to conventional anaerobic digestion technology, *Engineering in Life Sciences 6*, 285-292.

12. Gil, G. C., Chang, I. S., Kim, B. H., Kim, M., Jang, J. K., Park, H. S., and Kim, H. J. (2003) Operational parameters affecting the performance of a mediator-less microbial fuel cell, *Biosensors & Bioelectronics 18*, 327-334.

13. Rozendal, R. A., Hamelers, H. V. M., Rabaey, K., Keller, J., and Buisman, C. J. N. (2008) Towards practical implementation of bioelectrochemical wastewater treatment, *Trends in Biotechnology 26*, 450-459.

14. Tang, X., Li, H., Du, Z., Wang, W., and Ng, H. Y. (2015) Conductive polypyrrole hydrogels and carbon nanotubes composite as an anode for microbial fuel cells, *Rsc Advances 5*, 50968-50974.

15. Cheng, S., Liu, H., and Logan, B. E. (2006) Power densities using different cathode catalysts (Pt and CoTMPP) and polymer binders (Nafion and PTFE) in single chamber microbial fuel cells, *Environmental Science & Technology 40*, 364-369.

16. Tang, X. H., Li, H. R., Wang, W. D., Du, Z. W., and Ng, H. Y. (2014) A high-performance electrocatalytic air cathode derived from aniline and iron for use in microbial fuel cells, *Rsc Advances 4*, 12789-12794.

17. Wang, P., Lai, B., Li, H., and Du, Z. (2013) Deposition of Fe on Graphite Felt by Thermal Decomposition of Fe $(CO)_5$ for Effective Cathodic Preparation of Microbial Fuel Cells, *Bioresource Technology*.

18. Rand, M., Greenberg, A. E., and Taras, M. J. (1976) Standard methods for the examination of water and wastewater, Prepared and published jointly by American Public Health Association, American Water Works Association, and Water Pollution Control Federation.

19. McCarty, P. L., Bae, J., and Kim, J. (2011) Domestic Wastewater Treatment as a Net Energy Producer-Can This be Achieved?, *Environmental Science & Technology 45*, 7100-7106.

20. Huggins, T., Fallgren, P., Jin, S., and Ren, Z. (2013) Energy and

Performance Comparison of Microbial Fuel Cell and Conventional Aeration Treating of Wastewater, *J Microb Biochem Technol S 6*, 2.

21. Rabaey, K., and Verstraete, W. (2005) Microbial fuel cells: novel biotechnology for energy generation, *Trends in Biotechnology 23*, 291-298.
22. Zeeman, G., Kujawa, K., de Mes, T., Hernandez, L., de Graaff, M., Abu-Ghunmi, L., Mels, A., Meulman, B., Temmink, H., Buisman, C., van Lier, J., and Lettinga, G. (2008) Anaerobic treatment as a core technology for energy, nutrients and water recovery from source-separated domestic waste(water), *Water Science and Technology 57*, 1207-1212.
23. Shizas, I., and Bagley, D. M. (2004) Experimental determination of energy content of unknown organics in municipal wastewater streams, *Journal of Energy Engineering-Asce 130*, 45-53.
24. Xie, X., Ye, M., Hsu, P. C., Liu, N., Criddle, C. S., and Cui, Y. (2013) Microbial battery for efficient energy recovery, *Proceedings of the National Academy of Sciences of the United States of America 110*, 15925-15930.
25. Kim, B. H., Chang, I. S., and Gadd, G. M. (2007) Challenges in microbial fuel cell development and operation, *Applied Microbiology and Biotechnology 76*, 485-494.
26. Logan, B. E. (2010) Scaling up microbial fuel cells and other bioelectrochemical systems, *Applied Microbiology and Biotechnology 85*, 1665-1671.
27. Balat, M. (2010) Microbial Fuel Cells as an Alternative Energy Option, *Energy Sources Part a-Recovery Utilization and Environmental Effects 32*, 26-35.
28. Lee, H. S., Parameswaran, P., Kato-Marcus, A., Torres, C. I., and Rittmann, B. E. (2008) Evaluation of energy-conversion efficiencies in

microbial fuel cells (MFCs) utilizing fermentable and non-fermentable substrates, *Water Research 42*, 1501-1510.

29. Chae, K. J., Choi, M. J., Kim, K. Y., Ajayi, F. F., Park, W., Kim, C. W., and Kim, I. S. (2010) Methanogenesis control by employing various environmental stress conditions in two-chambered microbial fuel cells, *Bioresource Technology 101*, 5350-5357.

# Chapter 7 Conclusion and future work

## 7.1 Conclusion

This thesis is focused on power enhancement and applications of MFCs. The main conclusions are summarized as follows:

(1) Conductive polypyrrole hydrogels/carbon nanotubes (CPHs/CNTs) that synergized the advantageous features of hydrogels and organic conductors were synthezided *via* a liquid phase reaction using phytic acid as gelator and dopant. This anode reduced the interfacial charge transfer resistance from 19.2 Ω to 5.3 Ω and facilitated the direct electron transfer. Besides, the porous structure and hydrophilicity of this material improved the biofilm formation on anode surface. Consequently, this anode increased the maximum power density of MFCs by 118%.

(2) Anthraquinone-2-sulfonic acid (AQS), an electron transfer mediator, was covalently grafted onto graphite felt surface *via* spontaneous reduction of the *in situ* generated AQS diazonium cations. AQS grafted on graphite felt had a surface concentration of $5.37 \pm 1.15 \times 10^{-9}$ mol/cm$^2$. The redox potential of the modified graphite was about -0.248 V (vs.NHE), indicating that AQS functioned as a redox mediator to facilitate the mediated electron transfer from bacteria to electrode. This AQS modified anode enhanced the maximum power density of MFCs by 94%. This study demonstrates that graphite covalently immobilized with AQS via spontaneous reduction of its diazonium cation is an

effective and versatile method to facilitate mediated electron transfer and to enhance the power production in MFCs.

(3) A high-performance and low-cost electrocatalyst for oxygen reduction in the cathode of MFCs was synthesized. The catalyst was prepared by pyrolyzing iron-impregnated Polyaniline in $NH_3$ atmosphere under high temperature. The catalyst showed very positive onset potentials of about 0.92 V (vs. RHE). Also, the catalyst presented high selectivity towards the four-electron reduction of oxygen, as the yield of hydrogen peroxide was less than 3% in the whole potential range. These high catalyctic activity significantly reduced the overpotential caused by the slow kinetic of ORR and the competing two-electron reduction reaction. The catalyst considerably enhanced the maximum power density from 1.32 $W/m^3$ to 12.54 $W/m^3$ in MFCs. This study showed that iron coordinated with pyridinic nitrogen hosted in micropores was the active site for the high catalytic activity. The high catalytic activity combined with strong stability and low cost makes this catalyst an ideal cathode for MFCs.

(4) Bicarbonate buffer, as an alternative of phosphate buffer, was used in MFCs to help stabilize the solution pH for power production. Power densities of the MFCs with the two buffers were almost the same. Compared with the electrolyte with phosphate buffer, however, electrolyte with bicarbonate buffer effectively decreased the suspended bacteria, which had no contribution for electricity production in MFCs. The reduction of bacteria suspended in the

solution allowed more substrate to be consumed by biofilm formed on anode surface for electricity generation. Therefore, the electrolyte with bicarbonate buffer significantly enhanced the coulombic efficiency of MFCs. For example, the coulombic efficiency was increased by 174% in two-chambered MFCs with an acetate concentration of 11 mM. This study demonstrates that electrolyte with bicarbonate holds the potential to enhance the feasibility for practical applications of MFCs.

(5) The application of MFCs for electrical energy production from wastewater was studied. An energy recovery efficiency of 18.4% and an energy density of 0.89 kWh/(kg COD) was obtained in single chamber MFCs, which was comparable to anaerobic digestion combined with combustion. This study demonstrates that MFCs can be a self-sufficient technology for simultaneous energy recovery and wastewater treatment.

### 7.2 Future work

Although MFCs are promising for various kinds of applications, there are quite some challengers that need to be overcome. The power density is still quite low compared with anaerobic digestion. The power density should be further increased to enhance their applications. Besides, the construction cost is prohibitive. Novel high-performance and low-cost materials and bioreactor design need to be prepared to commercialize the technology. Further, the scale-up of MFCs is urgent for real-world applications of MFCs. The volume of most of the MFCs, however, is in the level of less than 10 L. As a result, pilot plant of large scale MFCs need to be studied for real-world applications.

Further work might consider the following aspects:

(1) CPHs/CNTs could enhance the biofilm formation, reduce the interfacial charge transfer resistance and facilitate the direct electron transfer from bacteria to anode surface, while AQS covalently grafted onto graphite felt surface via spontaneous reduction of the in situ generated AQS diazonium cations could serve as a redox mediator to facilitate the mediated electron transfer from bacteria to electrode surface. Therefore, grafting AQS onto CPHs/CNTs surface is expected to enhance both the direct electron transfer and the mediated electron transfer. This novel material might be an ideal anode in MFCs to enhance the power production.

(2) PANI-$Fe_{900}$ catalyst for ORR exhibited very positive onset potential, extremely high selectivity for the four-electron reaction pathway and high power density in MFCs. The pyrolysis method can be optimized to increase the micropore area and the pyridinic nitrogen content of this catalyst. The catalyst with higher micropore area and the pyridinic nitrogen content will further improve its electrocatalytic activity towards ORR and ultimately power density in MFCs. Besides, PANI-$Fe_{900}$ has demonstrated the potential for large scale application due to its high catalytic activity and extremely low cost. Therefore, its performance at large scale in MFCs should be investigated.

(3) Bicarbonate buffer could greatly enhance the coulombic efficiency of MFCs. Also, the coulombic efficiency of MFCs using bicarbonate buffer was very stable for different substrate concentration. An enhanced and stable

coulombic efficiency will greatly improve the MFC type biosensor for BOD detection, such as the accuracy and repeatability. Therefore, it is suggested to investigate the application of MFC type biosensor using bicarbonate buffer for BOD measurement.